



The Journal of Gemmology

2015 / Volume 34 / No. 5





Gem-A

THE GEMMOLOGICAL ASSOCIATION
OF GREAT BRITAIN



Get closer to the source 13–20 June 2015

Gem-A is hosting the trip of a lifetime to **Idar-Oberstein**: the home of gem carving. Visits include **Edelsteinminen Steinkaulenberg**, **Kupferbergwerk in Fischbach**, **DGemG**, **Schneider gem tools**, **Deutsches Mineralienmuseum**, **Historische Weiherschleife** and **lapidaries**, as well as the opportunity to sample the very best of small-town culture. Prices start at just **£1,545**, and include travel, accommodation, visits, breakfast and dinner.

For more information or to secure your place, contact events@gem-a.com.

Understanding Gems

Join us.



COLUMNS

381 What's New

GL Gem Spectrometer |
Photography accessory clips |
Presidium Gem Indicator |
Newsletters from the Gem
Testing Laboratory, GGTL and
ICGL | GIT Lab updates |
Gold demand trends | *Handbook
of Gemmology*, 3rd edn. | Oiled
gems lab alert | Pink and blue
CVD synthetic diamonds | *World
Diamond Magazine* | Coloured
stone app

384 Practical Gemmology

Colour grading of synthetic
moissanite

386 Gem Notes

Large kunzite from Brazil |
Marble-hosted ruby mine,
Mogok, Myanmar | Secondary
gem deposit in Mogok,
Myanmar | Pink play-of-colour
opal from Idaho | Dumortierite
inclusions in quartz from
Brazil | Quartz sphere with
large inclusion | Zawadi
sapphires | Tourmaline from
the Havey quarry, Maine, USA |
Greenland tugtupite | Orange
zircon from Myanmar | Glass
imitation of emerald | Large black
synthetic moissanite as a black
diamond imitation | Peridot-
polymer composite | Dyed
quartzite imitating bicoloured
tourmaline



Cover Photo:

The attractive appearance of this 54.10 ct Zawadi sapphire is created by its 'golden' sheen and contrasting network of dark fractures and twin planes. Courtesy of Primagem; photo by Jeff Scovil.



ARTICLES

Feature Article

404 The Potential of a Portable EDXRF Spectrometer for Gemmology

By Franz A. Herzog

Gemmological Briefs

420 Green Lead-Glass-Filled Sapphires

By Thanong Leelawatanasuk, Namrawee Susaewee, Supparat Promwongnan and Nicharee Atsawatanapirom

428 Demantoid from Balochistan, Pakistan: Gemmological and Mineralogical Characterization

By Ilaria Adamo, Rosangela Bocchio, Valeria Diella, Franca Caucia and Karl Schmetzer

434 Nail-head Spicules as Inclusions in Chrysoberyl from Myanmar

By Karl Schmetzer and Michael S. Krzemnicki

441 Letters

444 Conferences

AGA Tucson | GILC Tucson | GIT 2014

448 Gem-A Notices

453 Learning Opportunities

457 New Media

463 Literature of Interest

The Journal is published by Gem-A in collaboration with SSEF and with the support of AGL and GIT.





Editor-in-Chief

Brendan M. Laurs
brendan.laurs@gem-a.com

Production Editor

Mary A. Burland
mary.burland@gem-a.com

Marketing Consultant

Ya'akov Almor
bizdev@gem-a.com

Executive Editor

James H. Riley

Editor Emeritus

Roger R. Harding

Assistant Editor

Michael J. O'Donoghue

Associate Editors

Edward Boehm, *RareSource, Chattanooga, Tennessee, USA*; Alan T. Collins, *King's College London*; John L. Emmett, *Crystal Chemistry, Brush Prairie, Washington, USA*; Emmanuel Fritsch, *University of Nantes, France*; Rui Galopim de Carvalho, *Portugal Gemas, Lisbon, Portugal*; Lee A. Groat, *University of British Columbia, Vancouver, Canada*; Thomas Hainschwang, *GGTL Gemlab-Gemtechlab Laboratory, Balzers, Liechtenstein*; Henry A. Hänni, *GemExpert, Basel, Switzerland*; Jeff W. Harris, *University of Glasgow*; Alan D. Hart, *The Natural History Museum, London*; Ulrich Henn, *German Gemmological Association, Idar-Oberstein*; Jaroslav Hyršl, *Prague, Czech Republic*; Brian Jackson, *National Museums Scotland, Edinburgh*; Stefanos Karamelas, *Gübelin Gem Lab Ltd., Lucerne, Switzerland*; Lore Kiefert, *Gübelin Gem Lab Ltd., Lucerne, Switzerland*; Hiroshi Kitawaki, *Central Gem Laboratory, Tokyo, Japan*; Michael S. Krzemnicki, *Swiss Gemmological Institute SSEF, Basel*; Shane F. McClure, *Gemmological Institute of America, Carlsbad, California*; Jack M. Ogden, *Striptwist Ltd., London*; Federico Pezzotta, *Natural History Museum of Milan, Italy*; Jeffrey E. Post, *Smithsonian Institution, Washington DC, USA*; Andrew H. Rankin, *Kingston University, Surrey*; George R. Rossman, *California Institute of Technology, Pasadena, USA*; Karl Schmetzer, *Petershausen, Germany*; Dietmar Schwarz, *AIGS Lab Co. Ltd., Bangkok, Thailand*; Menahem Sevdemish, *GemeWizard Ltd., Ramat Gan, Israel*; Guanghai Shi, *China University of Geosciences, Beijing*; James E. Shigley, *Gemmological Institute of America, Carlsbad, California*; Christopher P. Smith, *American Gemological Laboratories Inc., New York*; Evelyne Stern, *London*; Elisabeth Strack, *Gemmologisches Institut, Hamburg, Germany*; Tay Thyie Sun, *Far East Gemological Laboratory, Singapore*; Pornsawat Wathanakul, *Gem and Jewelry Institute of Thailand, Bangkok*; Chris M. Welbourn, *Reading, Berkshire*; Joanna Whalley, *Victoria and Albert Museum, London*; Bert Willems, *Leica Microsystems, Wetzlar, Germany*; Bear Williams, *Stone Group Laboratories LLC, Jefferson City, Missouri, USA*; J.C. (Hanco) Zwaan, *National Museum of Natural History 'Naturalis', Leiden, The Netherlands*.

Content Submission

The Editor-in-Chief is glad to consider original articles, news items, conference/excursion reports, announcements and calendar entries on subjects of gemmological interest for publication in *The Journal of Gemmology*. A guide to the preparation of manuscripts is given at www.gem-a.com/publications/journal-of-gemmology.aspx, or contact the Production Editor.

Subscriptions

Gem-A members receive *The Journal* as part of their membership package, full details of which are given at www.gem-a.com/membership.aspx. Laboratories, libraries, museums and similar institutions may become Direct Subscribers to *The Journal* (see www.gem-a.com/publications/subscribe.aspx).

Advertising

Enquiries about advertising in *The Journal* should be directed to the Marketing Consultant. For more information, see www.gem-a.com/publications/journal-of-gemmology/advertising-in-the-journal.aspx.

Copyright and Reprint Permission

Abstracting with credit to the source, photocopying isolated articles for noncommercial classroom use, and photocopying by libraries for private use of patrons, are permitted. Requests to use images published in *The Journal* should be directed to the Editor-in-Chief. Give the complete reference citation and the page number for the image(s) in question, and please state how and where the image would be used.

The Journal of Gemmology is published quarterly by Gem-A, The Gemmological Association of Great Britain. Any opinions expressed in *The Journal* are understood to be the views of the contributors and not necessarily of the publisher.

Printed by DG3 (Europe) Ltd.

© 2015 The Gemmological Association of Great Britain

ISSN: 1355-4565



21 Ely Place
London EC1N 6TD
UK

t: +44 (0)20 7404 3334
f: +44 (0)20 7404 8843
e: information@gem-a.com
w: www.gem-a.com

Registered Charity No. 1109555
Registered office: Palladium House,
1-4 Argyll Street, London W1F 7LD

President

Harry Levy

Vice Presidents

David J. Callaghan, Alan T. Collins,
Noel W. Deeks, E. Alan Jobbins,
Michael J. O'Donoghue,
Andrew H. Rankin

Honorary Fellows

Gaetano Cavalieri, Terrence S.
Coldham, Emmanuel Fritsch

Honorary Diamond Member

Martin Rapaport

Honorary Life Members

Anthony J. Allnutt, Hermann Bank,
Mary A. Burland, Terence M.J.
Davidson, Peter R. Dwyer-Hickey,
Gwyn M. Green, Roger R. Harding,
John S. Harris, J. Alan W. Hodgkinson,
John I. Koivula, Jack M. Ogden,
C.M. (Mimi) Ou Yang, Evelyne Stern,
Ian Thomson, Vivian P. Watson,
Colin H. Winter

Chief Executive Officer

James H. Riley

Council

Jason F. Williams – Chairman
Mary A. Burland, Jessica M. Cadzow,
Steven J.C. Collins, Paul F. Greer,
Alan D. Hart, Nigel B. Israel, Jonathan
Lambert, Richard M. Slater, Miranda
E.J. Wells, Stephen Whittaker

Branch Chairmen

Midlands – Georgina E. Kettle
North East – Mark W. Houghton
South East – Veronica Wetten
South West – Richard M. Slater

Understanding Gems™

What's New

INSTRUMENTS AND TECHNIQUES

GL Gem Spectrometer NIR PL405

The GL Gem Spectrometer NIR PL405 is a dual purpose spectrometer for photoluminescence and Vis-NIR spectroscopy (550–1000 nm) that was released by Gemlab Group in December 2014. The spectrometer has a higher resolution but shorter wavelength range than Gemlab's previous GL Gem Spectrometer (300–1000 nm). It is equipped with a long-wave pass filter and is optimized for the NIR range. The unit is simply plugged into a computer's USB port; no additional drivers are necessary. It can be used to identify various gems such as ruby, sapphire, emerald, spinel and alexandrite based on their PL response, and it also may be used for quick diamond testing (to reveal the GR1 and Si centres at room temperature). For more information, visit www.cigem.ca/research-technology/gl-gemspec-nir-pl405.



Photography Accessory Clips

In 2014, Lithographie Ltd. started offering black flexible clips for gem and mineral photography. They are useful for holding reflectors, diffusers,



etc., and are available in two sizes: five joints (15.6 cm long) or 10 joints (23.6 cm long). Visit www.lithographie.org/bookshop/five_joint_black_flexible.htm.

Presidium Gem Indicator

The Presidium Gem Indicator was launched at the Hong Kong International Jewellery Show in March 2015. The instrument is an enhanced and more convenient handheld version of the Presidium Gem Tester/Colored Stone Estimator. It distinguishes between diamonds and various other gems using thermal conductivity, and it comes with a changeable probe tip to guard against equipment downtime. The probe consists of two linked thermometers; one is heated electronically while the other is cooled by the stone being tested. The difference in temperature creates an electrical output, which is then amplified and displayed on the LED screen. It features an input function that allows users to select from a range of 12 common gem colours, thereby achieving more accurate results. Visit www.presidium.com.sg/PGI.html.



NEWS AND PUBLICATIONS

Gem Testing Laboratory (Jaipur, India) Newsletter

The latest *Lab Information Circular* (Vol. 71, March 2015), available at www.gtijaipur.info/circulars/LIC_Vol71_March2015_Eng.pdf, describes emeralds with repaired (glued) fractures, a dendritic opal showing play-of-colour, an emerald parcel with imitations consisting of coated beryl and



glass, a strongly colour-zoned (green and light brown) synthetic moissanite, a dyed labradorite bead, photochromism and thermo-chromism displayed by CVD synthetic diamond, and multi-coloured dyed quartz.

GGTL Newsletters

In March 2015, GGTL Laboratories released its latest newsletters (Nos. 4 and 5), available at [www.ggtl-lab.org/media/newsletter/GGTL_Newsletter_No_4_March_2015_\(EN\).pdf](http://www.ggtl-lab.org/media/newsletter/GGTL_Newsletter_No_4_March_2015_(EN).pdf) and [www.ggtl-lab.org/media/newsletter/GGTL_Newsletter_ALERT_No_5_March_2015_\(EN\).pdf](http://www.ggtl-lab.org/media/newsletter/GGTL_Newsletter_ALERT_No_5_March_2015_(EN).pdf). Number 4 reports on a yellow CVD synthetic diamond found in a parcel of melee originating in Hong Kong (see *The Journal*, Vol. 34, No. 4, 2014, pp. 300–302) and also describes the DFI Mid-UV Laser+, an instrument designed and built by GGTL Laboratories



for the detection of near-colourless HPHT and CVD synthetic diamonds. Number 5 documents the first colourless melee-sized CVD synthetic detected in a parcel of natural diamonds during the Baselworld (Switzerland) show in March 2015.

GIT Lab Updates

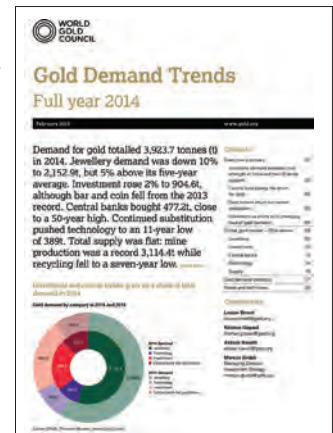
In March 2015, the Gem and Jewelry Institute of Thailand (GIT) issued an 'urgent release' on a new type of glass-filled ruby that is claimed to be toxin-free and marketed under the name 'Organic Ruby' by Spa Gems company in Chanthaburi (see www.git.or.th/2014/eng/testing_center_en/lab_notes_en/glab_en/2015/03/GIT_URGENT_RELEASE.pdf). This lead-glass-filled ruby reportedly has undergone further treatment to remove significant amounts of Pb from the glass filler in the stone. The 'Organic Ruby' name has created controversy among traders who fear that it could be misleading to consumers.

Also in March 2015, GIT released a lab update on a synthetic ruby overgrowth on natural corundum. The properties of the 1.84 ct gem showed that it was similar to material that circulated in the market in the early 2000s. The report can be downloaded at www.git.or.th/2014/eng/testing_center_en/lab_notes_en/glab_en/2015/03/Synthetic_Ruby_Overgrowth.pdf.

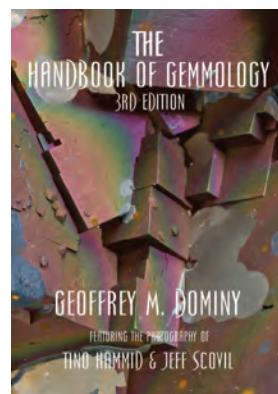


Gold Demand Trends 2014

In February 2015, the World Gold Council released their report on 2014 gold demand trends, available at www.gold.org/download/file/3691/GDT_Q4_2014.pdf. Gold jewellery demand was down 10% to 2,152.9 tonnes, but was 5% above its five-year average. Year-on-year declines in jewellery were widespread. A few markets were notable exceptions to the downward trend: India had a particularly good year, topping the 2013 total by 8%.



The Handbook of Gemmology, 3rd edn.



The 3rd edition of this book is now available on DVD or to download (see <http://handbookofgemmology.com>). Now with 1,056 pages, the book includes updated information on gem magnetism, inclusions, physical and optical properties, opal mining, and a new section titled GEMFACTS that gives comprehensive information on the 15 most common gem species.

ICGL Newsletter

The International Consortium of Gem-Testing Laboratories has released Newsletter No. 1/2015, available at <http://icglabs.org>. The theme of the newsletter is emerald, and it includes reports on composites of pale green beryl and green glass, hydrothermal synthetic emeralds with filled fractures, and recent developments in 'Soudé Emeralds' (quartz doublets).



Oiled Gems Lab Alert

In April 2015, Lotus Gemology (Bangkok, Thailand) issued a lab alert warning about the prevalence of gems submitted for testing that were fissure filled with oils or resins (see www.lotusgemology.com/index.php/library/articles/315-lotus-gemology-lab-alert-for-oiled-gems). Nearly all of these treated gems were of Burmese origin, consisting of ruby, sapphire, spinel and tourmaline. None of the clients who submitted the stones were aware of the oil/resin filling.

Pink and Blue CVD Synthetic Diamonds

In February 2015, M&A Gemological Instruments released an application note titled 'Large Amount of Pink and Blue CVD-grown Synthetic Diamonds on the Market' by Mikko Åström and Alberto Scarani (PDF available at www.gemmoraman.com/Articles.aspx).



on the Market' by Mikko Åström and Alberto Scarani (PDF available at www.gemmoraman.com/Articles.aspx). The report describes CVD synthetics tested during the 2015 Tucson gem shows, where they were available in relatively large quantities. The blue synthetics have created the most concern because their spectroscopic characteristics at room temperature are similar to those of irradiated blue natural (not synthetic) diamonds and also they are not electrically conductive.

World Diamond Magazine

The World Diamond Mark Foundation (WDMF), in close cooperation with the Turkish Jewelry Exporters Association (JTR), has launched a new quarterly periodical called the *World Diamond Magazine*. WDMF was established in 2012 by the World Federation of Diamond Bourses with the global objective to boost consumer demand for diamonds and diamond jewellery. JTR is one of the early adopters of the WDMF and its programs. The *Magazine* publishes WDMF-related articles and its

own editorials and news, in addition to carrying a carefully selected choice of articles from the international trade press. It was launched in September 2014, and the latest issue (March 2015) features an article from Gem-A's president, Harry Levy, about diamond grading standards. The magazine is available in print format at major trade shows and conferences, and PDF files of the issues can be downloaded at www.worlddiamondmark.org/world-diamond-magazine. For a free subscription, email communications@worlddiamondmark.org.



Ya'akov Almor

Media Relations Director, WDMA

OTHER RESOURCES

Coloured Gemstone App



Geoffrey Watt of Mayer & Watt (Maysville, Kentucky, USA) recently released an educational coloured gemstone app that is designed to be used by jewellery professionals and consumers. A January–February 2015 update enables users to search by keyword; both iOS and Android devices are supported by this free app.

Visit <http://mayerandwatt.com/gemipedia/mayer-and-watt-app-instruction>.

Erratum

The What's New entry on Historical Facet Designs (Vol. 34, No. 4, 2014, p. 279) should have reported that the website was launched in June 2013 not 2014.

What's New provides announcements of new instruments/technology, publications, online resources and more. Inclusion in What's New does not imply recommendation or endorsement by Gem-A. Entries were prepared by Mary Burland and Brendan Laurs unless otherwise noted.

Colour Grading of Synthetic Moissanite

Mary L. Johnson

Since its introduction to consumers in the 1990s (see Nassau et al., 1997), gem-quality synthetic moissanite has become a popular substitute for diamond. As used in the gem trade, it is generally near-colourless to pale yellow, green or grey, with high lustre and dispersion, and has a hardness greater than corundum; it is typically fashioned in shapes popular for diamonds. So far, all commercial synthetic moissanite diamond substitutes are doubly refractive.

The value of a diamond is determined by the 4Cs: colour, clarity, carat weight and cut. Most grading laboratories use the D-to-Z scale to colour grade near-colourless to yellow diamonds. In such a system, a diamond is compared *face-down* to face-down master stones along the D-to-Z scale. In GIA's laboratory, diamonds with more colour than the D-to-Z scale, or with hues other than yellow, brown or grey, are graded *face-up* using the GIA Fancy Color scale. This scale is applied when such hues first become perceptible (usually at about the H level in the D-to-Z system) for colours such as green, blue and pink. The colour grades are: Faint, Very Light, Light, Fancy Light, Fancy, Fancy Dark, Fancy Deep, Fancy Intense, and Fancy Vivid, with the hue name given after the



Figure 1: The conventional way to colour grade diamond simulants is as done for D-to-Z diamonds, with both the sample and master stone in the face-down position against a white or light grey background, using daylight-equivalent fluorescent light. Here, a master stone is on the left and a synthetic moissanite is on the right. Each gem is approximately 5 mm in diameter. Photo courtesy of Charles & Colvard Ltd.

grade (e.g. Fancy Light orangy yellow: see King et al., 1994).

During a recent visit to a facility operated by a major synthetic moissanite supplier (Charles & Colvard, Morrisville, North Carolina, USA), this author witnessed experienced gemmologists colour grading near-colourless synthetic moissanites for internal company purposes as if they were grading D-to-Z range diamonds: face-down compared to face-down master stones, on a light-coloured neutral background, with overhead daylight-equivalent fluorescent illumination (Figure 1). Other synthetic moissanite suppliers appear to use a similar technique (e.g.

“color grading is done on the bottom half to avoid faceting influencing the color grading”: Mira Moissanite – Less Responses, 2011).

It would seem intuitive that near-colourless diamond simulants should be colour graded in the same way as D-to-Z diamonds. However, the face-up colour-grading methodology used for fancy-colour diamonds is more applicable to synthetic moissanite for a simple reason: synthetic moissanite is pleochroic.

Factors in a Gemstone's Colour

Again, let's start with diamonds. There are three aspects that determine the face-up colour appearance of a high-clarity diamond: its body colour, the effect of the cutting style, and the environment in which the diamond is placed (with reference to the observer, lighting and other surroundings). Because diamonds in the D-to-Z range are being evaluated for their rarity and apparent colour purity, the *only* aspect being evaluated is the body colour. (Cut is evaluated separately, and the environment is standardized.) For this reason, diamond is colour graded in the face-down position so that the path of light through the stone,

showing its body colour, does not compete with distracting reflections or dispersion flares.

For fancy-colour diamonds, what matters most is the colour that is manifested face-up; therefore, coloured diamonds are evaluated in this position, and the grade is determined by the apparent face-up colour. This also means that it is sometimes possible to improve the colour grade of a fancy-colour diamond by recutting it. But what about those distracting reflections and/or dispersion flares? To minimize these, the diamond is colour graded within a mostly closed environment (i.e. the Macbeth Judge II viewing booth: see www.xrite.com/judge-ii). Also, the grader must be trained to recognize the *characteristic colour* that creates the overall colour impression of the diamond (again, see King et al., 1994).

Diamond is isotropic, meaning that its optical properties do not change with crystallographic direction. By contrast, gems that are doubly refractive, such as synthetic moissanite, may have different light absorption spectra (and therefore different colour appearances) in different directions—that is, they are pleochroic. Popular examples include tourmaline, ruby, sapphire and emerald. For strongly pleochroic gems, such as green tourmaline and iolite, the orientation of the stone relative to its crystallographic axes is important for determining face-up colour, and the gems are cut accordingly (otherwise, a green tourmaline might appear over dark, and an iolite

could look pale or yellowish instead of blue). Partly for this reason, the colour of coloured stones is evaluated in the face-up position.

Synthetic Moissanite Colour-grading Methodology

Synthetic moissanite as a D-to-Z diamond simulant is pleochroic, and it is logical to assume that it is cut in an orientation that minimizes its face-up colour. Because of this, colour grading synthetic moissanite face-down is inappropriate because its face-down colour may not be indicative of its face-up appearance.

Master stones for D-to-Z colour grading (both diamonds and cubic zirconia) are designed to be used in a face-down position, thus minimizing reflections and dispersion flares. Therefore, even though synthetic moissanite should be colour graded in a *face-up position*, it should be graded against *face-down master stones*

Figure 2: Pleochroic diamond simulants such as synthetic moissanite should actually be colour graded in the face-up position (see stone on the right) against face-down master stones (left). Each gem is approximately 5 mm in diameter. Photo courtesy of Charles & Colvard Ltd.

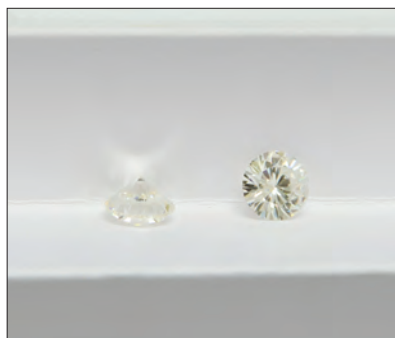


(Figure 2). A few preliminary experiments known to this author have indicated that this should not be a problem for trained graders, even for fancy shapes. It is important as well to indicate that the colour grade assigned to a synthetic moissanite is not equivalent to that of a D-to-Z (non-fancy-colour) diamond, since such diamonds are graded face-down while synthetic moissanite should be graded face-up. The author recommends terminology such as ‘this synthetic moissanite *faces up* F colour.’

References

- King J.M., Moses T.M., Shigley J.E. and Liu Y., 1994. Color grading of colored diamonds in the GIA Gem Trade Laboratory. *Gems & Gemology*, **30**(4), 220–242, <http://dx.doi.org/10.5741/gems.30.4.220>.
- Mira Moissanite – Less Responses, 2011. http://betterhandiamond.com/discussion/ubbthreads.php/topics/634123/all/Mira_Moissanite_Less_Responses, dated 1 June, accessed 5 November 2014.
- Nassau K., McClure S.F., Elen S. and Shigley J.E., 1997. Synthetic moissanite: A new diamond substitute. *Gems & Gemology*, **33**(4), 260–275, <http://dx.doi.org/10.5741/gems.33.4.260>.

Dr Mary Johnson is a former manager of research and development at the Gemological Institute of America in Carlsbad, California, USA. She now provides advice and services to the gem trade and the mineral specimen business through her company, Mary Johnson Consulting. Email: mlj@cox.net

Gem Notes

COLOURED STONES

Large Kunzite Gem Crystal from Brazil

The granitic pegmatites of Minas Gerais, Brazil, are well known for producing large crystals of gem-quality pink spodumene (kunzite). One such crystal documented by Sinkankas (1962), thought to be the world's largest at the time, measured 31.1 × 15.8 × 9.7 cm and weighed 7.41 kg. Sinkankas

Figure 1: This enormous gem-quality kunzite crystal weighs almost 30 kg. It was mined in 1998 from the Urucum pegmatite in Brazil. Photo by B. M. Laurs.



(1962, p. 287) also reported that “flawless gems exceeding 300 carats have been cut in Brazil, and the author has cut a number of much larger ones...which, unfortunately, were not entirely flawless.”

An important source of large kunzite crystals in Brazil is the Urucum mine in Minas Gerais State. In 1968, an enormous pocket at this mine reportedly yielded 3,000 kg of gem spodumene, although the largest crystals were modestly sized at just under 2 kg (Cassedanne, 1986). Three decades later, in October 1998, another large kunzite pocket was discovered at Urucum by Dilermando Rodrigues de Melo Filho of Geometa Ltda. (Governador Valadares, Minas Gerais). This cavity reportedly produced over 100 kg of high-quality crystals (Mauthner, 2011). Some of them were exceedingly large, such as the 37.1-cm-tall crystal pictured by Mauthner (2011). However, the largest kunzite crystal from this pocket was not exhibited until recently.

At the 2015 Tucson gem shows, Geometa displayed a gem-quality kunzite recovered from the 1998 pocket that weighed almost 30 kg (Figure 1). The crystal was deeply etched (as is typical of Brazilian kunzite), but had lustrous surfaces and was completely transparent. It was the first time it had been publically displayed outside of Brazil, and to this author's knowledge it is the largest gem-quality kunzite crystal in the world.

Brendan M. Laurs

References

- Cassedanne J.P., 1986. The Urucum pegmatite, Minas Gerais, Brazil. *Mineralogical Record*, **17**, 307–314.
- Mauthner M., 2011. The history of kunzite and the California connection. *Rocks & Minerals*, **86**(2), 112–131, <http://dx.doi.org/10.1080/00357529.2011.537171>.
- Sinkankas J., 1962. World's largest kunzite crystal. *Gems & Gemology*, **10**(9), 274–277, 287.

Gem-A Visit to a Marble-hosted Ruby Mine, Mogok, Myanmar

In December 2014, a team from Gem-A visited the gem mining area of Mogok in central Myanmar (for more information, see Laurs, 2015). Guided by Federico Bärlocher (a gem dealer and collector from Switzerland who specializes in top-quality Mogok gems and crystals), the group consisted of CEO James Riley, chairman of the Board of Trustees Jason Williams, and this author. Mogok was closed to foreigners for decades until it was reopened in 2012; a special permit from the Myanmar government is needed to visit there.

Numerous hard-rock (primary) ruby mines explore the ‘marble ark’ in the mountainous terrain of the Mogok area (Themelis, 2008). We visited one mine in the Bapawdan area, located approximately 5 km northwest of Mogok. The present mine owner has worked the deposit since 2007 in a joint venture with the Myanmar government. The property was initially worked in 2000.

The deposit is mined nearly 24 hours/day in two shifts. Access to the mine is provided by a 100-m-long adit (fitted with track for ore cars; Figure 2) and several shafts. The workings consist of a series of declines that follow a natural karst system in the marble that dips steeply to the south. Ruby mineralization locally occurs along specific horizons in the marble that partially follow the general trend of the natural cave system. A complex network of ladders (e.g. Figure 3) and platforms is used to access both primary and secondary deposits within the underground



Figure 2: Ore cars are lined up before the entrance to this ruby mine in the Bapawdan area of Mogok, Myanmar. Photo by B. M. Laurs.

workings. The miners use pneumatic drills and explosives (e.g. Figure 4) to break up the marble host rock in search of ruby, and they collect



Figure 3: A miner descends a steep ladder to the working face where marble is drilled and blasted in search of rubies. The cables on the right are used to hoist the marble to a haulage tunnel, where it is then loaded into ore cars. Photo by B. M. Laurs.

Figure 4: A miner dressed in a longyi (traditional Burmese skirt) uses a pneumatic drill to prepare the marble for blasting. His assistant in the left foreground holds several sticks of explosives. Photo by B. M. Laurs.



gravels from the floor of the cave system that have weathered from the marble. According to U San Myo, ruby mineralization is encountered only occasionally in the marble, and it is very rare to see gems in the mine exposures.

The marble pieces broken up by the explosives are immediately placed into heavy-duty bags and

Figure 5: The mine owner displays a small piece of ruby-bearing marble that was just recovered from the processing plant, while Jason Williams looks on. Photo by B. M. Laurs.



secured with a theft-proof tie until they are taken to the surface and processed for any possible rubies. At the processing facility, the marble is passed into a small jaw crusher that reduces it to <2 cm pieces. The crushed marble is washed into a jig using water from a nearby stream. All material that washes over the riffles is hand-sorted for pieces of ruby-bearing marble. At the end of the day, the gravel and rocks trapped in the riffles are placed into sieves (approximately 2 mm mesh size) for additional washing, followed by hand picking. The rubies recovered during this process are placed into a locked steel receptacle. The secondary gravels that are brought up from the mine are washed in the stream using the same sieves. In the brief time that we witnessed the processing of the ore, only one small ruby specimen was recovered (Figure 5), as well as one minute grain each of ruby and red-orange spinel that were sieved from the karst gravels. The secondary deposits reportedly also produce moonstone, apatite and other minerals.

We found this mine to be a very well-organized and professionally planned operation. Maps of the geology and mine workings that were displayed in the head office suggested that a considerable portion of the ruby-mineralized layers still remain to be mined in the future.

Brendan M. Laurs

References

- Laurs B., 2015. Journey to Mogok, Myanmar. *Gems & Jewellery*, **24**(1), 10–13.
- Themelis T., 2008. *Gems & Mines of Mogok*. Self-published, 352 pp.

Gem-A Visit to a Secondary Gem Deposit in Mogok, Myanmar



Figure 6. This secondary deposit in the Bernardmyo area of Mogok is a source of gem corundum, spinel, topaz, and other minerals. Photo by B. M. Laurs.

In December 2014, a team from Gem-A was led by Federico Bärlocher to visit the gem mining area of Mogok in central Myanmar (see also the preceding Gem Note on the marble-hosted ruby mine). The Mogok Stone Tract is famous for producing a diverse array of gem materials—sometimes of the highest quality—from both primary and secondary deposits (e.g. Themelis, 2008). We visited a secondary gem deposit (Figure 6) located 7.6 km northwest of Mogok, near the village of Ingyauk (or Injauk) in the Bernardmyo area. At the time of the visit, the mine owner had just completed the first year of his three-year lease. He works the mine for six months of the year, during the dry season.

Water cannons are used to wash material from the pit into a sump (Figure 7), and the slurry

is then pumped out of the pit to a washing plant (Figure 8). Larger stones (over 1 inch or 2.5 cm) are screened off, and the remainder of the material flows into a jig. The heavier stones (including gems) are caught in the riffles above the jig, and at the end of each day the miners remove the concentrate by hand. Material from the top half of the riffles is discarded, and the heavier gravels in the bottom portion are put into sacks for hand picking off-site. Any gems seen during this process are placed into a metal bowl.

During our visit a rather small amount of gems were extracted from the jig, but they did include one bright pink-red spinel pebble (Figure 9). The remainder consisted of low-quality ruby, sapphire and spinel with some small pieces of pale brown topaz, smoky quartz and black tourmaline. The



Figure 7. A water cannon is used to wash gem-bearing material into a small collecting area, or sump, from where it is pumped out of the pit to a processing plant. Photo by B. M. Laurs.



Figure 8. At the washing plant, rocks larger than 2.5 cm are screened off, and the remaining material is washed into a jig. Photo by B. M. Laurs.

sapphires were mostly colourless to yellow or blue, while the spinel was pink-to-red, purple-grey, yellow, blue or black. The corundum and spinel produced from this mine are only rarely of gem quality, and they typically occur as waterworn broken pieces or less commonly as somewhat rounded tabular pseudo-hexagonal crystals. By contrast, the topaz is mostly transparent and shows extremely variable degrees of rounding from alluvial transport. Some of the smoky quartz crystals recovered from the operation have sharp crystal faces and attain relatively large sizes (20+ cm long), suggesting that their original source rock was not far away.

The mine owner indicated that several weeks or months may pass with only low-quality production, although one good stone can cover expenses for the entire year. During the 2014 mining season, the best gem he recovered was a 'light' ruby pebble weighing 16 g. He mentioned that after a few months of the mining season have passed, it is common to see local families (especially children) picking tiny grains of gem material from the tailings of the mine. These are



Figure 9. A small assortment of gem material results from cleaning out a portion of the riffles at the end of each day. The inset shows a brightly coloured spinel pebble that is ~1.5 cm long. Photos by B. M. Laurs.

cut into melee-sized stones or (mostly) used in gem 'paintings' that are commonly seen in Mogok and in tourist centres throughout Myanmar.

Brendan M. Laurs

Reference

Themelis T., 2008. *Gems & Mines of Mogok*. Self-published, 352 pp.

Pink Play-of-Colour Opal from Idaho

It is well known that opal may be treated by various methods to change its body colour. This is particularly true for porous hydrophane opal, such as the material from Wollo, Ethiopia. Dyeing of this material has produced a variety of hues, especially purple (Renfro and McClure, 2011). Dyed pink

play-of-colour opal has also been documented in recent years (e.g. Leelawatanasuk and Susawee, 2013). It was therefore refreshing to see play-of-colour opal showing natural pink body colour at the 2015 Tucson gem shows. Mined in Spencer, eastern Idaho, USA, small amounts of this material



Figure 10: This 14 carat gold pendant features a 2.41 ct pink play-of-colour opal from Spencer, Idaho. It is set together with a diamond and a pink Tanzanian spinel. Photo by Ed Barker.

have been produced for years, but it is not well known in the international opal trade.

A pendant containing a 2.41 ct pink opal from Spencer was shown to this author by Ed Barker (Artistry in Gold, Yountville, California, USA).

He purchased the rough material in 1984, and then cut and mounted the cabochon himself. The cabochon showed a noticeable orangy pink body colour along with flashes of green, blue and violet play-of-colour (Figure 10). Barker indicated that such material continues to be produced by Spencer Opal Mines LLC. A visit to their booth in Tucson revealed both rough and cut pink opal showing weak-to-strong play-of-colour. Most of the material was opaque, but some was translucent. According to co-owner Claudia Couture, since early 2012 Spencer Opal Mines has focused on more actively recovering the pink opal, and they have polished several thousand pieces as doublets or solid cabochons ranging from 2–3 ct up to 20+ ct. Couture indicated that the pink opal is only known from certain areas of the mine. Not surprisingly, opal showing the pink body colour is much less common than white opal at this deposit.

Brendan M. Laurs

References

- Leelawatanasuk T. and Susawee N., 2013. Lab update—An unusual pink opal. Gem and Jewelry Institute of Thailand, Bangkok, 19 August, www.git.or.th/2014/eng/testing_center_en/lab_notes_en/glab_en/2013/dyed_pink_opal.pdf.
- Renfro N. and McClure S.F., 2011. Dyed purple hydrophane opal. *Gems & Gemology*, **47**(4), 260–270, <http://dx.doi.org/10.5741/gems.47.4.260>.

Dumortierite Inclusions in Quartz from Brazil

At the 2015 Tucson gem shows, Luciana Barbosa (Gemological Center, Minas Gerais, Brazil) had an impressive display of various gems with inclusions, including a new find of quartz with dumortierite needles from Brazil. She indicated that the material is from western Bahia State, near the Vaca Morta quarry. She first encountered this quartz in late 2013, and the rough mostly contained very fine hair-like inclusions or blue clouds. Approximately 100 kg of quartz was produced, but most did not have the inclusions. By mid-2014, high demand combined with limited supply resulted in skyrocketing prices for this material. In late 2014 to early 2015, additional production came on the market as slightly larger

pieces with inclusions consisting of thicker bluish grey needles. A small number of pieces containing deep blue inclusions were also found at that time. The blue and bluish grey inclusions were subsequently identified by Raman analysis as dumortierite by John Koivula and Nathan Renfro at the Gemological Institute of America in Carlsbad, California. To their knowledge, this is the first time that well-formed, eye-visible crystals of dumortierite have been found in rock crystal quartz (N. Renfro, pers. comm., 2015).

Barbosa reported obtaining a total of ~20 kg of better-quality rough, but only about 20–30% contained desirable inclusions. The dumortierite is usually concentrated on one side of the quartz

Figure 11: A discovery of quartz with dumortierite inclusions recently occurred in Brazil's Bahia State. Shown together with an included quartz crystal are an 11.40 ct cabochon containing bluish grey sprays of dumortierite and a 34.50 ct cabochon with a 'carpet' of deep blue dumortierite inclusions. Courtesy of James Zigras; photo by Jeff Scovil

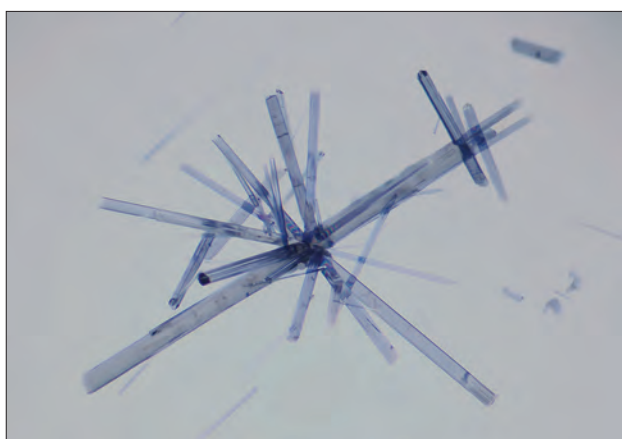


Figure 12: These dumortierite inclusions in quartz form a conspicuous star-shaped cluster. Photomicrograph by Nathan Renfro, © GIA; image width 7.8 mm.

crystal. Therefore, the cabochons are commonly cut so that the adjacent quartz face (on the bottom of the cabochon) is unpolished to preserve as many of the inclusions as possible. The inclusions typically form 'carpets' or radiating clusters in the quartz (Figures 11 and 12); phantom-like clouds of dumortierite are also encountered. Barbosa has cut approximately 200 cabochons of this quartz so far, but most of her stock consists of polished crystals containing the inclusions. She indicated that much of the rough material has been purchased by Chinese buyers. Small quantities of rough continue to be produced from several diggings in western Bahia State.

Brendan M. Laurs

Quartz Sphere with Large Well-formed Inclusion

'Crystal balls' or spheres polished from rock crystal quartz are typically cut from material that is very pure in appearance (i.e. free of distracting inclusions). However, it has also become common for quartz spheres to showcase visually pleasing inclusion features. A quick internet search will reveal numerous examples containing a variety of inclusions such as rutile, tourmaline and reflective partially healed fractures, among many others.

At the 2015 Tucson gem shows, Steve Ulatowski (New Era Gems, Grass Valley, California) had an 8.5-cm-diameter quartz sphere containing a remarkably large and well-formed inclusion

(Figure 13). The sphere was brought to Tucson by William M. dos Reis (WR Cut Stone Comércio Ltda., Rio de Janeiro, Brazil), who stated that the rough material was probably mined from Brumado, Bahia, Brazil. The magnesite deposits of Brumado are famous for producing a variety of collectible minerals, including transparent quartz crystals and well-formed rhombohedrons of magnesite and dolomite (e.g. Barbosa et al., 2000). Consideration of the reported locality, rhombohedral morphology and yellow colour of the inclusion suggest that it is dolomite, calcite, or a mineral of the magnesite-siderite series.

Brendan M. Laurs

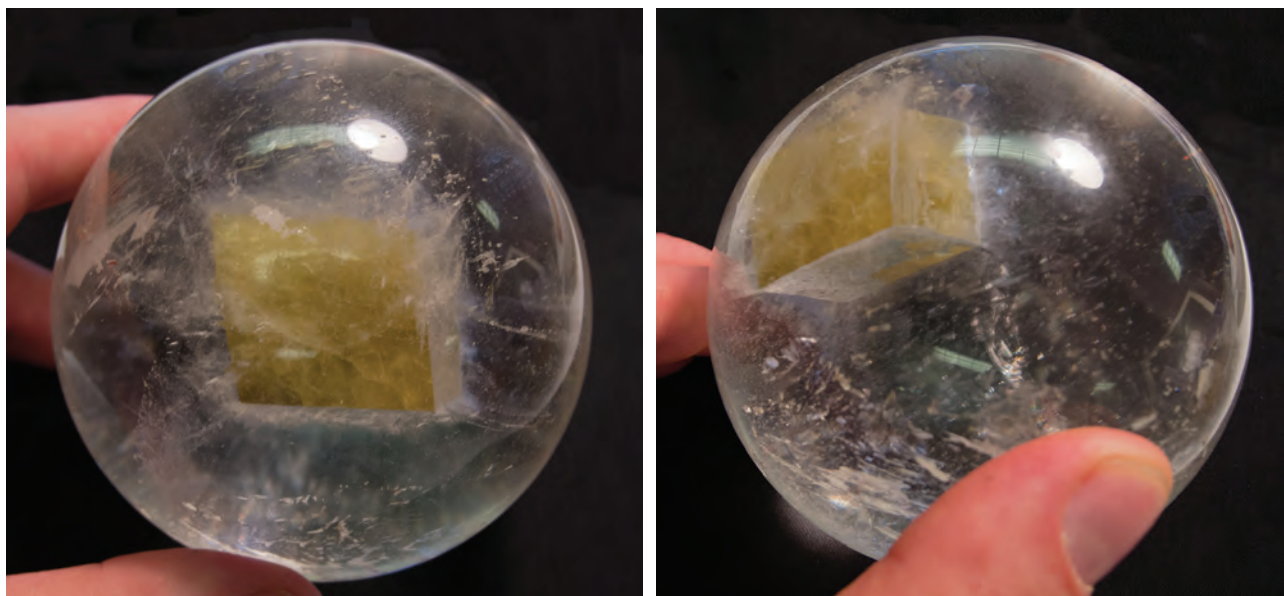


Figure 13: These two views of an 8.5-cm-diameter quartz sphere, reportedly from Brumado, Brazil, show a large well-formed inclusion that has the appearance of a carbonate mineral. Courtesy of James Zigras; photos by B. M. Laurs.

Reference

Barbosa C.P., Falster A.U., Simmons W.B., Webber K.L., Nizamoff J. and Gaines R.V., 2000. Minerals of

the Brumado magnesite deposits, Serra das Éguas, Bahia, Brazil. *Rocks & Minerals*, **75**(1), 32–39, <http://dx.doi.org/10.1080/00357520009602572>.

‘Zawadi’ Sapphires

During the 2015 Tucson gem shows, Jeffery Bergman (Primagem, Bangkok, Thailand) had some attractive sapphires from a relatively new find in East Africa (most likely eastern Kenya). They were notable for their ‘golden’ sheen, and in some cases for their intricate network of dark linear patterns (see Figure 14 and the cover of this issue). He was selling them as ‘Zawadi’ sapphires (after the Swahili word meaning ‘gift from the earth’). He indicated that most of the production occurred in early 2013, and his Bangkok-based supplier of the material has reportedly obtained over 20 tonnes of rough.

According to Bergman, about 20,000 carats have been cut so far. Since most of the material is opaque, the gems are typically cut with wide tables (commonly covered by checkerboard facets) and are oriented to best display the sheen. Faceted stones may weigh up to 100+ ct, although most are in the range of 0.50–10 ct with an emphasis on calibrated sizes for volume manufacturers. Numerous cabochons have also been cut in a variety of shapes. The material is reportedly not treated in any way.



Figure 14: The Zawadi sapphires shown here range from 5 to 20 ct. Most exhibit wide tables with checkerboard cuts to emphasize the ‘golden’ sheen. Photo by Jeffery Bergman.

The sheen displayed by Zawadi sapphire is somewhat reminiscent of black star sapphire from Thailand. However, the Zawadi material only occasionally shows asterism, and it derives its attractive appearance from the sheen combined with the dark patterns caused by fractures and polysynthetic twin planes in the corundum.

Brendan M. Laurs

Tourmaline from the Havey Quarry, Maine, USA

During the past few years, activities at the Havey quarry (Poland, Androscoggin County, Maine, USA) by mine owner Jeffrey W. Morrison have yielded significant quantities of high-quality tourmaline crystals and gem rough. Examples of rough and cut stones—mostly bluish green—were seen most recently by this author at the 2015 Tucson gem shows, where the material was offered by Larry Woods (Jewels from the Woods, Blanco, Texas, USA) and displayed by the Smithsonian Institution, as well as by Morrison himself.

The Havey quarry explores a portion of the Berry-Havey pegmatite, which belongs to the Oxford pegmatite field in southern Maine. According to Morrison, the pegmatite first produced gem tourmaline in 1910–1912. It lay mostly idle until 1976, when Terry Szenics produced small amounts of green and ‘cinnamon’-coloured tourmaline. It then lay idle again until 2007, when Morrison acquired the property. After completing the necessary preparations for organized mining of the deposit, Morrison found his first tourmaline pocket in late 2009, although it contained mostly smoky quartz. His first significant tourmaline discovery occurred in 2011, and in 2012 he found additional small cavities containing gem tourmaline.

However, 2013 was much more productive, with the discovery of a series of pockets. Detailed accounts of these finds are available at <https://crossmainetourmaline.wordpress.com>,

Figure 15: One of the most recent tourmaline finds (October 2014) at the Havey quarry was the ‘Fireworks’ pocket. A flashlight illuminates the inside of the excavated cavity. The buckets contain some of the pocket contents. Photo by Jeffrey Morrison.



and several videos of mining and sorting the tourmaline can be viewed at www.crossjewelers.com/video. These finds were important for producing attractive bluish green crystals that contained excellent gem rough for faceting. During the most recent mining season, in 2014, Morrison found several small-to-medium pockets, as well as one significant pocket (Figure 15) with green tourmaline crystals, some showing a ‘navy’ blue termination.



Figure 16: Tourmaline pockets at the Havey quarry are commonly filled with soft white clay. This 2013 discovery shows a tourmaline crystal that had been broken by natural forces into three pieces. Although the top two sections of this crystal were of fine gem quality (see Figure 17), the remainder of the rough material from this pocket was suitable for cutting only small stones. Photo by Jeffrey Morrison.

Morrison mines the Havey quarry in an open pit that measures approximately 35 × 35 m and 10 m deep. He typically drills holes that are 2½ inches (6.5 cm) in diameter and 12–14 feet (3.7–4.3 m) long that are loaded with explosives. (Shorter and narrower holes are drilled in potentially pocket-bearing zones.) The blasted material is removed from the pit with an excavator and dump truck. The gem pockets are carefully dug by hand. The tourmaline is commonly enclosed in soft white clay (Figure 16) that is washed away with a hose. Most of the tourmaline pockets are football sized or smaller, with varying quantities of gem rough (from a few grams to hundreds of grams). The largest tourmaline pocket was 1.5 × 1.5 m and consisted of two connected chambers. In addition to tourmaline, the pockets may contain smoky

quartz, lepidolite, feldspar, apatite, etched beryl (morganite and goshenite) and several accessory minerals.

Within each pocket the colour of the tourmaline is very consistent. Morrison reported that of all of the Havey tourmaline he has mined, approximately 60% is bluish green (e.g. Figure 17), 10–20% is ‘watermelon’ (pink/green) and the remainder is pure green. He has also rarely encountered other colours, such as pink, ‘fuchsia’, grey-blue, etc. Most of the tourmaline cut to date has been faceted by Sean Sweeny (Bar Harbor, Maine), and the majority of the gemstones were then sold to Cross Jewelers (Portland, Maine). Cross has produced an extensive line of jewellery featuring the ‘minty green teal’ colour of tourmaline that they call ‘SparHawk’. Morrison retains the largest gem rough for custom cutting by accomplished faceters such as Sean Sweeny, Larry Woods and Dalan Hargrave (GemStarz Jewelry, Spring Branch, Texas), and stones weighing up to 38 ct have been faceted.

Tourmaline from the Berry-Havey pegmatite was recently studied in detail by Roda-Robles et al. (2015). Samples from the gem pockets mined by Morrison proved to be mainly elbaite with some zones corresponding to rossmanite and darrellhenryite. The latter mineral is a relatively new species of Li-bearing tourmaline that belongs to the oxy-tourmaline series (Novák et al., 2013). Although Roda-Robles et al. (2015) have documented darrellhenryite for the first time in gem quality from the Havey quarry, it is possible that other occurrences exist worldwide but have been misidentified as elbaite.

The Havey quarry is on private property and is closed to the public. However, it will be visited by participants of the 2015 Maine Pegmatite Workshop, which will take place 29 May–6 June in Poland, Maine (<http://pegworkshop.com>). For more information about the Havey quarry, see



Figure 17: The Havey tourmaline on the right is the upper section of the crystal shown in Figure 16, and the 23.53 ct stone on the left (now in the Maine Mineral and Gem Museum) was cut from the centre section of this crystal by Sean Sweeney. The ~12.6 g crystal on the right was subsequently cut by Larry Woods into a 30.62 ct stone that is now in the collection of the Smithsonian Institution in Washington D.C., USA. Photo by Jeff Scovil.

Morrison’s blog at <http://haveymine.blogspot.com>, which also provides a list of significant gem pockets.

Brendan M. Laurus

References

- Novák M., Ertl A., Povondra P., Galiova M.V., Rossman G.R., Pristacz H., Prem M., Giester G., Gadas P. and Skoda R., 2013. Darrellhenryite, $\text{Na}(\text{LiAl}_2)\text{Al}_6(\text{BO}_3)_3\text{Si}_6\text{O}_{18}(\text{OH})_3\text{O}$, a new mineral from the tourmaline supergroup. *American Mineralogist*, **98**(10), 1886–1892, <http://dx.doi.org/10.2138/am.2013.4416>.
- Roda-Robles E., Simmons W., Pesquera A., Gil-Crespo P.P., Nizamoff J. and Torres-Ruiz J., 2015. Tourmaline as a petrogenetic monitor of the origin and evolution of the Berry-Havey pegmatite (Maine, USA). *American Mineralogist*, **100**(1), 95–109, <http://dx.doi.org/10.2138/am-2015-4829>.

Recent Production of Greenland Tugtupite

In 2014, mining activities by native Greenlandic prospectors yielded additional production of high-quality tugtupite, some of which was shown at the 2015 Tucson gem shows (e.g. Figure 18). The ma-

terial was produced by two companies, Ice Cold Gems Co. and Red Ice Gem Co., which were also the first to ethically market fair-trade ruby mined and polished by local Greenlanders in that country.

Figure 18: This photo shows some of the recently produced Greenland tugtupite seen at the 2015 Tucson shows. The five gem-quality rough pieces weigh 0.38–0.83 g, and the 1.22 ct marquise-cut gemstone was faceted by Jens Mikkel Fly (Nuuk, Greenland). The pendants were made by Mikael Møller (Nuuk) and feature 26 × 16 mm tugtupite cabochons that are set in silver with caribou antler, in the traditional design of the ulu (arctic knife). The rock specimen contains a gem-quality tugtupite veinlet 4 cm in width. Photo by Jeff Scovil.



Tugtupite ($\text{Na}_4\text{AlBeSi}_4\text{O}_{12}\text{Cl}$) is an unusual feldspathoid mineral known in gem quality only from the Ilímaussaq intrusive complex in southwest Greenland (Jensen and Petersen, 1982). The initial discoveries occurred between 1957 and 1965, at various sites within an area centred on Tugtup agtâkorfia, also known as Kvanefjeld, in the Narsaq region. The Ilímaussaq igneous complex is known for its extreme enrichment in rare elements, which resulted in the formation of more than 225 different minerals, some indigenous only to this locality (Petersen, 2001). The name *tugtupite* is derived from the Greenlandic Inuit word for reindeer or caribou (*tuktu*). The red and white colour of the rock in the field reminded the traditional hunters of tracking reindeer blood across the snow, considered an auspicious sign.

Tugtupite in Greenland occurs as vitreous, transparent, translucent and opaque masses that most commonly range from white to pink to 'crimson' red. It has a Mohs hardness of 6½, but highly included masses can give artificially low readings of 4 due to contamination by other minerals. Tugtupite is typically found associated with albite, analcime, beryllite, aegirine, neptunite and pyrochlore (Sørensen, 2006). Most tugtupite is microcrystalline and massive; very few well-developed crystals have been found.

Greenland tugtupite displays tenebrescence, also known as reversible photochromism, which is the ability of the mineral to change or intensify in colour when exposed to radiation of a particular wavelength. In darkness or under sustained low

light, such as the long arctic night, tugtupite loses its colour and fades to white. But with the bright sunlight of the arctic summer, tugtupite becomes red. Greenland tugtupite is also strongly fluorescent, especially the gem-quality material: it fluoresces bright 'crimson' red to short-wave UV radiation, and a weak 'salmon'-pink to long-wave UV. Even brief illumination of just several minutes with short-wave UV intensifies the tenebrescent red colour in tugtupite.

Gem tugtupite occurs within hydrothermal veins as disseminations, clots and veinlets, in seams measuring up to 4 cm thick and 1–2 m in length and depth (Secher and Johnsen, 2008). The principal surface exposure of the ore zone measures approximately 10 × 50 m, and has been excavated to a depth of up to 5 m. Some half-dozen smaller prospects are known from other locations elsewhere in the district. The tugtupite is gathered by village hunting parties employing simple hand mining methods, and also by small teams of trained prospectors (who are responsible for the recent production) using specialized tools and portable equipment.

The Tucson 2015 delivery of tugtupite was noteworthy for its relatively high transparency, which is unusual for the species. A select amount was suitable for faceting, and stones up to 1.22 ct were on display. Some translucent and semi-translucent material has also been produced, as well as the massive and microcrystalline opaque material traditionally sold as tugtupite. Several kilograms of rough material were included in the Tucson delivery, with about two dozen faceted

stones polished so far. Clean faceted gems are great rarities for tugtupite, yet the important news from Tucson 2015 is that Greenlandic cutters are now producing fine gemstones and cabochons that weigh some 1–4 ct.

William Robtert (william.Robtert@cox.net)
Phoenix, Arizona, USA

References

- Jensen A. and Petersen O.V., 1982. Tugtupite: A gemstone from Greenland. *Gems & Gemology*, **18**(2), 90–94, <http://dx.doi.org/10.5741/gems.18.2.90>.
- Petersen O.V., 2001. List of all minerals identified in the Ilímaussaq alkaline complex, South

Greenland. In H. Sørensen, Ed., The Ilímaussaq Alkaline Complex, South Greenland: Status of Mineralogical Research with New Results. *Geology of Greenland Survey Bulletin* 190, 25–30.

Secher K. and Johnsen O., 2008, *Minerals in Greenland*. Geology and Ore No. 12, Geological Survey of Denmark and Greenland, Copenhagen, Denmark, 12 pp., www.geus.dk/minex/go12.pdf.

Sørensen H., 2006, Ilímaussaq alkaline complex, south Greenland—An overview of 200 years of research and an outlook. Contribution to the Mineralogy of Ilímaussaq No. 130, *Meddelelser om Grønland Geoscience*, **45**, The Commission for Scientific Research in Greenland, Copenhagen, Denmark, 70 pp.

Large Orange Zircon from Myanmar

Recently, a 21.87 ct transparent brownish-reddish orange cushion mixed-cut zircon (Figure 19) was submitted to American Gemological Laboratories for an identification report by Hussain Rezayee (Rare Gems and Minerals, Los Angeles, California, USA). The RI was over the limit of the refractometer (>1.81). The gem readily displayed a uniaxial optic figure in the polariscope, and it fluoresced weak orange to both long- and short-wave UV radiation. Microscopic examination revealed only a few fine needles and lines of reflective pinpoints. As is typical of zircon (e.g. O'Donoghue, 2006), the stone displayed numerous lines in the spectroscope: 432, 484, 521, 537, 562, 589, 660, 662 and 691 nm. Mid-infrared spectroscopy also was consistent with zircon.

Rezayee obtained this stone in July 2014 while visiting Myanmar, and according to his supplier it had not been heated. It is well known in the gemmological community that brown zircon may be heat treated to colourless or blue. This occurs in a reducing environment at approximately 1,000–1,400°C. When, on occasion, off-colours are created via this process, the stones are commonly reheated to approximately 900°C in an oxidizing environment, resulting in colourless, yellow, orange or red colours (see www.gemologyproject.com/wiki/index.php?title=Zircon and Nassau, 1994). To date, there is no definitive way to consistently distinguish between heated and unheated zircon. As a result, all colours of zircon



Figure 19: This 21.87 ct zircon from Myanmar shows both high transparency and a strong brownish-reddish orange colour. Photo by Bilal Mahmood.

other than brown and green may potentially be the result of a heating process.

Measuring 16.37 × 12.32 × 10.22 mm, this zircon is very rare for its size, colour and clarity. The dispersion of zircon is close to that of diamond which, combined with the intense colour of the stone, added to its beauty.

Wendi M. Mayerson (wmayerson@aglgemlab.com)
American Gemological Laboratories
New York, New York

References

- Nassau K., 1994. *Gemstone Enhancement—History, Science and State of the Art*, 2nd edn. Butterworth-Heinemann, Oxford, 200–202.
- O'Donoghue M., Ed., 2006. *Gems*, 6th edn. Butterworth-Heinemann, Oxford, 284–288.

SYNTHETICS AND SIMULANTS

A Convincing Glass Imitation of Emerald



Figure 20: The green gem (12 × 10 mm) in this platinum and diamond ring strongly resembles emerald, but proved to consist of lead glass. Photo by B. Williams.



Figure 21: Microscopic examination of the green glass revealed straight and curved planar arrangements of gas bubbles. Photomicrograph by B. Williams; magnified 20×.

Recently submitted to Stone Group Laboratories for identification by Sushil Goyal (Liberty Gems, New York, New York) was a platinum and diamond ballerina-style ring featuring a large green gem (Figure 20). Its general appearance was typical of lighter-coloured Colombian emeralds, and it contained a few eye-visible inclusions. Closer inspection with a loupe revealed what looked like oiled fissures containing numerous minute, rounded gas bubbles (Figure 21).

In some cases, it is more interesting to run laboratory tests in the reverse order of what is typically done, especially when anticipating a certain result based on visual observations. In this case, due to 'something missing' from the gem's colour and its lack of reaction with a Chelsea colour filter, the next test performed was energy-dispersive X-ray fluorescence (EDXRF) spectroscopy to determine the gem's chemical composition and possible chromophores. This showed the unexpected presence of Pb, and since there was no significant Cr or V, further tests were in order. Raman analysis readily

identified the gem as glass, but the nature of the strange veins containing tiny trapped gas bubbles remained a mystery. Fourier-transform infrared (FTIR) spectroscopy was performed next, but no polymers were detected. The RI was recorded as 1.52, and we concluded that this gem consisted of a solid piece of green lead glass.

Viewed with the microscope, an experienced eye might sense that there was something unusual about the 'emerald', but the veins of fine bubbles masked many of the properties that would normally indicate glass. The veins did not conform to a typical emerald fissure pattern, yet were not obviously 'wrong' in their appearance. Surface scratches and abrasions were more typical of glass than emerald. When observed with the Chelsea colour filter, the gem remained green despite having the general appearance of a Colombian emerald. Also, the broad table and low crown are not often seen with emerald, nor are they typical of imitation stones. The diamond mounting certainly added credibility to the centre stone.

The process of creating the inclusion features in this glass remains a mystery. Theoretically, cracks could have been induced and then filled with a different high-lead glass. Another possibility is that when the green lead glass was still molten, a wire could have been inserted, twisted and removed, leaving the material laced with gas bubbles.

This was the most recent item seen in a series of unusual and convincing glass imitations that have come through our laboratory in the past few years. These clever imitations are nothing like the more obvious

examples commonly seen in gemmological coursework. Glass imitations of tiger's-eye, jadeite, peridot, tourmaline, aquamarine and now emerald have been encountered by these authors, and the tourmaline and aquamarine look-alikes initially fooled even experienced eyes looking for tell-tale signs. Outside of lab testing, the polariscope or refractometer will yield the best initial clues that a material is a glass imitation.

Bear and Cara Williams (info@stonegrouplabs.com)

*Stone Group Laboratories
Jefferson City, Missouri, USA*

New Large Black Synthetic Moissanite as a Black Diamond Imitation

Two black, opaque, flat round gems were received at GGTL-Laboratories (Geneva, Switzerland) in October 2014 for certification as black diamonds (Figure 22). The samples weighed approximately 29 and 34 ct, and measured 28.0–28.3 × 3.7 mm and 29.2–29.5 × 4.0 mm, respectively.

Microscopic observation piqued our attention because the gems did not show features consistent with natural black diamond (i.e. an irregular distribution of brown-to-black inclusions of various shapes, dense clouds, etc.), heat-treated black diamond (minute graphite inclusions), or 'classic' black synthetic moissanite (very dark green-to-blue or brown body colour, etc.). Strong fibre-optic illumination revealed a dark grey body colour with an olive tinge (Figure 23), and reflected light showed a very fine-grained homogeneous texture (Figure 24-left). The microtexture was very similar to that of a black ceramic material (boron carbide) imitating black diamond that was described by Choudhary (2013; see Figure 24-right), but was different from the mosaic pattern in black synthetic moissanite described by Moe et al. (2013). Minute interstitial spaces in our samples measured 5–150 µm (mostly ~50 µm).

The two gems were inert to long- and short-wave UV radiation, but showed faint orange fluorescence when exposed to the intense 300–410 nm excitation of the GGTL DFI luminescence microscopy system. Their RI was over the limit



Figure 22: These large black diamond imitations (left, 29 ct and right, 34 ct) consist of very fine-grained synthetic moissanite. Photo by C. Caplan.

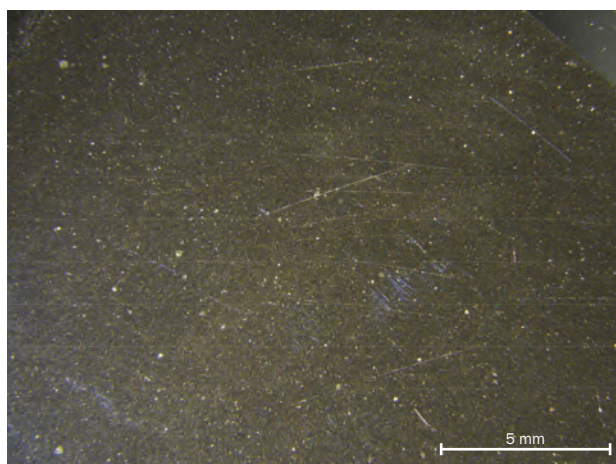


Figure 23: Viewed with the microscope and 250 W fibre-optic illumination, the synthetic moissanite samples showed a dark grey body colour with an olive tinge. Photomicrograph by F. Notari.

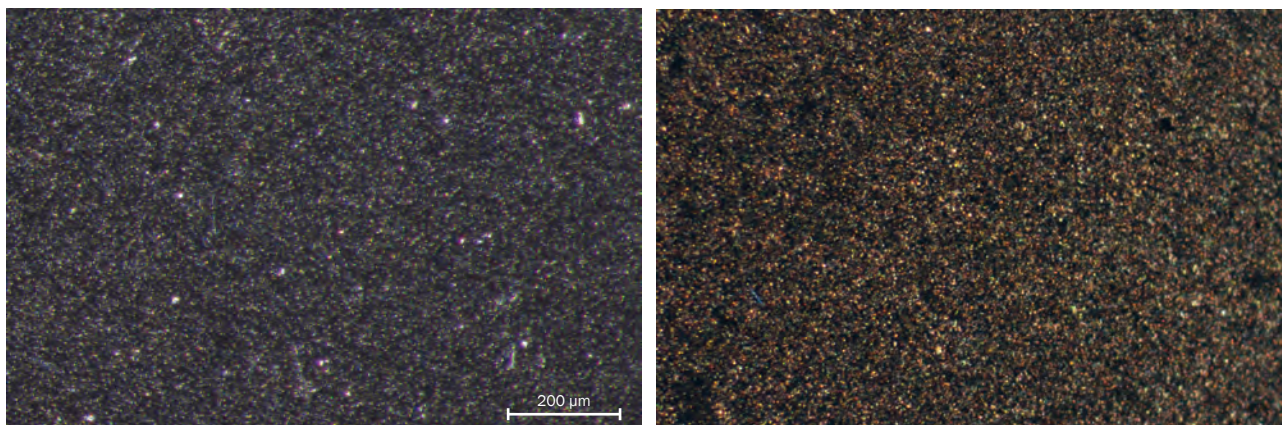


Figure 24: On the left, the 34 ct synthetic moissanite shows a very fine-grained homogeneous texture with minute reflecting particles. A similar texture is shown in the image on the right of a boron carbide black diamond imitation. Photomicrograph on the left by F. Notari, and on the right by Gagan Choudhary (magnified 48×; reprinted with permission from Choudhary, 2013).

of our refractometer (>1.81), and they tested positive for diamond with a thermal conductivity tester. The hydrostatic SG of the two samples was 3.16, and a hardness test showed >9 on the Mohs scale. (Hardness was tested with the client's permission on the girdle at 160× magnification.)

Specular reflectance FTIR spectra were recorded for both gems using a Thermo Nicolet Nexus spectrometer with a DTGS (deuterated triglycine sulphate) detector, by accumulating 20 scans at room temperature at a resolution of 4 cm^{-1} . The spectra showed features corresponding to a reference sample of green synthetic moissanite (Figure 25).

EDXRF chemical analysis was also performed on both gems, using a Thermo Noran QuanX-EC

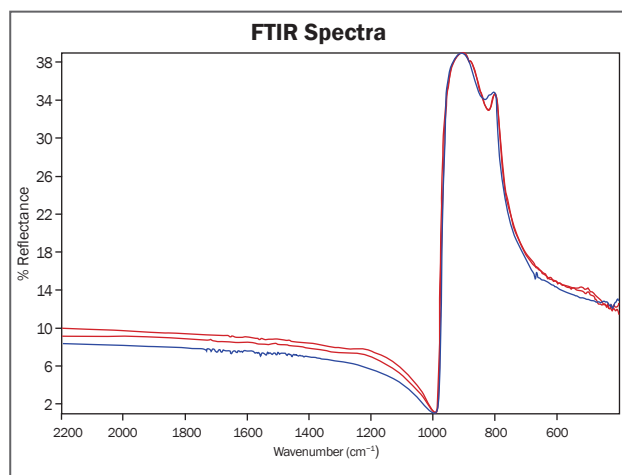
instrument with all available filters (count time of 300 s and beam diameter of 3.5 mm). The analyses showed major amounts of Si and traces of Fe, Cr and Ti. This is consistent with synthetic moissanite, which has a chemical formula of SiC (carbon cannot be detected by this instrument). The Fe, Cr and Ti are likely contained in the impurities that give the black appearance to this material.

Our analyses indicate that these two gems are opaque black synthetic moissanite with a very fine-grained structure. The SG of 3.16 is helpful for its identification (compared to diamond's 3.54 and boron carbide's 2.40). Monocrystalline synthetic moissanite has a typical SG of 3.22, and the lower value obtained for these samples is probably due to their being some type of sintered product rather than a monocrystalline material. Such sintered dark grey synthetic moissanite is available for industrial applications (e.g. Sadow and Agarwal, 2004). Conclusive identification of this material as synthetic moissanite was shown by specular reflectance FTIR spectroscopy and EDXRF analysis.

This type of black synthetic moissanite is now clearly available in the market as large cut gems. In October 2014 we bought a sample weighing 210.65 ct (diameter ~ 41 mm) for comparison, and our observations and analyses of this gem were consistent with those described here.

*Candice Caplan (candice.caplan@ggtl-lab.org),
Thomas Hainschwang and Franck Notari
GGTL-Laboratories, Geneva, Switzerland, and
Balzers, Liechtenstein*

Figure 25: The specular reflectance FTIR spectra of the two gems (red lines) provide a close match to the reference sample of green synthetic moissanite (blue line).



References

- Choudhary G., 2013. Gem News International: Boron carbide: A new imitation of black diamond. *Gems & Gemology*, **49**(3), 180–181.
- Moe K.S., Johnson P. and Lu R., 2013. Lab Notes:

- Large synthetic moissanite with silicon carbide polytypes. *Gems & Gemology*, **49**(4), 255–256.
- Saddow S.E. and Agarwal A., Eds., 2004. *Advances in Silicon Carbide Processing and Applications*. Artech House, Norwood, Massachusetts, USA, 228 pages.

Peridot-Polymer Composite



Figure 26: This 3.25 ct bead turned out to be a composite, made up of pieces of peridot embedded in a polymer matrix. Photo by G. Choudhary.

Composites assembled from opaque-to-translucent gem materials such as turquoise, chalcedony, opal and chrysocolla have become popular during the past few years, as evidenced by the number of samples received for identification at the Gem Testing Laboratory in Jaipur, India. We recently examined a translucent yellowish green, round faceted bead (Figure 26) that turned out to be a composite gem featuring peridot.

The bead weighed 3.25 ct and measured 9.09 × 8.91 × 5.36 mm. At first glance, it appeared to be peridot due to its typical colour. However, microscopic observation revealed numerous gas bubbles, which made us think otherwise. Further examination showed that the bead was actually composed of several pieces of yellowish green material that were embedded in a pale yellow matrix containing gas bubbles (Figure 27). This was further confirmed by the difference in surface lustre of the two materials when viewed with reflected light. The individual pieces were transparent with curved and smooth surfaces; although a few of them contained fractures, most were free of inclusions. Looking closely through



Figure 27: The bead in Figure 26 consisted of several pieces of yellowish green peridot embedded in a pale yellow polymer matrix. Note the presence of gas bubbles confined to the interstitial polymer areas. Photomicrograph by G. Choudhary; magnified 24×.

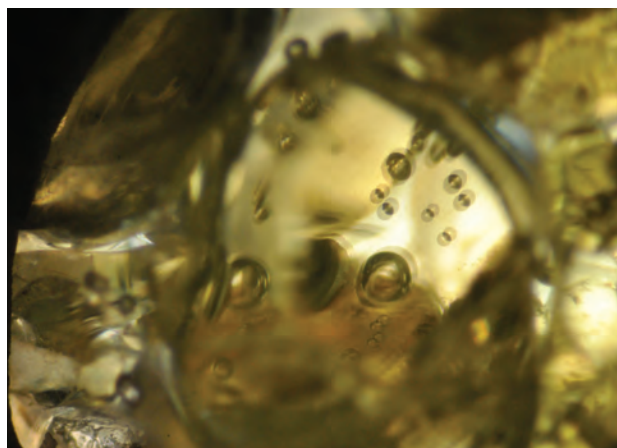


Figure 28: When viewed through the individual pieces of peridot, doubling of gas bubbles within the polymer matrix was visible. Photomicrograph by G. Choudhary; magnified 48×.

the individual pieces, we observed doubling of the gas bubbles within the polymer matrix (Figure 28).

Although it was obvious that the bead was a composite, its major component had yet to be

identified. A spot RI of ~1.67 was obtained with a distinct birefringence blink, as expected for the doubling mentioned above. When exposed to long- and short-wave UV radiation, the bead remained largely inert, except for a weak whitish glow overall. The desk-model spectroscope revealed three bands in the blue-green region at ~450, 470 and 490 nm, and these also were recorded with ultraviolet-visible-near infrared spectroscopy. These properties suggested that

the individual yellowish green pieces were peridot. Raman spectroscopy confirmed they were peridot and that the matrix was a polymer.

The identification of this bead as a composite was straightforward, and determining the identity of its components was relatively simple using basic gemmological tools. The use of peridot for such a composite is surprising.

*Gagan Choudhary (gagan@jepcindia.com)
Gem Testing Laboratory, Jaipur, India*

Dyed Quartzite as an Imitation of Bicoloured Tourmaline

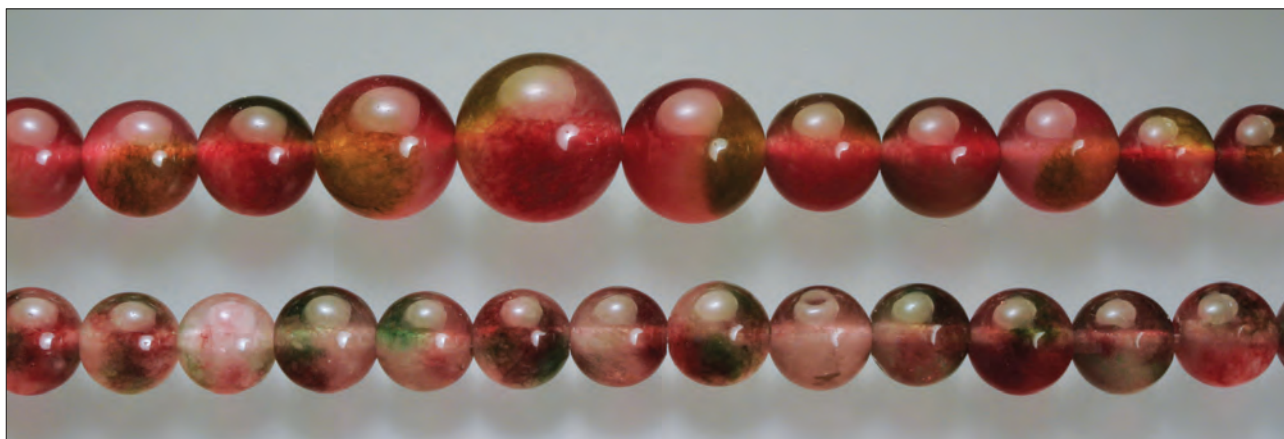


Figure 29: These bead necklaces initially appear to consist of bicoloured tourmaline, but they proved to be dyed quartzite. The largest bead is 14 mm in diameter. Photo by J. Hyršl.

Bicoloured 'watermelon' tourmaline is a popular gem material, but it is becoming rarer and more expensive. Two necklaces recently studied by the author consisted of a clever imitation of bicoloured tourmaline (Figures 29 and 30). They very probably originated from China (as the owner bought them from a Chinese dealer), and they measured 43 and 46 cm long with spherical beads of 6–14 mm in diameter. All of the beads in one necklace were bicoloured, with red prevailing over green. The other necklace contained tricoloured beads, with red, green and colourless portions. At first glance both necklaces looked like typical tourmaline, but a closer look showed that the coloration was concentrated along fractures. The RI measured by the distant vision method was 1.54, indicating that the granular quartz variety, quartzite, was used as the starting material for this imitation. Viewed under both long- and short-wave UV radiation, the red part on both necklaces fluoresced red-

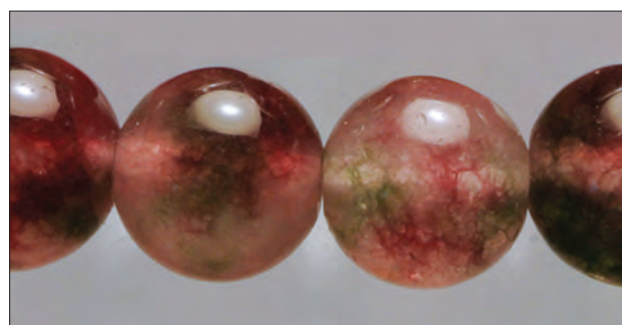


Figure 30: The dyed quartzite beads (here, up to 7 mm in diameter) show obvious colour concentrations along fractures. Photo by J. Hyršl.

orange and yellow, while the other colour(s) appeared inert. The dichroscope is also helpful for revealing such imitations, since tourmaline is strongly dichroic but dyed quartzite shows no pleochroism.

*Jaroslav Hyršl (hyrsl@hotmail.com)
Prague, Czech Republic*

FOR THE ADVANCEMENT OF
GEMMOLOGICAL SCIENCE

We are proud to announce the call for applications for the second annual Dr. Eduard Gübelin Research Scholarship, a grant supporting a scientific research project in the field of gemmology in the broadest sense.

The annual value is USD 30,000.

Submission deadline:

June 30th, 2015.

For guidelines, application forms and further information please see:

www.gubelingemlab.com/scholarship/



DR. EDUARD GÜBELIN
ASSOCIATION

FOR RESEARCH & IDENTIFICATION
OF PRECIOUS STONES

The Potential of a Portable EDXRF Spectrometer for Gemmology

Franz A. Herzog

Energy-dispersive X-ray fluorescence (EDXRF) spectroscopy is an important and well-established technique for the non-destructive chemical analysis of gem materials. The suitability of a portable EDXRF instrument for gemmological use was examined with a Niton XL3t GOLDD+ Analyzer manufactured by Thermo Scientific. Analysis of a variety of gem samples (natural, treated and synthetic) yielded qualitative data in the element range from Na to U that were comparable with results obtained from typical bench-top EDXRF instruments. The spectra measured by the portable unit showed well-resolved peaks, and gemmologically important intensity ratios of various elements were easily obtained. Using different collimators and measuring times, loose as well as mounted gems could be measured qualitatively. Although quantitative chemical data were not obtainable in this study, such results should be feasible using a calibration procedure that is optimized for gem analysis. This portable instrument, in conjunction with the use of an He purge unit for a better signal-to-noise (S/N) ratio when analysing light elements, is deemed very useful for smaller laboratories, as well as for larger laboratories offering off-site testing.

The Journal of Gemmology, 34(5), 2015, pp. 404–418, <http://dx.doi.org/10.15506/JoG.2015.34.5.404>
© 2015 The Gemmological Association of Great Britain

Introduction

Gemmological laboratories are routinely tasked with establishing the identity of gem samples as well as their natural, treated or synthetic origin. In some cases, the determination of a stone's geographical origin is also requested by the client. Much can be determined by a well-trained gemmologist using standard gemmological instruments, but in many cases it is necessary to perform additional non-destructive analyses. One technique commonly

used in gem labs is chemical analysis by EDXRF spectroscopy. The EDXRF spectra provide a quick display of most of the chemical components that may be present, including major (typically >1 wt.%), minor (0.1–1 wt.%) and trace (<0.1 wt.%) elements. While major and minor elements are useful for defining the mineral species, trace elements may indicate whether a gem is natural or synthetic, as well as the presence of some treatments and in some cases a stone's geographical origin. Chemical data are considered *qualitative*

if they are non-quantifiable and simply indicate the presence of an element. In the case of EDXRF spectroscopy, the pattern of a certain element is visually detected through the presence of peaks seen in the X-ray fluorescence spectra. To be *quantitative*, the data must be calibrated against samples of known composition. In that case, the actual concentrations of elements/oxides found in the sample are reported numerically with an inferred accuracy. A limitation of EDXRF analysis is that light elements (atomic mass <11, or lighter than Na) cannot be detected.

Portable instruments for EDXRF spectroscopy have been geared toward a wide range of applications (e.g. Zurfluh et al., 2011; Shugar and Mass, 2012), including archaeology, art conservation, mining exploration, environmental studies and industrial applications (particularly cement and metals). To investigate whether such instrumentation is suitable for gemmology (e.g. Voynick, 2010), the author tested a portable device made by Thermo Scientific (Niton XL3t GOLDD+) on a variety of gem samples (e.g. Figure 1). Although other manufactures have marketed similar instruments (e.g. Bruker, Olympus, Oxford Instruments, Spectro, etc.), these were not tested in this study.

Materials and Methods

When a sample is analysed by an EDXRF instrument, an X-ray beam is used to excite a unique fluorescent X-ray energy spectrum from each element present in the gem. The simultaneous measurement of various elements in the stone yields a type of compositional 'fingerprint'. With an appropriate calibration procedure, the concentration of most elements can be quantified down to parts-per-million levels. More about EDXRF spectroscopy can be found in, for example, Lachance and Claisse (1995) and Jenkins (1999).

Instrumentation

For this study, a Niton XL3t GOLDD+ Analyzer together with an appropriate stand for the safe handling of gem samples was loaned by Thermo Scientific for two weeks. The instrument is shown in Figures 2 and 3, and some of its parameters are listed in Table I. The device offers four excitation



Figure 1: Some of the samples analysed in this study are shown here (clockwise, from top left): an 8.60 ct lapis lazuli slab from Afghanistan (sample 16), an ~100 ct jadeite slab from Myanmar (sample 9), a 20.85 ct zircon from Sri Lanka (sample 15); a 21.65 ct apatite from Madagascar (sample 17); a 3.97 ct Verneuil synthetic spinel (sample 6) and a 1.78 ct spinel from Vietnam (sample 5). The blue spinels were selected to assess testing for the Co chromophore (which is typically not present in detectable amounts using EDXRF), and the other samples were chosen to test for the detection of light (Na to Cl) or heavy (Th and U) elements. Photo by F. A. Herzog.



Figure 2: The portable EDXRF device (Niton XL3t GOLDD+ from Thermo Scientific) tested for this study is shown on the left, together with cables for its power and USB connections. On the right is the He purge unit that is used for light-element analysis. The image scale can be judged from the size of the AC power adapter (6 × 10 cm). Photo by F. A. Herzog.

Figure 3: The EDXRF unit is seen here mounted in a stand used for analysing small samples. The sample chamber (18 × 8 cm) is large enough to accommodate a variety of unmounted samples, but may be too small for bulky jewellery items; larger stands are available. Photo by H. A. Hänni.



ranges (Table II), each with a pre-assigned primary filter that is used to optimize the signal over the background noise in the corresponding energy range. Within each range, a fixed amount of energy excites specific ranges of elements. Due to the X-ray excitation, elements may undergo *K*-, *L*- or *M*-shell ionization, resulting in diagnostic *K*-, *L*- or *M*-lines in the EDXRF spectra.

X-ray devices must follow strict safety protocols, and only those that fulfil country-specific safety regulations can be sold. After

buying a Niton Analyzer, user training (including safety aspects) is provided. For small samples (like most gemstones), an appropriate safety-approved enclosure that shields the user from X-rays is mandatory (e.g. Figure 3). Different logins provide various levels of access to the instrument, and the X-rays can only be activated when ‘Analyze’ is selected and the trigger is pressed (in all other modes, the instrument cannot start operating). Used correctly, the Niton Analyzer is extremely safe.

Table I: Main features of the Niton XL3t GOLDD+ portable EDXRF instrument.

Size	<1.3 kg, 24.4 × 23.0 × 9.5 cm
X-ray tube	Ag anode, 6–50 kV, 0–200 μA
Collimator	8 mm (standard) or 3 mm (optional)
Measurement area	10 mm circle
Primary filters	See Table II
Detector	<ul style="list-style-type: none"> Geometrically optimized large-area drift detector (GOLDD) Si drift detector (SDD), operated at approximately –30 °C Resolution: <185 eV @ 60,000 cps
Connectivity	USB cable for PC connection
Power supply	Two rechargeable Li batteries (8 h each) and AC power adapter
Software	<ul style="list-style-type: none"> NDT (Niton Data Transfer) for data transfer between unit and PC NDTr for remote control of unit
Accessories	<ul style="list-style-type: none"> He purge unit, for improved signal/noise for light elements (see Figure 2) Various stands with interlock mechanism and shielding (e.g. Figure 3)

Table II: Excitation ranges available for the XL3t GOLDD+ device.^a

Range	Excitation	Element range	Typical energy range (keV)	Primary Filter	Measurement time (sec) ^b
Main	Maximal energy	K-lines: Ti to Mo L-lines: Ta to Bi	4.0–20.0	Light metal combination	120
Low	Mid-energy	K-lines: K to Cr L-lines: Ba to Nd M-lines: Ir to U	2.5–6.0	Cu	120
High	Maximal energy	Rh to Nd	20.0–44.0	Mo	90
Light	Minimal energy	Na (qualitative) to Cl	1.0–3.0	No filter	150

^a The current is self-adjusting for optimal 'dead' time, range 0–200 μ A.

^b These times are optimal for the 3 mm collimator, but also were used for the 8 mm collimator.

Analytical Considerations

Although this instrument can be employed in a variety of disciplines, in this study only the 'Mining Cu/Zn' menu was used (in the 'Soils & Minerals' section). The factory calibration for this mode uses a Fundamental Parameter calculation specifically designed for the identification of mineral elements, based on pure elements and mining reference standards.

To operate properly, the device should be 'system checked' at least weekly. This is performed by the user, with a specific menu item on the main display, after the unit has warmed up for at least three minutes. This procedure ensures the energy scale of the system is properly calibrated (i.e. that the $\text{Cu}(K\alpha)$ peak is correctly located at 8.041 keV).

For accurate measurements of gem materials, appropriate sample holders must be used. They should fulfil two conditions:

1. The gem must sit firmly against the Analyzer during the measurement.
2. The sample holder itself should not interfere with the EDXRF spectrum of the gem.

For most analyses, the sample holder consisted of a thin (0.1 mm) transparent polyethylene sheet (as used for overhead projectors) with a hole of 4 mm in diameter (Figure 4, left). For small stones of <5 mm in diameter, an acrylic sample holder was used in addition to the polyethylene sheet (Figure 4, right). The acrylic has only a minute influence on backscattering of the X-rays and its sulphur content can be neglected.

The Niton XL3t GOLDD+ Analyzer itself consists of several components densely packed into its casing, and hence some of these materials show up as peaks when performing a blank test—an analysis done without any sample, but with the sample holder installed—as they are

Figure 4: The sample holder used in this study is shown on the left. It consists of a square sheet of polyethylene with a 4-mm-diameter hole punched in the centre. Scotch tape is used to affix the sheet to the Analyzer. The sample holder on the right consists of an acrylic block with a 10-mm-diameter hole drilled halfway through it, and a smaller hole drilled through the remainder of the block to fit a central, moveable pin (plastic tube from a ballpoint pen) to which the sample is attached with Blu-Tack. This assemblage, which is useful for smaller stones, is then placed over the hole in the polyethylene sheet mentioned above. Photos by F. A. Herzog (left) and H. A. Hänni (right).

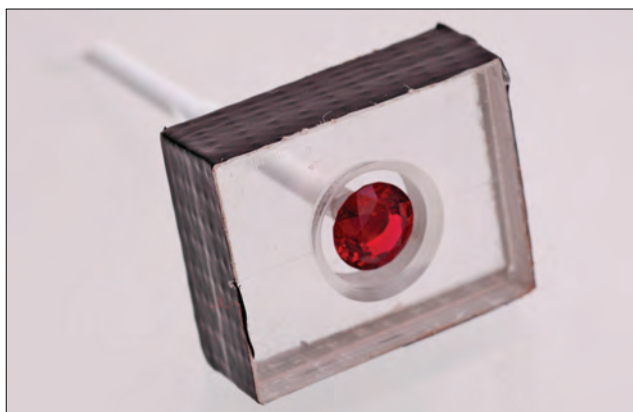
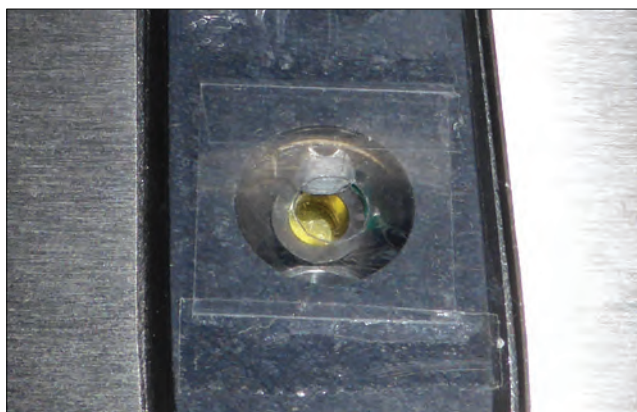


Table III: Elements showing up as system peaks and their excitation range.

Range*	System Peaks
Main	L-lines of W from primary excitation beam Ni from contribution of the system in the emerging beam Low Fe from unknown source L-lines of Au from detector enclosure, if backscattering occurs
Low	Low Cr from unknown source L-lines of Sb
High	Sn from solder in detector Mo from filter Ag from tube
Light	L-lines of Ag from tube

* See Table II for range descriptions.

part of the system's chemistry. These *system peaks* (see Table III) should not be mistaken for peaks from the sample. The specific elements appearing as system peaks depend on the energy range that is selected by the excitation energy and the primary filter (Table II). The Ni peak is most significant, as its signal is quite strong and it occurs in an area of high interest for many gem materials—in the vicinity of Fe. Nevertheless, such system peaks are taken into account in the quantitative analysis by an appropriate calibration, and their contributions

are subtracted from the chemical data. For qualitative analysis, the system peaks are part of the background spectra (shown as a black curve in the spectra included in this article). The blank spectrum in Figure 5 shows an example of system peaks in the main excitation range. Examples of blank spectra for the other excitation ranges can be downloaded from the online data depository on *The Journal's* website.

In the range of the light elements (Na to Cl), the absorption by air is quite high and hence their signals are attenuated. For many EDXRF instruments this problem is solved by evacuating the sample chamber. However, the necessary vacuum pumps are heavy and power consuming, and therefore are not feasible for battery-operated portable instruments. For the Niton Analyzer, this problem is solved by purging with He gas, where the very small volume between the tube, the outlet window (itself sealed with a very thin piece of foil) and the detector is flushed with He. This provides a very good improvement for the signal-to-noise (S/N) ratio for light elements, and also drastically reduces interfering fluorescence peaks (at 2.95 and 3.19 keV) caused by the presence of Ar in air. The He purge unit (Figure 2) is itself quite portable, although it cannot be transported on commercial airliners due to security regulations.

Figure 5: This 'blank' EDXRF spectrum, taken with an empty sample holder in place, shows the system peaks in the main excitation range. The Ni contribution is most significant, but the count rates are not very high.

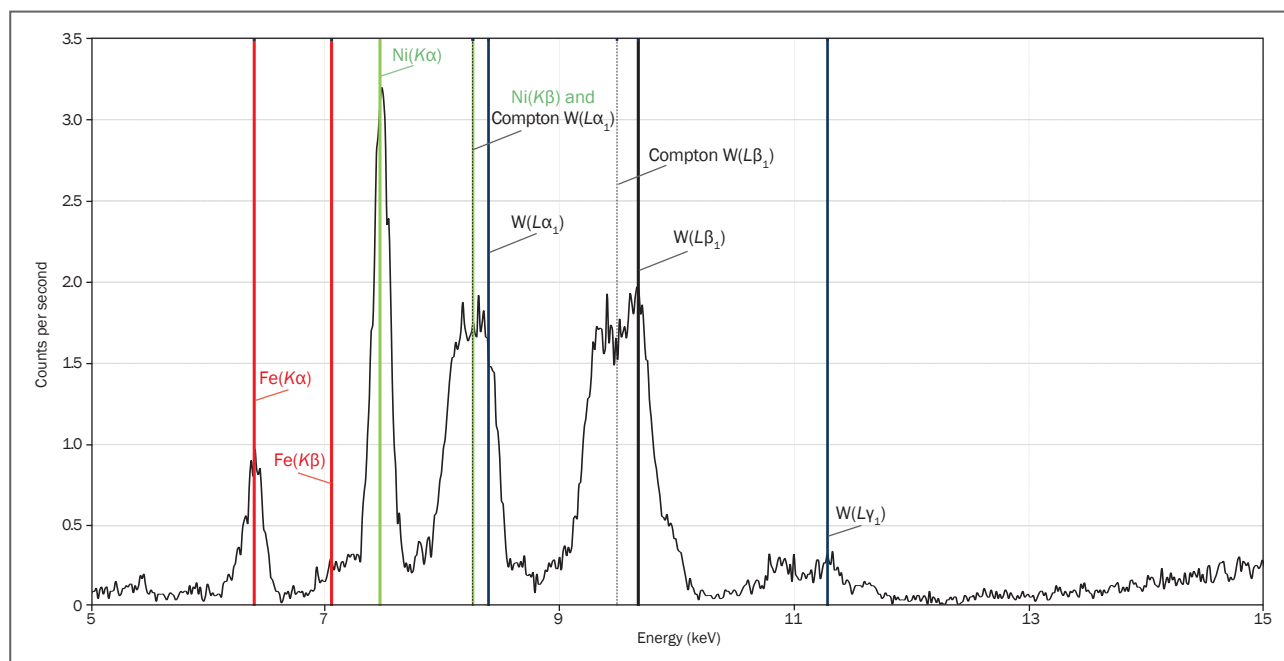




Figure 6: The corundum gems analysed for this study are (clockwise from top left): a 9.10 ct Verneuil synthetic ruby (sample 1), a 4.83 ct ruby with Pb-glass filling (sample 4), a 1.86 ct flux-grown synthetic ruby from Ramaura (sample 2), and a 4.12 ct natural untreated star ruby from Mogok (sample 3). Photo by H. A. Hänni.

Samples and Analytical Procedure

To evaluate the instrument for its suitability in gem testing, a diverse array of materials often found in gem laboratories were analysed (see, e.g., Figures 1, 6, 7 and 8, and Table IV). The analytical procedure was as follows:

- All samples were cleaned with isopropyl alcohol and dried with lint-free paper.
- A 3 mm collimator was used for mounted stones and an 8 mm collimator was employed for loose gems. The device was factory calibrated for both collimators.
- All excitation ranges (main, low, high and light) in the 'Mining Cu/Zn' mode were analysed, and the measurement times for each range are given in Table II.
- After each measurement, spanning all four excitation ranges, the Niton Analyzer automatically provided a 'quantitative' analysis. If a specific calibration is not first set by the user, the standard factory calibration is applied. Since this calibration is not optimized for gemmological samples, such 'quantitative' results cannot be trusted and the data should be considered qualitative.
- All data/spectra were exported to a PC using the Niton Data Transfer (NDT) software supplied with the instrument. Visual evaluation of the spectra was done after they were imported into Microsoft Excel.



Figure 7: The emerald samples analysed in this study consist of (clockwise from top left): a 5 × 4 cm matrix specimen from Panjshir, Afghanistan, with a prismatic 3.0 × 0.3 cm emerald (sample 11); a 9.77 ct loose crystal specimen with pyrite and calcite from La Pita, Colombia (sample 10); a 0.76 ct Chatham flux-grown synthetic emerald (sample 13); and a 2.53 ct Biron hydrothermal synthetic emerald (sample 12). Photo by H. A. Hänni.

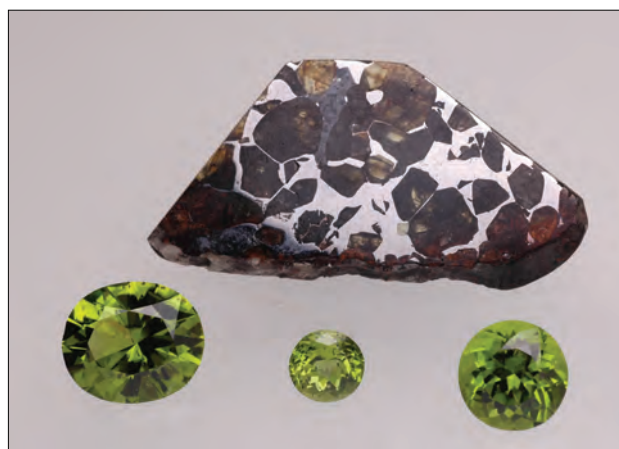


Figure 8: The olivines analysed in this study comprise (clockwise from top): a 67.5 ct Seymchan 1967 pallasitic meteorite slab from Magadan, Russia (sample 8) and a group of terrestrial olivines (sample 7) from Pakistan (11.75 ct), Norway (4.39 ct) and Myanmar (16.72 ct). Photo by H. A. Hänni.

Results

The NDT software used to operate the device and to download data, spectra and images from the Analyzer to the user's PC was clear and straightforward to use. The spectra could be scanned with a cursor, indicating the likely element responsible for a particular peak. All of the spectral lines of a given element were

Table IV: Samples tested for this study.^a

Sample no.	Mineral	Source	Weight (ct)	Composition	Elements to check
1	Corundum, Verneuil synthetic ruby	Djeva	9.10	Al ₂ O ₃	Low Fe, missing Ga Only colouring agent: Cr
2	Corundum, flux synthetic ruby ^b	Ramaura	1.86	Al ₂ O ₃	Low Fe, missing Ga Only colouring agent: Cr Residues of flux (Pb, Bi, La)
3	Corundum, untreated star ruby	Mogok, Myanmar	4.12	Al ₂ O ₃	V, Cr, Fe, Ga V should be visible, apart from Ti (because of rutile silk); Cr>Fe.
4	Corundum, ruby with Pb-glass filling ^b	Unknown	4.83	Al ₂ O ₃	V, Cr, Fe, Ga, Pb Check the possibility of deconvoluting the Ga peaks below the Pb peaks
5	Spinel, blue	Luc Yen, Vietnam	1.78	MgAl ₂ O ₄	Fe, Co, Zn, Ga Co peak, as it is visible in the UV-Vis spectrum
6	Spinel, synthetic blue	Verneuil	3.97	MgAl ₂ O ₄	Co Mg deficiency
7	Peridot	Norway Pakistan Myanmar	4.39 11.75 16.72	(Mg, Fe) ₂ SiO ₄	Ni
8	Peridot in Fe-Ni meteorite	Extraterrestrial	67.5	(Mg, Fe) ₂ SiO ₄	Ni
9	Jadeite	Myanmar	~100	NaAlSi ₂ O ₆	Na, as it is quite difficult to detect with EDXRF
10	Beryl, emerald (loose crystal)	La Pita, Colombia	9.77	Be ₃ Al ₂ Si ₆ O ₁₈	V, Cr, Fe Cr>V, Cr>Fe
11	Beryl, emerald (matrix specimen)	Panjshir, Afghanistan	~200	Be ₃ Al ₂ Si ₆ O ₁₈	Sc, V, Cr, Fe, Cs, Rb Fe>Cr Possible to see Sc?
12	Beryl, hydrothermal synthetic emerald ^b	Biron	2.53	Be ₃ Al ₂ Si ₆ O ₁₈	Cl as needed to get Cr into solution
13	Beryl, flux synthetic emerald ^b	Chatham	0.76	Be ₃ Al ₂ Si ₆ O ₁₈	Residues of flux (Pb, Bi), V, Mo
14	Tourmaline ^b	Paraíba, Brazil	1.32	Complex borosilicate	Among others: Mn, (Fe), Cu, Ga, Bi
15	Zircon	Sri Lanka	20.85	ZrSiO ₄	U and radioactive decay products (Th, Ra, Bi, Pb)
16	Lapis lazuli	Afghanistan	8.60	Mixture of lazurite, hauynite, sodalite, nosean	Na, Al, Si, S, Cl, Ca Detection possibilities for light elements (Na, S, Cl)
17	Apatite	Madagascar	21.65	Ca ₅ (PO ₄) ₃ (OH,Cl,F)	P, Cl, La, Ce, etc. Detection possibilities for P, Cl and REE
18	Scapolite, yellow	Madagascar	17.89	Al-silicate with additional anions	Check for halogen elements
19	Scapolite, purple	Tanzania	33.52	Al-silicate with additional anions	Compare to sample 18 as the colour is different
20	Tourmaline, magenta	Mozambique	23.28	Complex silicate	Compare results for different collimators
21a	Rhodolite, mounted in ear clip	Montana, USA	0.52	Mg ₃ Al ₂ (SiO ₄) ₃	Check usability of the 3 mm collimator; Cr, Fe as chromophores
21b	Andradite, mounted in ear clip	Ural Mountains, Russia	0.51	Ca ₃ Fe ₂ (SiO ₄) ₃	Check usability of the 3 mm collimator; Cr, Fe as chromophores

^a EDXRF spectra for samples 10–21 can be found in *The Journal's* online data depository.

^b Loaned by H. A. Hänni.

shown by the software. However, Na was not in the list of elements since it is not considered to be quantifiable with the current version of this instrument (even with the He purge unit). In the 'Overlay' mode, where each curve can be coloured differently, it was easily possible to compare different spectra within the same range (e.g. a natural emerald and a synthetic emerald in the 'low range'). To export the numerical data and the spectra in ASCII format is self-explanatory. Since the NDT software provided only limited reporting capabilities, the spectra were exported to Excel for further analysis. It was then possible to perform more evaluation steps such as drawing the spectra in their respective ranges, peak labelling, peak-fitting routines by use of a solver add-on, etc.

The qualitative analytical results given in subsequent sections of this article were visually derived from the corresponding spectra. The presence or absence of an element was determined by observing the peaks in the spectra, and the intensity ratios of the elements also could be estimated. For example, the Fe/Cr ratio of a Mogok ruby could be compared with that of an East African ruby—and it was clear that for a given Cr content the East African stone contained more Fe than the one from Mogok.

However, when evaluating EDXRF spectra, three important precautions must be taken:

- The identification of an element should be based on as many peaks as possible (deriving from possible *K*-, *L*- and *M*-shell transitions). The shape of the peaks should be symmetric around the energy of its emission. Overlap of peaks from different elements will cause asymmetry. Additional peaks belonging to the same element (possibly even in spectra of other excitation ranges) can help to identify the interfering elements.
- Peaks that cannot be assigned to any element—even after scanning through all of the elements from Mg to U—are suspicious, as they could be diffraction peaks from Bragg reflections of the sample's crystal lattice (see, e.g., Jenkins 1999). Usually diffraction peaks are somewhat broader than fluorescence peaks. In such cases, the sample should be placed in a different orientation (by rotation or tilting) and remeasured. Apart from

diffraction peaks, the interpretation of spectra may be complicated by 'sum peaks' as well as 'escape peaks' (see Lachance and Claisse, 1995). Although Thermo Scientific claims that these peak types are automatically removed by the software, any unallocated peak should be checked accordingly.

- For elements that may appear as system peaks, especially Fe and Ni in the main excitation range, any quantitative results have to be checked. Although the factory calibration of the Analyzer is not optimal for gemstones, it nevertheless gives indications for possible contributions of system-peak elements above their detection limit. As part of the underlying calibration process, the system-peak contributions are subtracted (taking into account matrix effects). If there are uncertainties regarding the presence of Fe and/or Ni in a sample, investigating its UV-Vis spectrum may help clarify the situation.

Examples of EDXRF Spectra

A small selection of the spectra obtained during this study is presented below, and several additional examples are provided in *The Journal's* online data depository; samples of the latter group are shown with a grey screen in Table IV. In all the spectra, the Y-axis shows 'counts per second', which is a measure of the X-ray-induced fluorescence intensity of the various elements. Along the X-axis, the energy of the emitted fluorescence lines is given in units of kiloelectron volts (keV). Element-specific fluorescence peaks are labelled in the form X(Yz), where X denotes the element, Y refers to the atomic shell (*K*, *L* or *M*) of the fluorescence transition and z is the series name of the transition (α , β , etc.). The background spectra (system peaks of the specified range) are always shown in black. The abbreviation 'LOD' (limit of detection) is the term used within the NDT software; it is equivalent to the more familiar 'bdl' (below detection limit) or 'nd' (not detected).

Ruby: 'Main range' spectra for rubies are shown in Figure 9. In the spectrum of a Mogok star ruby (sample 3), Ga and Cr could be identified by their $K\alpha$ and $K\beta$ pair of peaks (for the importance of Ga in natural corundum, see Hänni et al., 1982). The Fe and Ni peaks followed the background

Figure 9: 'Main range' EDXRF spectra are shown for a Mogok star ruby (sample 3) and a Pb glass-filled ruby (sample 4). The star ruby shows the classic Mogok pattern, with low Fe and rather high Cr. Its Ga peak certifies its natural origin. For the Pb glass-filled ruby, a natural origin cannot be determined by its Ga content since the Pb peaks completely overlap the Ga region; its Fe content and visual examination nevertheless indicate its natural origin.

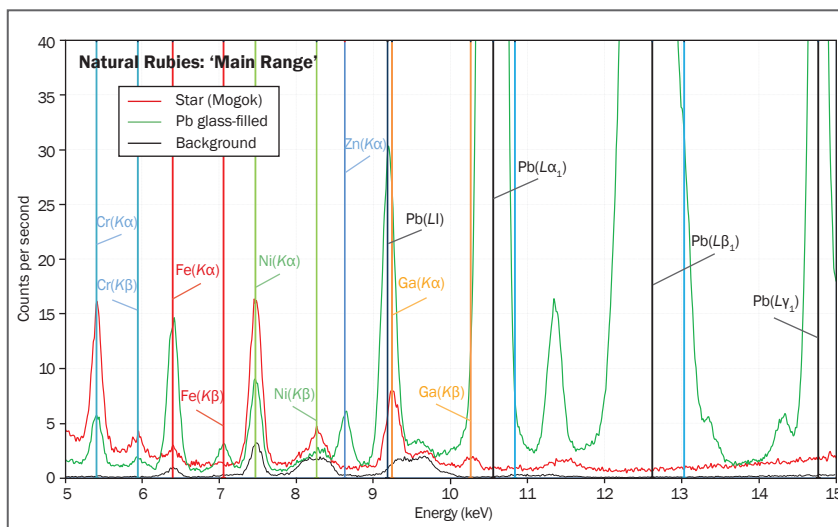
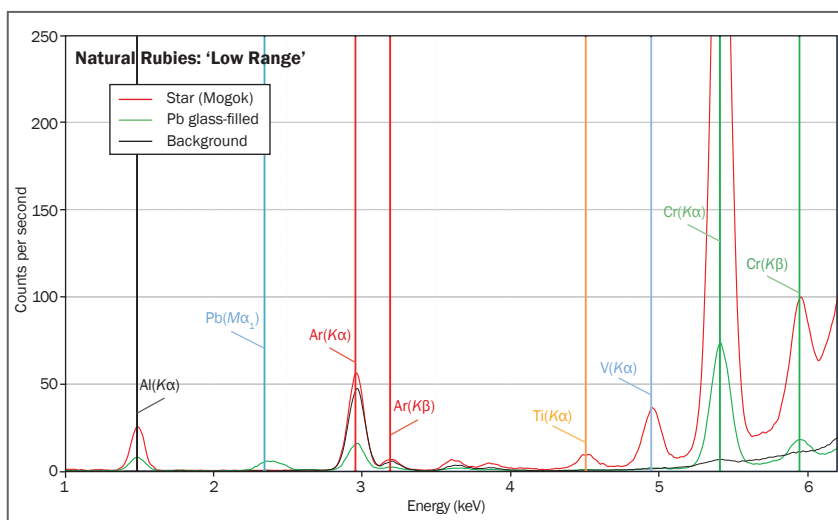


Figure 10: These 'low range' EDXRF spectra are from the same rubies analysed in Figure 9. In the Mogok star ruby, the presence of V supports its claimed origin and the Ti content is consistent with the rutile inclusions that are responsible for its asterism. For the Pb glass-filled ruby, only a small M-line of Pb can be observed in this excitation range.



curve, and therefore these elements do not occur in this ruby, or their concentrations are below the detection limit. A check of the quantitative results indeed showed 'LOD' for both elements in the star ruby. The spectrum of a Pb glass-filled ruby (sample 4) can be recognized as natural (i.e. not synthetic) by its relatively large Fe peak; Ga could not be detected as those peaks were overshadowed by the relatively large peaks of Pb(LI) and Pb(L α_1). The Zn peak is somewhat surprising—its origin is not clear, although it could be a constituent of the glass filling.

'Low range' spectra of these same rubies are shown in Figure 10. The V content of the star ruby (sample 3) supported its Burmese origin. The Ti originated from the network of fine rutile inclusions that is responsible for its asterism. In the Pb glass-filled ruby (sample 4), only one peak related to lead, Pb(M α_1), could be seen in this low-energy spectrum.

'Main range' spectra of two synthetic rubies are shown in Figure 11. For the Verneuil synthetic ruby (sample 1), the only feature was the Cr pair (K α , K β); together with the absence of Fe, Cr is responsible for the bright red colour of this sample. In the flux synthetic ruby (sample 2), apart from the chromophore Cr, the flux-related elements Pb and Bi were visible (cf. Muhlmeister and Devouard, 1991; Muhlmeister et al., 1998). Signals for Fe and Ni were also clearly visible, but they correspond to system peaks that have been enhanced by the corundum matrix. The mechanism of this fluorescence enhancement has not been studied in detail, but such system peaks are subtracted by the instrument's quantitative analysis calculations, and 'LOD' was reported for both Fe and Ni in this flux-grown sample. The absence of Ga peaks is obvious in the case of the Verneuil synthetic. The presence of Ga in the flux synthetic is not clear due to interference from Pb in the Ga(K α)

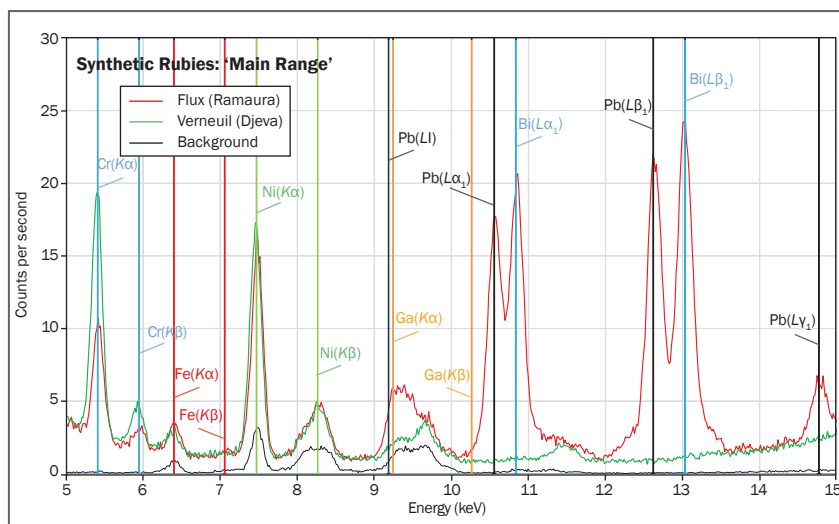


Figure 11: The 'main range' EDXRF spectra are shown for synthetic rubies: Verneuil (flame fusion; sample 1) and Ramaura (flux; sample 2). Both rubies show no Fe and high Cr contents. In the Verneuil sample, Ga is below the detection limit, but this is not so obvious in the Ramaura sample. The flux used for its growth contains Pb (and Bi and La), and the Ga K-lines are hidden by the Pb L-lines—a similar situation as in Figure 9. The Bi lines are also obvious.

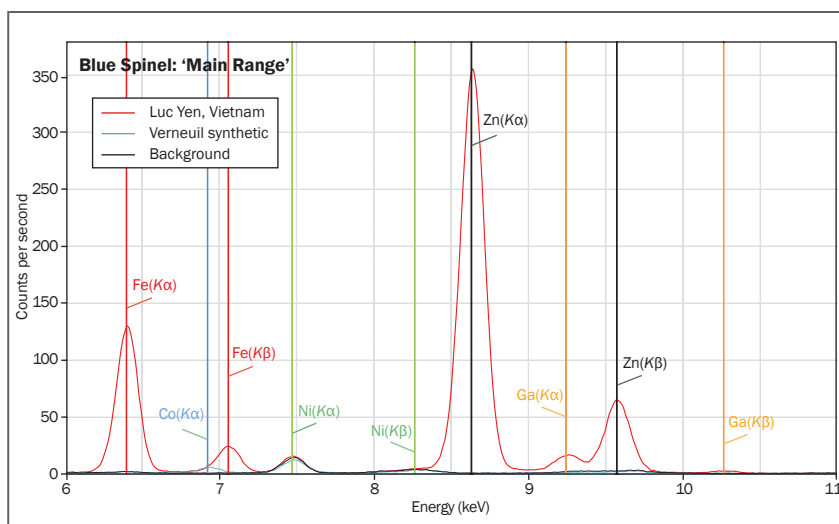


Figure 12: 'Main range' EDXRF spectra of a blue spinel from Vietnam (sample 5) and a Verneuil synthetic blue spinel (sample 6) are shown for comparison. The trace-element pattern of the natural spinel is classic: high Zn with a clear Ga peak and some Fe. All these elements are missing from the synthetic spinel. Only Co (the blue chromophore) is visible for the synthetic spinel.

region. Together with a visual inspection of this sample (which shows multiphase flux residues), the EDXRF spectrum clearly indicated this gem to be a Ramaura flux-grown synthetic ruby (see also Kane, 1983, and Muhlmeister et al., 1998). (In addition, the presence of La, also typical of Ramaura synthetic ruby, could be seen in the low- and high-range spectra.)

Spinel: 'Main range' spectra of one natural and one synthetic blue spinel are shown in Figure 12. The natural origin of the stone from Luc Yen (sample 5) is revealed by the large Zn peak, the clear presence of Ga and an obvious Fe contribution. The Verneuil synthetic spinel (sample 6) contained, apart from its main constituents (not visible in this spectrum), only the chromophore Co. This element could not be detected in the attractively coloured blue gem from Vietnam.

The 'light range' spectra of these natural and synthetic spinels are shown in Figure 13. To improve the S/N ratio, the He purge unit was used for better detection of the light elements. The relative excess Al in the synthetic spinel, as compared to the natural stone, is obvious.

Peridot: 'Main range' spectra of various peridot gems (sample group 7 and sample 8) are shown in Figure 14. As mentioned above and in Figure 5, Ni is a system peak, and this may be problematic in cases where the signal from this element is crucial. The Ni content of terrestrial olivine is higher than for the extraterrestrial counterpart found in pallasites (Shen et al., 2011; Williams and Williams, 2014). The spectra shown in this figure, all measured under exactly the same conditions, clearly confirm these findings (despite the contribution from the Ni system peak). The quantitative results indeed indicated the presence

Figure 13: 'Light range' EDXRF spectra are shown for the same samples as in Figure 12. These spectra were recorded with the He purge unit, and they clearly show the relative Al excess in the synthetic spinel.

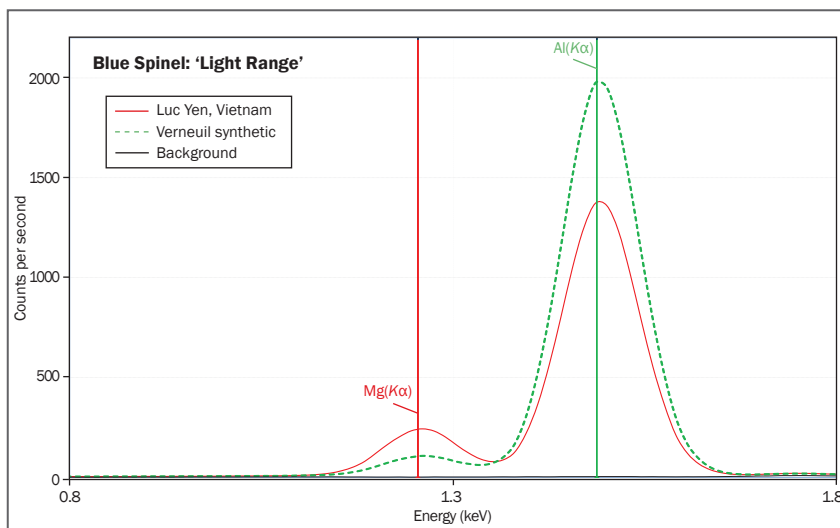


Figure 14: These 'main range' EDXRF spectra of peridot from various origins show lower contents of Ni in the pallasitic gem (sample 8) compared to terrestrial samples (sample group 7) from Myanmar, Pakistan and Norway.

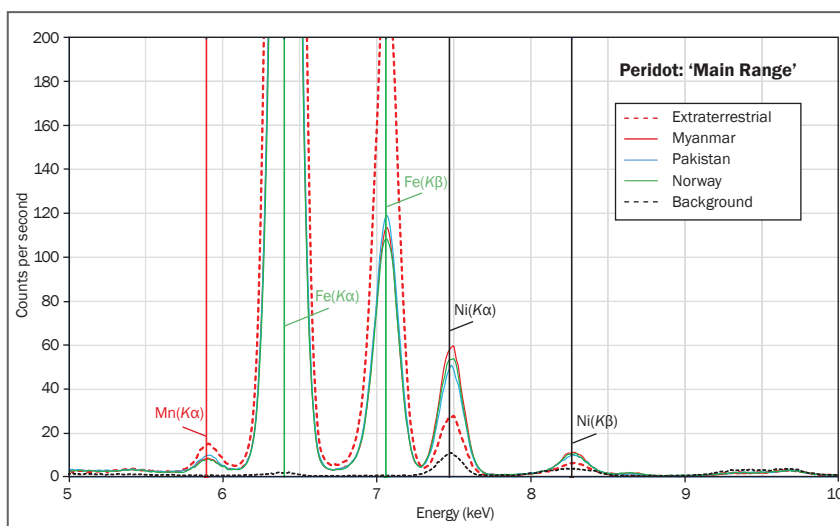
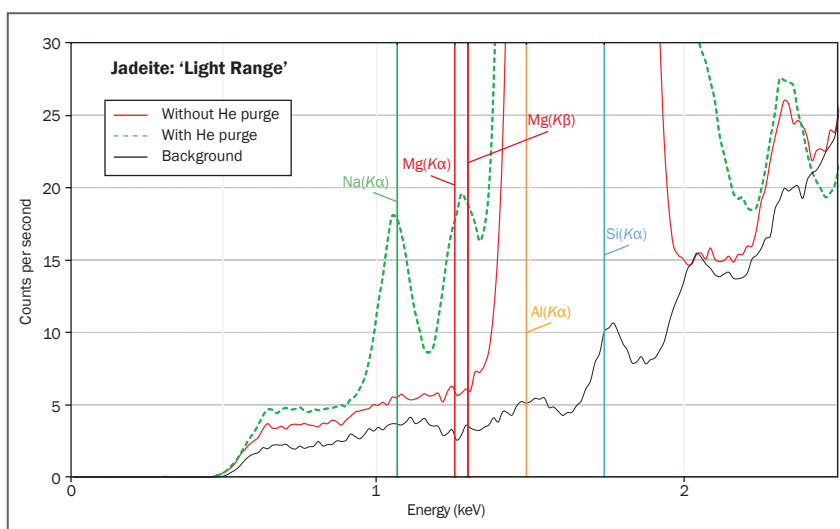


Figure 15: 'Light range' EDXRF spectra of jadeite (sample 9) are shown under normal conditions and with the He purge unit. The presence of Na and Mg can only be seen in the latter spectrum.



of Ni in all the samples, but with a clearly lower value for the pallasitic peridot. The spectra also show that Mn was relatively more abundant in the pallasitic peridot than in the terrestrial samples.

Jadeite: The 'light range' spectrum of jadeite (sample 9) is shown in Figure 15. Using the He purge unit, the important Na signal is obvious, and even a small Mg contribution is observed.

For the following samples, corresponding EDXRF spectra can be found in *The Journal's* online data depository.

Beryl: Four emerald samples were analysed. The trace-element concentrations of emerald are mainly used for locality determination and/or to establish natural versus synthetic origin. The Colombian stone (sample 10) was characterized by low Fe, higher Cr, substantial V and the absence of alkali elements such as Rb. In the Panjshir emerald (sample 11), Sc could be identified with the help of the 3 mm collimator; the 8 mm collimator measurement sampled too much of the carbonate matrix, and the Ca peak overlapped the Sc signal. The Cr content of this Afghan stone was quite low, but the V peak was surprisingly strong.

For the hydrothermal synthetic emerald (sample 12), the existence of Cl could be demonstrated (cf. Hänni and Kiefert, 1994). Flux residues (Mo) were clearly evident in sample 13, a Chatham synthetic emerald (cf. Nassau, 1980).

Using the He purge unit, it was shown that a natural emerald (sample 10) contained traces of Na and Mg whereas a synthetic stone (sample 12) lacked these elements (cf. Hänni, 1982).

Tourmaline: An elbaite from Paraíba, Brazil (sample 14), showed a small liddicoatite component as indicated by Ca in its 'low range' spectrum. Peaks for Mn and Cu that are characteristic of this tourmaline were obvious in the 'main range' spectrum. The ratio Cu/Mn <1 and the presence of Zn and moderate Bi recorded in the EDXRF spectra may support its Brazilian origin. Nevertheless, origin determination for Cu-bearing tourmaline by means of EDXRF analysis is not rigorous, since quantitative data is required—including for light elements that cannot be detected by EDXRF spectroscopy (Fritsch et al., 1990; Laurs et al., 2008).

Zircon: Sample 15 (see Figure 1) was analysed to test the device's ability to measure heavy elements, such as U and its decay products. In the 'main range' spectrum, these heavy elements may be seen by their *L*-shell fluorescence peaks, whereas Zr shows up with *K*-lines. In sample 15, apart from Zr, the elements Hf, U, Bi and Pb could be

identified by at least two peaks—although quite close to the resolution of the instrument. Only one peak for Th was visible, $L\alpha_1$, and to prove the existence of this element at least one more peak should be identified: $L\beta_1$ at 16.215 keV. Since that peak was hidden by the Zr signal, the presence of Th in this zircon was not conclusive.

Lapis Lazuli: Sample 16 (see Figure 1) was chosen for the study of lighter elements such as Na, S and Cl. For this purpose, spectra were recorded with and without the He purge unit. In the 'light range' spectrum, these elements were clearly seen with the He purge unit, but Na was invisible without the purge unit. To prove the existence of Cl within the 'light range', one has to be careful with the nearby Ag system peak [Cl($K\alpha$) = 2.622 keV and Ag(*LI*) = 2.634 keV]. There is no filter suppressing the Ag(*LI*) line, which originates from the X-ray tube. To confirm the presence of Cl in lapis lazuli, the 'low range' spectrum must be consulted, in which the Cu filter absorbs the Ag(*LI*) line.

Apatite: Sample 17, an apatite from Madagascar (see Figure 1), was chosen for its P and rare-earth element (REE) contents, and to check whether it might be a Cl-containing chlorapatite. (However, differentiation between fluorapatite and hydroxylapatite is not possible by EDXRF.) This apatite showed a clear P signal (as apatite is a phosphate), a small Cl contribution, significant Sr (substitution of Ca by Sr), and substantial traces of Y, La, Ce and Nd.

Scapolite: Both analysed samples (18 and 19; see Figure 16) showed clear Cl and Br peaks (cf. Dong, 2005), and their spectra were quite similar with respect to transition-metal elements, even though their colours were quite different (purple and yellow). To properly evaluate the marialite component (Na), the He purge unit should be used.

Comparison of Results from Different Collimators: Sample 20, a tourmaline from Mozambique (see Figure 16), was analysed with both 3 mm and 8 mm collimators, but otherwise under the same conditions (including measurement time). The results clearly showed

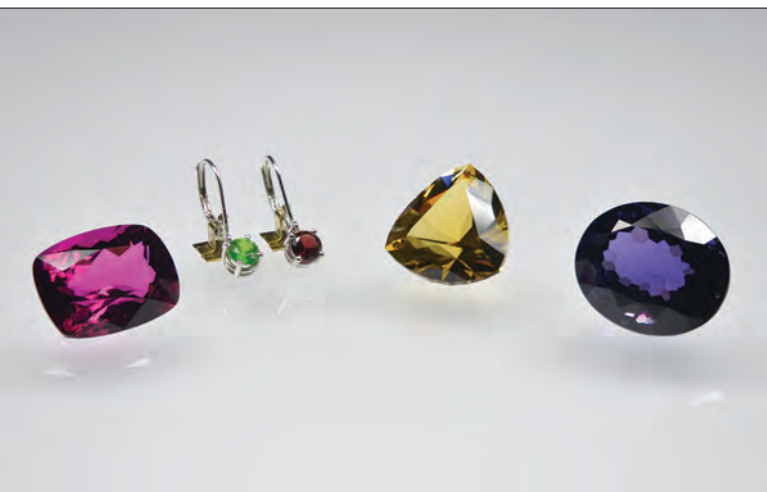


Figure 16: Also analysed for this article were the following samples (left to right): a 23.28 ct tourmaline from Mozambique (sample 20), a pair of ear clips with garnets mounted in white gold (sample 21b, a 0.51 ct andradite from Russia, and sample 21a, a 0.52 ct rhodolite from Montana, USA), a yellow 17.89 ct scapolite from Madagascar (sample 18) and a purple 33.52 ct scapolite from Tanzania (sample 19). Photo by F. A. Herzog.

that all elements visible in a certain range could be detected using either collimator. This is very important for the device's use on mounted gems.

Analysing Mounted Gemstones: Two 3-mm-diameter garnets (samples 21a and 21b; see Figure 16) that were mounted in white-gold ear clips were analysed using the 3 mm collimator. Both the rhodolite and andradite could clearly be identified with minimal disturbance from the mounting. The position of each of these stones within their respective garnet series was shown, as well as their colouring trace elements. The spectra were as good as those taken of a loose gem with an 8 mm collimator.

Discussion

The main motivation for this study was to investigate whether a portable EDXRF instrument, widely used in the mining industry and in other fields, can also be useful in gemmology. Analysis of a broad range of gem samples, either loose or mounted in jewellery, was quickly performed in a qualitative manner. Well-resolved spectra for almost all naturally occurring elements (Na to U) can be recorded with this portable EDXRF instrumentation, and trace elements (and their

intensity ratios) were effectively revealed that are useful for identifying geographical origin, chromophores and methods of synthesis.

Do we really need quantitative data for the routine analysis of gem materials? Certainly quantitative data are necessary for research purposes, as well as in some gem identification cases (e.g. determining the geographical origin of certain gem varieties). These situations require more sophisticated instrumentation such as an electron microprobe or laser ablation–inductively coupled plasma–mass spectrometry (LA-ICP-MS) equipment (see, e.g., Schmetzer, 2010). By contrast, EDXRF chemical analysis is often performed because the gemmologist wants confirmation of findings derived from standard gem testing techniques. If the interpretation of qualitative results (element ratios, existence of a certain element, etc.) is all that is needed, then EDXRF spectroscopy is sufficient, provided that the spectra are carefully evaluated for (1) peak overlaps, (2) the correct ‘fingerprint’ for each element and (3) the possibility of escape and sum peaks as well as diffraction peaks.

How does this portable analyzer compare to a typical bench-top EDXRF instrument? On the qualitative level, based on this author's experience with this portable unit and two bench-top EDXRF units (Thermo Fisher ARL Quant'X and Helmut-Fischer Fischerscope XUV 773), spectra from both types of instruments are comparable, even for light elements. An evaluation of quantitative data from this portable unit is beyond the scope of this study (see Box A). Nevertheless, it is certain that the calibration software accompanying bench-top instruments is more advanced; this probably also applies to the software for data quantification, based on the Fundamental Parameter method. However the advantages of the Niton Analyzer are obvious: It is portable, can be operated using a battery for eight hours and has a lower price (the actual price will vary depending on the analytical capabilities and accessories desired by the user).

Conclusions

The portable instrument evaluated for this report would be a great asset to a smaller gemmological laboratory as a principal EDXRF device, and would

Box A: Quantitative Chemical Analysis with the Niton Analyzer

For this study, none of the tested samples was analysed by a quantitative technique such as LA-ICP-MS to obtain a fully quantified concentration profile. Therefore, it is not possible to assess the data quantification process used by the Niton Analyzer when analysing gem samples. Nevertheless, this author suspects that the factory calibration using mining reference standards and pure elements does not produce satisfactory results for gemmological analysis. This raises the question of whether the calibration and hence a quantification can in principle be improved for gem analysis.

Indeed, the calibration for a specific sample's matrix (e.g. corundum) can be done

by the user, provided that several measured reference samples of the same species are available. (The process to set up a collection of EDXRF reference samples is complex and is not covered here.) To do this, all the reference samples are analysed with the Niton unit and the results for each element are plotted (e.g. in Excel) against the known values of those elements in the reference samples (see, e.g., the hypothetical example shown in Figure A-1). The resulting slope and intercept parameters can then be entered into the appropriate menu of the device's software. The device allows for concentrations to be given as ppm values of pure elements or as wt.% oxides.

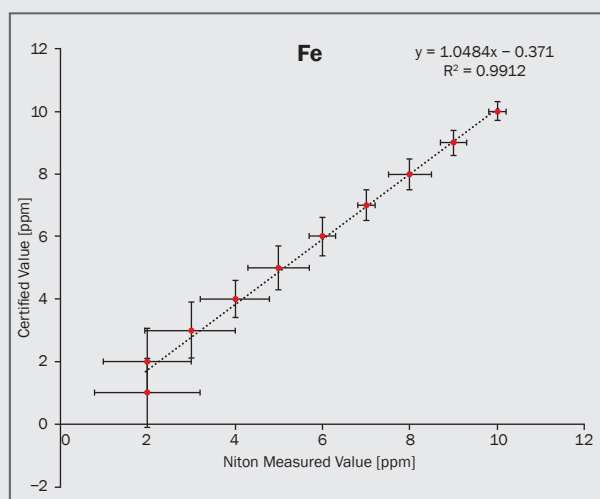


Figure A-1: This hypothetical calibration curve for Fe is shown for 10 reference samples of a given matrix (e.g. corundum). The data measured by the Niton Analyzer are plotted along the X-axis, and the known values (e.g. from LA-ICP-MS) are plotted along the Y-axis. A linear regression analysis calculates the two parameters for the calibration of Fe within the given matrix: slope (1.0484) and intercept (-0.371). These values can be entered into the user-defined cal-factor set of the Niton software for Fe. A similar procedure would have to be applied to all elements of interest to set up the instrument for quantitative analysis of a given gem species.

also be very useful for larger laboratories offering off-site testing. In addition to its portability, the instrument provides good-quality spectra in a simple and rapid way, for all possible sample types that may be submitted to gemmological laboratories. The elements present in a sample can be qualitatively identified (in the Na to U range), whether they are main constituents or present only in trace amounts. In addition, the intensity ratios of various elements are easily visible in the well-resolved spectra. Both of these aspects support the gemmologist in the decision-making path to correctly identifying a sample, including possibly its origin.

References

- Dong P., 2005. Halogen-element (F, Cl and Br) behaviour in apatites, scapolite and sodalite: An experimental investigation with field applications. Ph.D. thesis, University of Saskatchewan, Saskatoon, Canada.
- Fritsch E., Shigley J.E., Rossman G.R., Mercer M.E., Muhlmeister S. and Moon M., 1990. Gem-quality cuprian-elbaite tourmalines from São José da Batalha, Paraíba, Brazil. *Gems & Gemology*, **27**(3), 189–205, <http://dx.doi.org/10.5741/gems.26.3.189>.
- Hänni H.A., 1982. A contribution to the separability of natural and synthetic emeralds. *Journal of Gemmology*, **18**(2), 138–144, <http://dx.doi.org/10.15506/jog.1982.18.2.138>.

- Hänni H.A. and Stern W.B., 1982. Über die gemmologische Bedeutung des Gallium-Nachweises in Korunden. *Zeitschrift der Deutschen Gemmologischen Gesellschaft*, **31**(4), 255–261.
- Hänni H.A. and Kiefert L., 1994. Preliminary results on AGEE hydrothermal emeralds from Japan. *Journal of the Gemmological Association of Hong Kong*, **17**, 46–54.
- Jenkins R., 1999. *X-ray Fluorescence Spectrometry*, 2nd edn. Vol. 152 of *Chemical Analysis: A Series of Monographs on Analytical Chemistry and Its Applications*. John Wiley & Sons Inc., New York, New York, USA, 207 pp., <http://dx.doi.org/10.1002/9781118521014>.
- Kane R.E., 1983. The Ramaura synthetic ruby. *Gems & Gemology*, **19**(3), 130–148, <http://dx.doi.org/10.5741/gems.19.3.130>.
- Lachance G.R. and Claisse F., 1995. *Quantitative X-ray Fluorescence Analysis*. John Wiley & Sons Inc., Chichester.
- Laurs B.M., Zwaan J.C., Breeding C.M., Simmons W.B., Beaton D., Rjisdijk K.F., Befi R. and Falster A.U., 2008. Copper-bearing (Paraíba-type) tourmaline from Mozambique. *Gems & Gemology*, **44**(1), 4–30, <http://dx.doi.org/10.5741/gems.44.1.4>.
- Muhlmeister S. and Devouard B., 1991. Determining the natural or synthetic origin of rubies using energy-dispersive X-ray fluorescence (EDXRF). In A. S. Keller, Ed., *Proceedings of the 1991 International Gemological Symposium*, Gemological Institute of America, Santa Monica, California, 139–140.
- Muhlmeister S., Fritsch E., Shigley J.E., Devouard B. and Laurs B.M., 1998. Separating natural and synthetic rubies on the basis of trace-element chemistry. *Gems & Gemology*, **34**(2), 80–101, <http://dx.doi.org/10.5741/gems.34.2.80>.
- Nassau K., 1980. *Gems Made by Man*. Gemological Institute of America, Santa Monica, California.
- Schmetzer K., 2010. *Russian Alexandrites*. E. Schweizerbart'sche Verlagsbuchhandlung, Stuttgart, Germany.
- Shen A.H., Koivula J.I. and Shigley J.E., 2011. Identification of extraterrestrial peridot by trace elements. *Gems & Gemology*, **47**(3), 208–213, <http://dx.doi.org/10.5741/gems.47.3.208>.
- Shugar A.N. and Mass J.L., Eds., 2012. *Handbeld XRF for Art and Archeology. Studies in Archeological Sciences*, **3**, Leuven University Press, Leuven, Belgium.
- Voynick S., 2010. X-ray fluorescence analyzers. *Rock & Gem*, **40**(9), 20–28.
- Williams B. and Williams C., 2014. Alien sightings: Pallasite. *GemGuide*, **33**(2), 7–9.
- Zurfluh F.J., Hofmann B.A., Gnos E. and Eggenberger U., 2011. Evaluation of the utility of handheld XRF in meteoritics. *X-ray Spectrometry*, **40**(6), 449–463, <http://dx.doi.org/10.1002/xrs.1369>.

The Author

Dr Franz Herzog FGA is a retired physicist who has worked as an analyst at the Swiss Gemmological Institute SSEF in Basel, (where he learned about EDXRF analysis of gemstones), and at GRS in Lucerne, Switzerland. Email: f.a.herzog@bluewin.ch

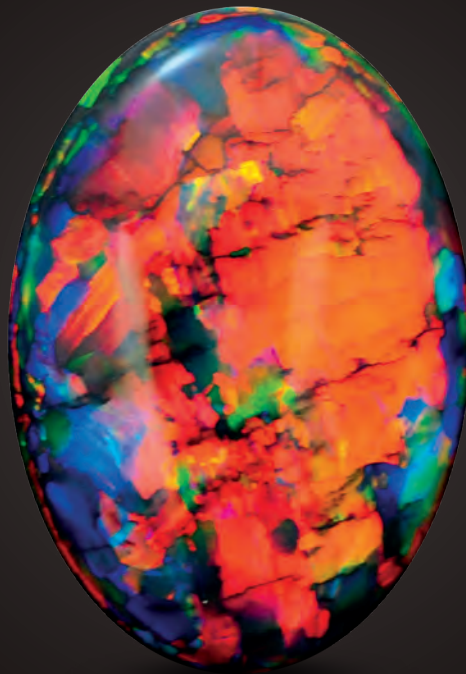
Acknowledgements

This article would not have been possible without the help of Marc Dupayrat, Niton technical support in Switzerland, and the cooperation of Thermo Scientific Europe in loaning the instrument. Thanks also go to Chris Calam of Thermo Scientific UK, who proof-read the article and provided support during the author's seminar at the Gem-A Conference 2014 in London. Prof. Dr H. A. Hänni (SEEF, Basel) is gratefully acknowledged for his interest in this project and for thorough discussions of this article. He also loaned samples of synthetic gem materials and a Paraíba tourmaline, and supplied photos of some of the analysed samples. Special thanks also go to the peer reviewers, who helped to improve this paper.

The Fire Within

“For in them you shall see the living fire of the ruby, the glorious purple of the amethyst, the sea-green of the emerald, all glittering together in an incredible mixture of light.”

- Roman Elder Pliny, 1st Century AD



BLACK OPAL 15.7 CARATS

Suppliers of Australia's finest opals to the world's gem trade.

CODY  OPAL

LEVEL 1 - 119 SWANSTON STREET MELBOURNE AUSTRALIA

T. +61 3 9654 5533 E. INFO@CODYOPAL.COM

WWW.CODYOPAL.COM


INTERNATIONAL
COLORED GEMSTONE
ASSOCIATION
MEMBER

Green Lead-Glass-Filled Sapphires

*Thanong Leelawatanasuk, Namrawee Susawee,
Supparat Promwongnan and Nicharee Atsawatanapirom*

In April 2014, the Gem and Jewelry Institute of Thailand's Gem Testing Laboratory (GIT-GTL) received several rough and cut samples of green lead-glass-filled sapphire for examination, and in December 2014 the treater invited GIT to tour his facility. These stones show many characteristics similar to those of previously known cobalt-doped lead-glass-filled blue sapphires: orange and blue flash effects and colour concentrations along filled fissures, flattened gas bubbles trapped within the filler, and chalky blue fluorescence of the filler when viewed with the DiamondView instrument. Chemical analysis of the green glass showed mostly Pb with some Si, minor Cu, and traces of Fe and Cr. The latter three elements could possibly be responsible for the green coloration of the glass filler.

The Journal of Gemmology, 34(5), 2015, pp. 420–427, <http://dx.doi.org/10.15506/JoG.2015.34.5.420>
© 2015 The Gemmological Association of Great Britain

Introduction

Lead-glass-filled corundum was introduced to the gem market in 2004 (see, e.g., Rockwell and Breeding, 2004; Smith et al., 2005). Initially, highly fractured rubies from various sources in East Africa were used as raw material for this treatment, and the finished products were sold under the trade name 'Newly Treated Ruby' in local markets in Bangkok and Chanthaburi, Thailand. Shortly thereafter, the fillers were proven to consist of lead-containing glasses (see references above and McClure et al., 2006; Milisenda et al., 2006). The principle behind this technique of filling fractures was not new, as it had already been applied to diamond (see, e.g., Koivula et al., 1989). However, some modifications were made by using high-temperature furnaces for melting the glass and filling fissures in corundum. Due to the poor durability of the filling material, many problems occurred during jewellery manufacturing/repair

and cleaning. The glass filler could be etched by certain acidic or basic solutions, and heat from a jeweller's torch might easily melt the glass.

Although the lead-glass fillers may pose durability problems, there are still certain advantages of these treated products. With proper precautions during jewellery making, repairing and cleaning (e.g. using cold mounting techniques and avoiding contact with acidic or basic solutions), the drawbacks can be avoided. And due to their affordability, mass availability and wide range of quality, these products are still in demand after almost a decade on the market.

In 2012, a new type of blue cobalt-doped lead-glass-filled corundum entered the market (Leelawatanasuk, 2012; Leelawatanasuk et al., 2013). This product showed many identifying features similar to those of the previous lead-glass-filled rubies. Subsequently, Henn et al. (2014) documented additional coloured lead-glass



Figure 1: The five green lead-glass-filled sapphires studied for this report weigh 0.89, 2.79, 5.90, 2.64 and 1.06 ct (from left to right). Photo by N. Atsawatanapirom.

fillings in corundum that were red and pale green. Most recently, in April 2014 GIT-GTL received for examination several rough and cut stones (Figures 1 and 2) that were claimed to be ‘the latest lead-glass-treated sapphire’. In December 2014 the owner of the process, Dhiranant Charoenjit (Figure 3), kindly allowed authors NS and SP to visit his facility at Nichima Gems in Chanthaburi Province, eastern Thailand.

According to Charoenjit, the starting material is sorted from low-quality, highly fractured pale-coloured sapphire rough. Some of the corundum shows well-formed hexagonal crystal shapes. The stones are cleaned in an acidic solution to remove impurities from the surface and within the open fissures. After this process, the material appears dull white (Figure 4, left) or is somewhat transparent with many open fissures. The stones are put into an alumina crucible with a sufficient amount of glass powder. The crucible is then heated in an electric furnace to approximately 1,300°C. After treatment, the stones are usually fused together into a glassy mass (e.g. Figure 2). The treatment is reportedly successful on only ~20% of the material, and the remaining 80% is rejected.

Material and Methods

Three pieces of rough and five faceted samples of the treated green sapphire were selected for this study. Standard gemmological equipment was used to obtain refractive indices, hydrostatic specific gravity, pleochroism, and fluorescence to long- and short-wave UV radiation for all of the faceted samples; they also were examined with a gemmological microscope. Chemical analysis by energy-dispersive X-ray fluorescence (EDXRF)



Figure 2: Shown here is an example of the low-quality pale coloured corundum that is used as the starting material for glass filling (bottom right, 3.15 g), together with two fused pieces of corundum and green glass after the treatment process (10.17 and 1.76 g). Photo by N. Atsawatanapirom.

spectroscopy was performed on all samples with an Eagle III instrument using an Rh X-ray tube, an accelerating voltage of 30 kV and a beam current of 200 mA. The diameter of the X-ray beam was 2,000 µm, and diffraction artefacts were avoided by sample rotation. Absorption

Figure 3: Dhiranant Charoenjit, managing director of Nichima Gems in Chanthaburi Province, explains the treatment process and shows the material before and after glass filling. Photo by S. Promwongnan.





Figure 4: These images show the corundum starting material after acid cleaning (left), and rough and faceted lead-glass-filled green sapphires after the treatment (centre and right). The rough stones weigh 1–5 g and the faceted samples are 1–3 ct. Photos by S. Promwongnan and N. Susawee.

spectra were recorded on all samples in the mid-infrared range ($4000\text{--}400\text{ cm}^{-1}$) with a Thermo Nicolet 6700 Fourier-transform infrared (FTIR) spectrometer equipped with a KBr beam splitter, at a resolution of 4 cm^{-1} . Ultraviolet-visible–near infrared (UV-Vis-NIR) spectra of all samples were recorded in the range $250\text{--}800\text{ nm}$ using a PerkinElmer Lambda 950 spectrophotometer with a sampling interval of 3.0 nm and scan speed of 441 nm per minute . X-radiography of all samples was performed using a Softex SFX-100 instrument, and one faceted stone was examined with a DiamondView deep-ultraviolet ($<230\text{ nm}$) luminescence imaging system.

To investigate some of the durability issues associated with lead-glass-filled corundum, preliminary testing was performed on three

representative cut stones, which were separately subjected to a soap solution in an ultrasonic cleaning unit, a jewellery torch and a rhodium electroplating agent.

Gemmological Properties

A distinctive feature of this product is its colour appearance: The faceted stones were yellowish green with low saturation, and the rough samples were a strong green and were coated with deep green glassy material (Figures 1 and 2).

The gemmological properties obtained from the faceted stones (Table I) are consistent with corundum in general. The samples were doubly refractive with RI values of $1.760\text{--}1.770$. SG was approximately $4.00\text{--}4.02$. Viewed with a dichroscope, they showed slight dichroism from greenish yellow to slightly yellowish green; the intensity of the green hue remained essentially constant whereas that of the yellow hue varied from pale to almost colourless. Figure 5 shows the differences in dichroism between an untreated green sapphire and this treated material. The dichroism of the treated sapphires suggests that their colour is mainly due to the isotropic green glass filler, and the underlying body colour of the material is likely to be light yellow to almost colourless. The stones were inert to short-wave UV radiation and luminesced weak orange or were inert to long-wave UV.

Microscopic examination proved to be a simple and important method for identifying these treated stones. The five faceted stones all showed features characteristic of natural (i.e. not synthetic) sapphire, such as tube-like features, ‘fingerprints’ and polysynthetic twinning (Figure 6). In addition, the gems showed many distinct

Table I: Properties of five faceted green lead-glass-filled sapphires.*

Refractive indices	1.760–1.770 (birefringence 0.010)
Polariscope reaction	Doubly refractive
Pleochroism	Slightly dichroic, in greenish yellow to slightly yellowish green
Specific gravity	4.00–4.02
Internal features	Growth tubes, ‘fingerprints’, lamellar twinning, orange and blue flash effects along filled fissures, green colour concentrations in filled fissures and cavities, flattened gas bubbles trapped in the glass filler
UV fluorescence	
Long-wave	Inert to weak orange
Short-wave	Inert

*Based on the testing of five stones weighing 0.89, 1.06, 2.64, 2.79 and 5.90 ct (see Figure 1).

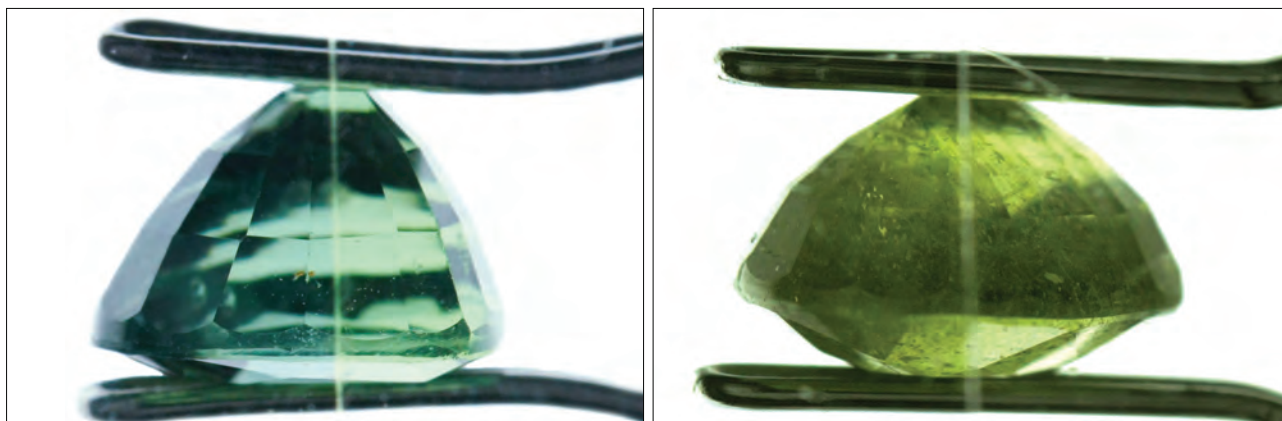


Figure 5: The 2.40 ct untreated green sapphire on the left shows typical bluish green to yellowish green dichroism, in contrast to the 2.79 ct green lead-glass-filled corundum on the right that displays greenish yellow and slightly yellowish green pleochroism. Photos by S. Promwongnan.

microscopic features associated with lead-glass-filled corundum, such as orange and blue flash effects, green colour concentrations along fissures and in cavities, and flattened gas bubbles trapped within filled fissures (Figures 7–9). Reflected light was useful for detecting cavities and fissures that were glass filled, as the surface lustre of the filler was noticeably lower than that of the host sapphire (Figures 9 and 10).

Chemical Composition

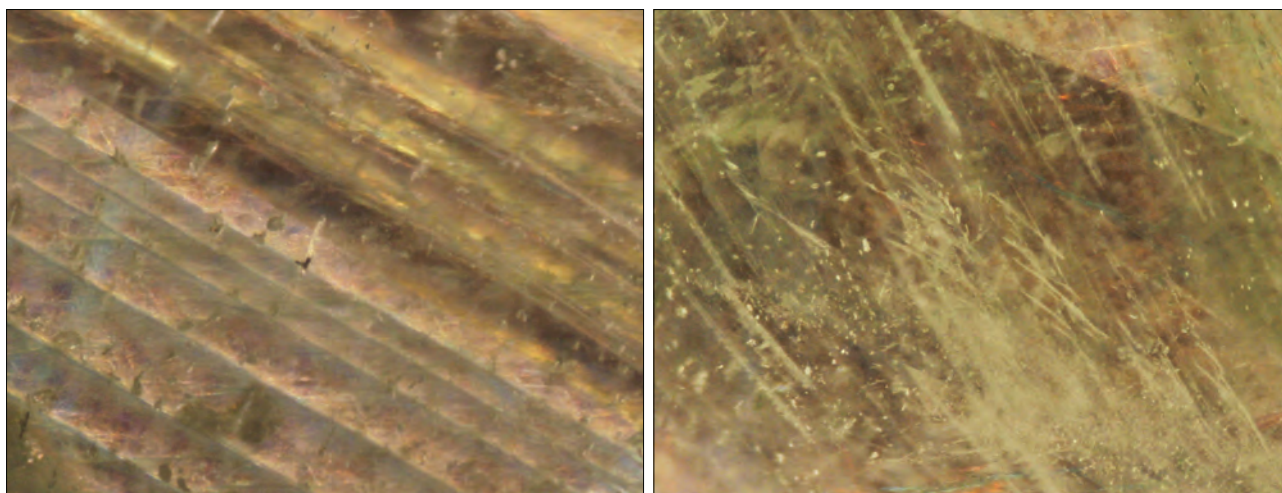
Semi-quantitative chemical analysis was performed by EDXRF spectroscopy on the green glassy residue at the surface of a 1.76 g rough sample (see Figure 2) to avoid sampling the host corundum. The analysis showed mostly Pb with some Al (from the corundum) and Si, minor Cu,

and traces of Fe and Cr. By contrast, chemical analysis of the cut stones mainly showed the composition of the host sapphire with small amounts of the glassy constituents.

Spectroscopy

The mid-FTIR spectra of the green glass clearly showed strong absorption bands at approximately 3400, 2597 and 2256 cm^{-1} that are related to the glass filler (Figure 11). A UV-Vis-NIR spectrum of the green glass residue protruding from the surface of a rough sample showed strong absorption through almost the entire visible spectrum, except for a transmission window in the green region at ~500–570 nm (Figure 12). This spectral pattern and the presence of Fe, Cu and Cr (measured by EDXRF spectroscopy) suggest that the green coloration

Figure 6: Polysynthetic twinning (left) and tube-like features (right) are characteristics of the natural corundum starting material used for these green lead-glass-filled sapphires. Photomicrographs by N. Atsawatanapirom; magnified 10 \times .



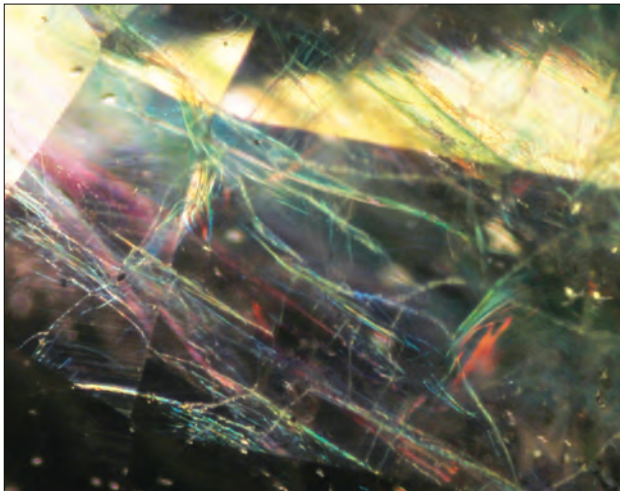


Figure 7: The lead-glass-filled fissures in the corundum show green colour concentrations as well as orange and blue flash effects depending on their orientation to the viewer. Photomicrograph by N. Atsawatanapirom; magnified 16 \times .

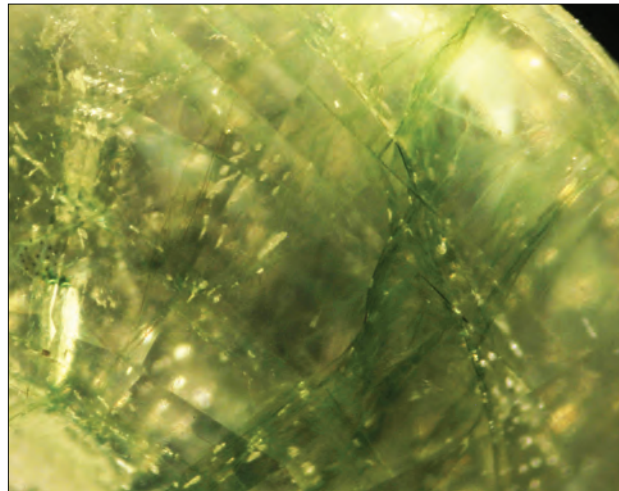


Figure 8: This 2.64 ct lead-glass-filled sapphire exhibits green colour concentrations along fissures that also contain flattened gas bubbles. Photomicrograph by N. Atsawatanapirom; magnified 10 \times .

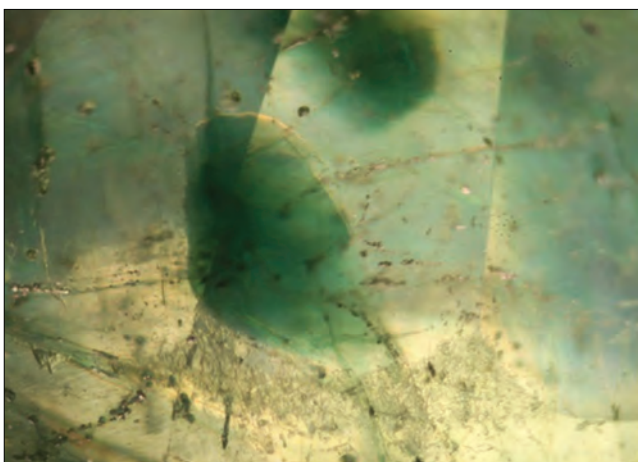


Figure 9: These views show a glass-filled cavity within a treated sapphire in darkfield (left) and reflected light (right). Photomicrographs by N. Susawee; magnified 20 \times .

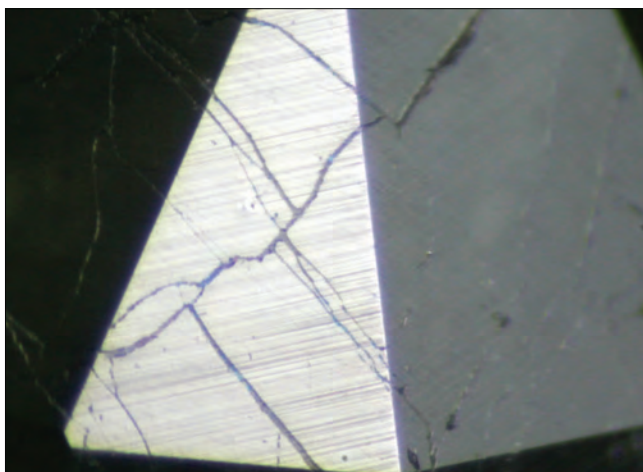


Figure 10: Reflected light reveals the lower lustre of the lead-glass filler in fissures (left, magnified 32 \times) and in a cavity (right, magnified 16 \times) as compared to the host sapphire. Photomicrographs by N. Atsawatanapirom.

of the glass filler is related to those elements. By comparison, the UV-Vis-NIR absorption spectra of the faceted samples showed strong absorption from around 500 nm toward shorter wavelengths, with a small Fe³⁺-related peak at ~450 nm and a weak, broad absorption band from ~600 to 800 nm (again, see Figure 12). This pattern is typical of Sri Lankan yellow sapphire (for which the colour is due to the stable colour centres; Pisutha-Arnond et al., 2004) in combination with some absorption contributed by the green glass filler in fissures and/or cavities. This result is consistent with the dichroism observed in the treated material (see Figure 5, right).

X-radiography

As expected, X-radiography of all the samples clearly revealed areas of glass filler within fissures and cavities in the faceted stones (Figure 13) and along the outer surfaces or rims of the rough samples. The filler appears darker than the host sapphire in these positive images; the light and dark patterns correspond to differences in the penetration capability of the X-rays through corundum versus lead glass. Such an appearance is also common for the previous types of lead-glass-filled corundum (e.g. SSEF, 2009).

DiamondView Imaging

The DiamondView instrument showed intersecting patterns of distinctly chalky blue fluorescence along the glass-filled fissures (Figure 14). Such images can provide valuable information not only for the identification of this type of treatment, but also for giving a rough estimate of the amount of

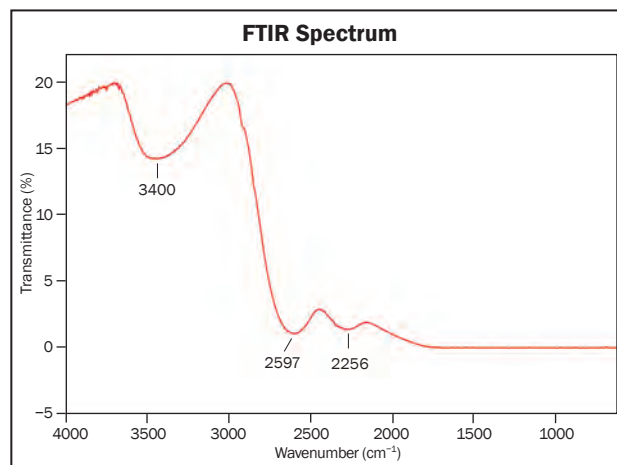


Figure 11: The mid-FTIR spectrum of green glassy residue on the surface of a treated rough sapphire shows strong absorption bands at approximately 3400, 2597 and 2256 cm⁻¹.

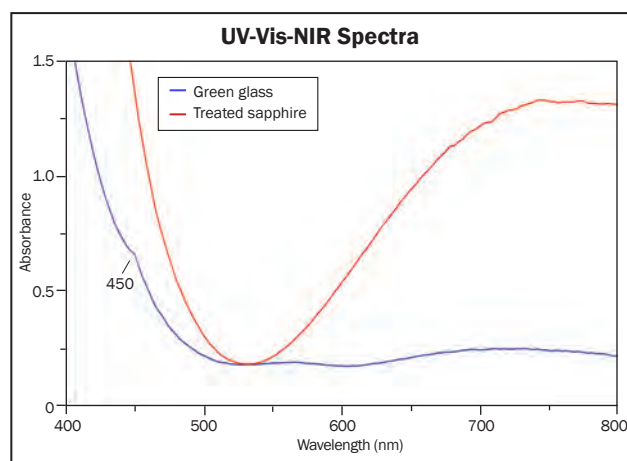
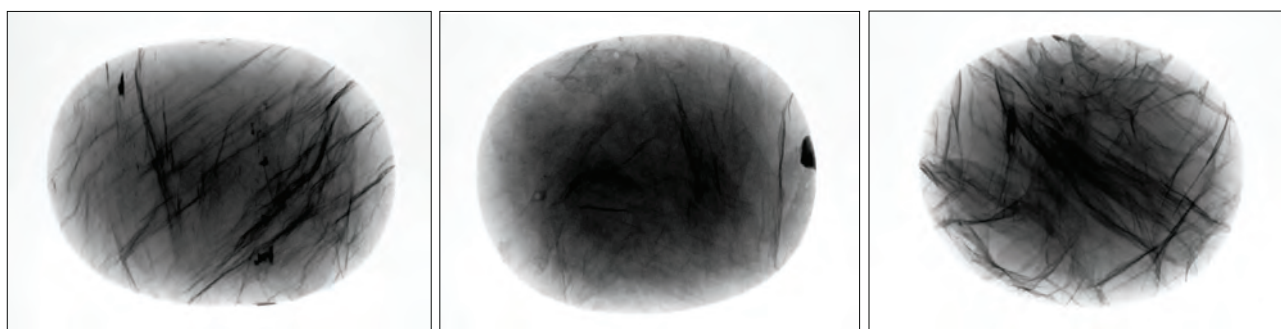


Figure 12: The UV-Vis-NIR spectrum of green glass protruding from a treated rough sapphire shows strong absorption through much of the visible range except for a transmission window in the green region at ~500–570 nm. By contrast, the spectrum of a faceted green lead-glass-filled sapphire shows an absorption edge at ~500 nm extending toward shorter wavelengths, with a small Fe³⁺-related absorption peak at ~450 nm and a weak, broad absorption band at ~600–800 nm.

Figure 13: These X-radiographs of three faceted green glass-filled sapphires (2.64, 5.90 and 2.79 ct, from left to right) show distinct opaque areas along the fractures and cavities. Images by S. Promwongnan.



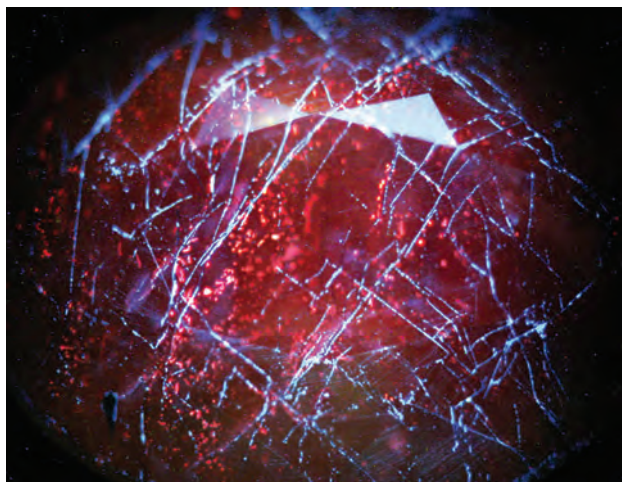


Figure 14: This DiamondView image reveals strong chalky blue fluorescence along the fissures of a 2.64 ct green glass-filled sapphire. Photo by S. Promwongnan.

glass filler that is present in a sample, similar to the X-radiographs.

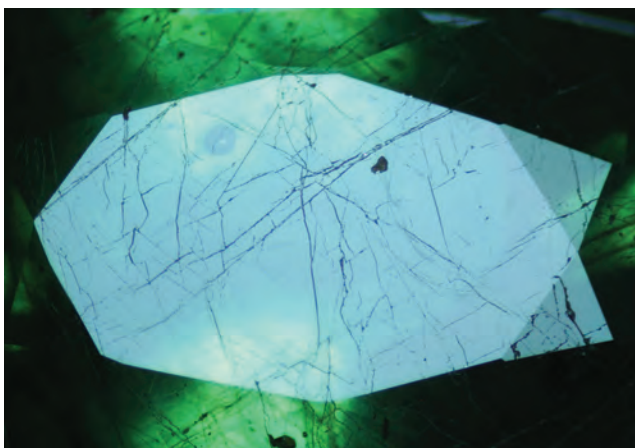
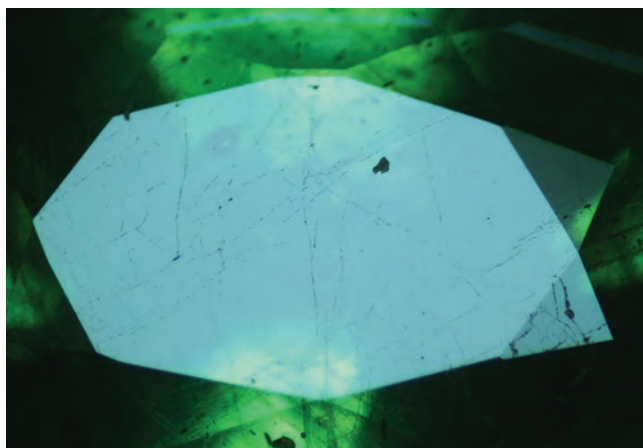
Preliminary Durability Testing

No damage to the lead-glass filler was observed after ultrasonic cleaning in an ordinary liquid soap solution for 15 minutes.

After exposure to a jewellery torch flame for one minute, some damage was observed on the surface of the lead-glass filler. Subsequent exposure to a strong direct torch flame for 30 seconds caused further damage to the filler.

Immersion in the rhodium electroplating agent for two minutes caused significant damage to the glass filler (Figure 15).

Figure 15: Lead-glass-filled fractures within the table of a sapphire are shown in reflected light before (left) and after (right) immersion in a rhodium electroplating agent for two minutes. The filler significantly dissolved, leaving many open fractures. Photomicrographs by S. Promwongnan; magnified 15 \times .



Conclusions

The identification of green lead-glass-filled sapphire is straightforward based on the same criteria used to distinguish previous lead-glass-type treatments. Microscopic observation is probably the simplest method to positively identify such treatments. The most prominent characteristics are orange and blue flash effects and green colour concentrations along fissures, and also flattened gas bubbles trapped within the glass-filled fissures.

EDXRF chemical analyses can reveal the presence of Pb and Si, along with Fe, Cu and Cr that probably act as colouring agents for the green glass filler. Furthermore, FTIR spectroscopy is also useful for proving the existence of a glass filling in such stones. X-radiography can help confirm the presence of lead glass, as well as give a rough estimation of the amount of filling material present in a sample. DiamondView images show chalky blue fluorescence along fissures and cavities, and also can help quantify the degree of filling.

Preliminary durability testing revealed some damage to the glass filler from a jewellery torch and rhodium electroplating solution, similar to results obtained previously for lead-glass-filled corundum (McClure et al., 2006; Leelawatanasuk, 2012; LMHC, 2012; Leelawatanasuk et al., 2013). Thus, we recommend that jewellers and consumers handle these treated stones with the special care that is typically recommended for lead-glass-filled materials.

Glass-filled corundum has been circulating in the gem market for many years. With recent developments in this type of treatment, green glass-filled sapphires are now available. There also is the potential for additional colours of glass fillers to be developed in the future.

References

- Henn U., Schollenbruch K. and Koch S., 2014. Gem Notes: Corundum with coloured lead-glass fillings. *Journal of Gemmology*, **34**(2), 111–112.
- Koivula J.I., Kammerling R.C., Fritsch E., Fryer C.W., Hargett D. and Kane R.E., 1989. The characteristics and identification of filled diamonds. *Gems & Gemology*, **25**(2), 68–83.
- Leelawatanasuk T., 2012. Urgent Lab Info: Blue dyed and clarity modified sapphire with cobalt+lead-glass filler in fractures and cavities. Gem and Jewelry Institute of Thailand, Bangkok, 29 May, www.git.or.th/2014/eng/testing_center_en/lab_notes_en/lab_en/2012/Cobalt_Lead_Glass_FF_Sapphire_Final.pdf.
- Leelawatanasuk T., Atichat W., Pisutha-Arnond V., Wattanakul P., Ounorn P., Manorotkul W. and Hughes R.W., 2013. Cobalt-doped glass-filled sapphires: An update. *Australian Gemmologist*, **25**(1), 14–20, www.git.or.th/2014/eng/testing_center_en/lab_notes_en/lab_en/2013/cobalt_doped_glass_filled_sapphires.pdf.
- LMHC, 2012. Information Sheet #3—Corundum. Laboratory Manual Harmonization Committee, Version 9, December, 3 pp., www.lmhc-gemology.org/pdfs/IS3_20121209.pdf.
- McClure S.F., Smith C.P., Wang W. and Hall M., 2006. Identification and durability of lead glass-filled rubies. *Gems & Gemology*, **42**(1), 22–34, <http://dx.doi.org/10.5741/gems.42.1.22>.
- Milisenda C.C., Horikawa Y., Manaka Y. and Henn U., 2006. Rubies with lead glass fracture fillings. *Journal of Gemmology*, **30**(1–2), 37–42, <http://dx.doi.org/10.15506/jog.2006.30.1.37>.
- Pisutha-Arnond V., Häger T., Wathanakul P. and Atichat W., 2004. Yellow and brown coloration in beryllium-treated sapphires. *Journal of Gemmology*, **29**(2), 77–103, <http://dx.doi.org/10.15506/jog.2004.29.2.77>.
- Rockwell K.M. and Breeding C.M., 2004. Lab Notes: Rubies, clarity enhanced with a lead glass filler. *Gems & Gemology*, **40**(3), 247–249.
- Smith C.P., McClure S.F., Wang W. and Hall M., 2005. Some characteristics of lead-glass-filled corundum. *Jewellery News Asia*, **255**, November, 79–84.
- SSEF, 2009. How much glass is in the ruby? *SSEF Facette*, **19**, 8–9, www.ssef.ch/fileadmin/Documents/PDF/facette16.pdf.

The Authors

Thanong Leelawatanasuk, Namrawee Susawee, Supparat Promwongnan and Nicharee Atsawatanapirom

The Gem and Jewelry Institute of Thailand, ITF Tower, Silom Rd., Bangkok 10500, Thailand.
Email: lthanong@git.or.th

Acknowledgements

The authors thank GIT's academic advisors, Dr Visut Pisutha-Arnond, Wilawan Atichat and Boontawee Sriprasert for their extensive reviews of this article.



Save the date | Gem-A Conference 2015
incorporating the 18th FEEG Symposium

Saturday 21 November — Sunday 22 November

Demantoid from Balochistan, Pakistan: Gemmological and Mineralogical Characterization

*Ilaria Adamo, Rosangela Bocchio, Valeria Diella,
Franca Caucia and Karl Schmetzer*

During the past few years, small demantoid crystals, indicated as coming from the Muslim Bagh area of Balochistan Province, have been available occasionally in the gem market in Peshawar, Pakistan. The gemmological properties and chemical data for this material are reported here. These bright green to yellowish green garnets are almost pure andradite (typically ≥ 98 mol.%, with RI > 1.79 and SG = 3.80–3.90). They contain inclusions of serpentine-group minerals, including the well-known fibrous ‘horsetails’, which are characteristic of a serpentinitic geological origin. Black crystals of Cr-rich magnetite are also common inclusions in demantoid from this relatively new locality. Iron and traces of chromium cause the green colour of these garnets.

The Journal of Gemmology, 34(5), 2015, pp. 428–433, <http://dx.doi.org/10.15506/JoG.2015.34.5.428>
© 2015 The Gemmological Association of Great Britain

Introduction

Demantoid, the green variety of andradite [$\text{Ca}_3\text{Fe}_2(\text{SiO}_4)_3$], is one of the most appreciated gems of the garnet group (O’Donoghue, 2006). The traditional sources are Russia and Italy, whereas commercially important deposits recently have been found in northern Madagascar, south-east Iran, northern Pakistan (Kaghan Valley) and central Namibia (Philips and Talantsev, 1996; Lind et al., 1998; Quinn, 2005; Du Toit et al., 2006; Adamo et al., 2009, 2011; Pezzotta et al., 2011).

In recent years, gem-quality demantoid crystals have occasionally appeared in Pakistan’s Peshawar gem market that are indicated as having come from the Muslim Bagh area of Balochistan, a large province in south-west Pakistan. Brown and orange-brown andradite gems from Balochistan

have previously been reported by Fritz and Laurs (2007), whereas recently Palke and Pardiou (2014) also described the occurrence of green samples (demantoid).

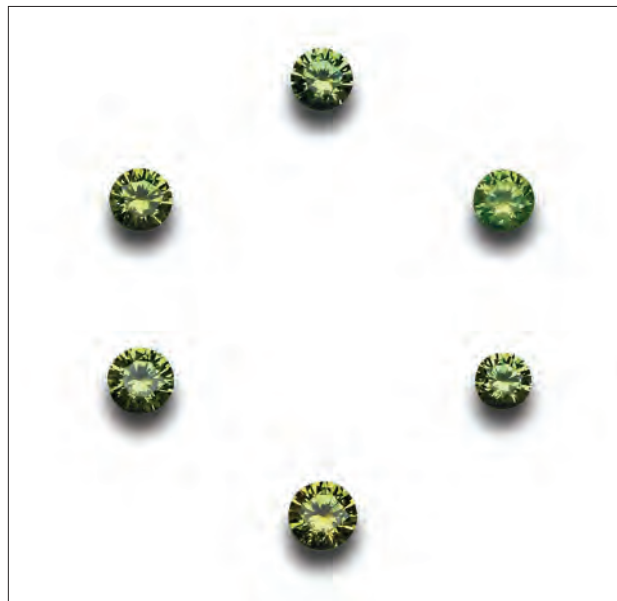
The garnets consist of well-formed dodecahedral crystals with an attractive green to yellowish green colour, although they are typically very small, rarely exceeding 1 ct (e.g. Figure 1). Bigger pieces of rough (up to 25 ct) are also available, but they are too included to cut larger stones.

The geology of the Muslim Bagh area locally consists of a nearly complete ophiolite sequence, mainly composed of peridotite (i.e. harzburgite and dunite) that is partially to completely serpentinitized, with many outcrops of dunite containing chromite deposits (Kakar et



Figure 1 (above): A small demantoid deposit in Balochistan, Pakistan, is reportedly the source of these fine demantoid crystals (0.78–0.98 ct), which were among those studied for this article. Photo by Stefan Hanken.

Figure 2 (right): These round brilliants (0.05–0.10 ct) are some of the demantoid gems from Balochistan investigated for this study. Photo by Andrea Zullino.



al., 2013). Naeem et al. (2014) briefly mentioned a variety of gems and minerals that are found in this area, including ‘tsavorite garnet’, but not demantoid.

This study provides a gemmological and mineralogical characterization of demantoid from Balochistan, investigating rough and cut samples by means of standard gemmological methods, as well as electron microprobe and laser ablation–inductively coupled plasma–mass spectroscopy (LA-ICP-MS) chemical analyses.

Materials and Methods

We examined 30 demantoid samples from Balochistan, consisting of 20 pieces of rough (0.18–0.98 ct; e.g. Figure 1) and 10 melee-sized faceted specimens (0.05–0.10 ct; e.g. Figure 2). All of the samples, which were kindly provided by a collector, were examined by standard gemmological methods to determine their optical properties, SG, UV fluorescence and microscopic features.

Quantitative chemical analyses were obtained from polished surfaces of four rough samples by electron microprobe analysis (EMPA) using a JEOL JXA-8200 instrument in wavelength-dispersive mode, with an accelerating voltage of 15 kV, beam current of 15 nA, and count times of 60 s on peaks and 30 s on background. The following elements were measured: Na, Mg, Al, Si, K, Ca, Ti, V, Cr, Mn, Co and Fe. The raw data were corrected for matrix effects using a conventional $\rho\rho Z$ routine in the JEOL software package.

To compare the composition of these Balochistan samples with demantoid from various localities (see Bocchio et al., 2010), we measured the trace-element composition of five rough samples from Balochistan (including the four analysed by EMPA) by means of LA-ICP-MS. The instrument consisted of a Quantel Brilliant 266 nm Nd:YAG laser coupled to a PerkinElmer DRCE quadrupole ICP-MS. The external calibration standard was NIST-SRM612 glass, and Ca was the internal standard. The spot size was 50 μm . The following elements were analysed: Sc, Ti, V, Cr, Co, Ni, Zn, Sr, Y, Zr, La, Ce, Nd, Sm, Eu, Gd, Tb, Dy, Er, Yb and Lu.

Results and Discussion

Standard Gemmological Properties

The standard gemmological properties of the Balochistan samples are summarized in Table I, and are typical of andradite (cf. O’Donoghue, 2006). All the samples were bright green or yellowish green with low-to-moderate saturation (Figures 1 and 2). The crystals were well formed, with the dodecahedron {110} as the dominant form (Figure 1). A few specimens also showed some intergrown individuals that may be associated with dodecahedral twinning (Figure 3). Nearly all the samples contained fibrous crystalline inclusions, identified as chrysotile by EMPA, in the typical ‘horsetail’ arrangement (Figure 4). These curved fibres of chrysotile were sometimes associated

with opaque whitish masses, chemically identified as serpentine-group minerals, probably antigorite (Figure 4, right). Opaque black crystalline inclusions, identified by EMPA as Cr-bearing magnetite, were often present (Figure 5). These internal features are characteristic of serpentinite-hosted demantoid, as is also the case for stones from Russia, Italy, Iran and northern Pakistan (Phillips and Talantsev, 1996; Milisenda et al., 2001; Gübelin and Koivula, 2005; Du Toit et al., 2006; Adamo et al., 2009). In particular, the inclusions closely resemble those in demantoid from Val Malenco, Italy (Adamo et al., 2009), whereas the acicular diopsides reported in some demantoid samples from Russia (Krzemnicki, 1999) were not observed in our Balochistan samples.

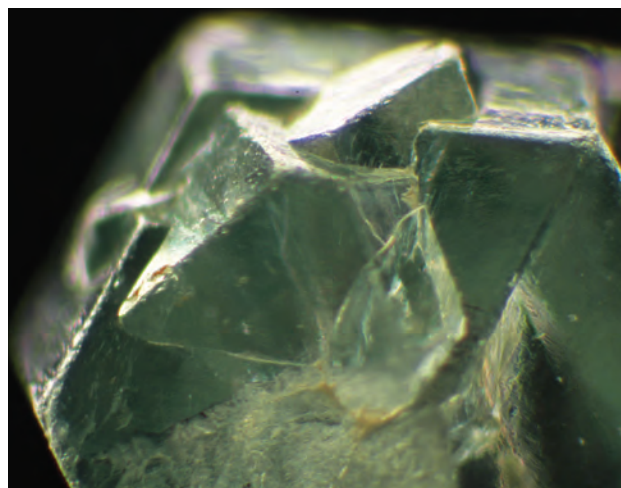


Figure 3: Several intergrown crystals show re-entrant angles that may indicate dodecahedral twinning in this demantoid sample from Balochistan. Photomicrograph by Andrea Zullino; magnified 20x.

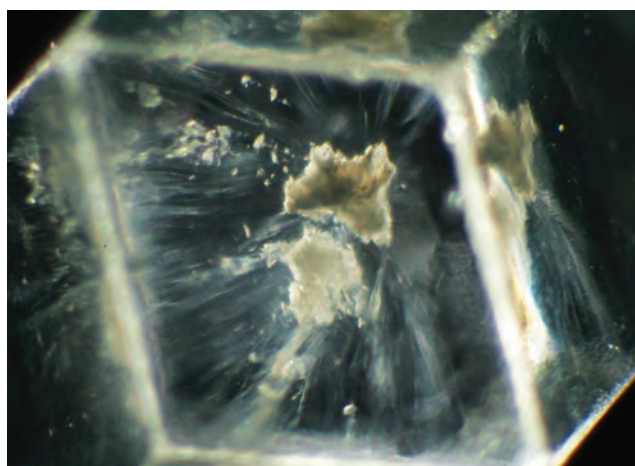
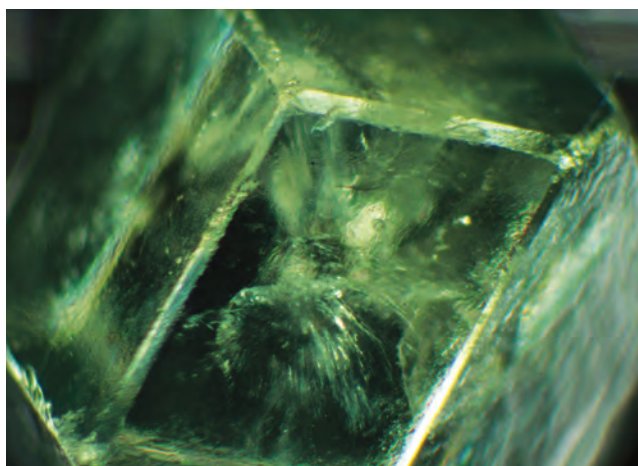


Figure 4: Fibrous (chrysotile; left) and massive (probably antigorite; right) serpentine-group mineral inclusions are seen in these demantoid samples from Balochistan. Photomicrographs by Andrea Zullino; magnified 45x.

Table 1: Gemmological properties of demantoid from Balochistan, Pakistan.

Colour	Green to yellowish green
Diaphaneity	Transparent
Optic character	Optically isotropic with moderate to strong anomalous double refraction
RI	Greater than 1.79
SG	3.80–3.90
Fluorescence	Inert to long- and short-wave UV
Internal features	'Horsetail' and fibrous crystalline inclusions (chrysotile), whitish opaque inclusions (probably antigorite), black opaque crystals (Cr-bearing magnetite), growth structures and fractures

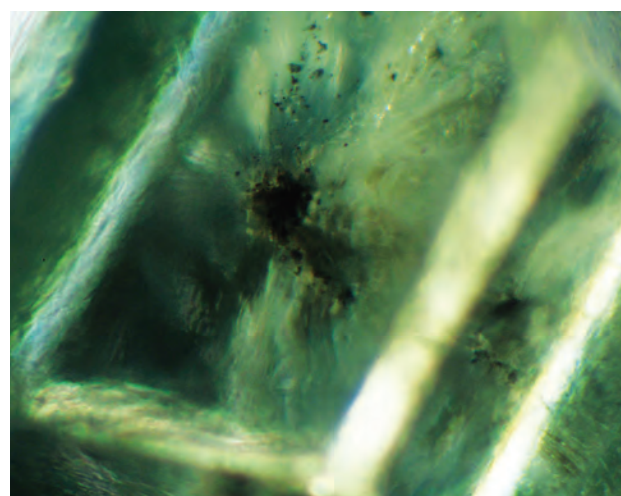


Figure 5: Inclusions of Cr-rich magnetite are present in this demantoid crystal from Balochistan. Photomicrograph by Andrea Zullino; magnified 45x.

Table II: Chemical composition obtained by EMPA of demantoid from Balochistan, Pakistan.^a

Sample	1	3	4	21	4-5 ^b	4-6 ^b	4-7 ^b	4-2 ^b
No. analyses	40	40	60	40	1	1	1	1
Oxides (wt.%)								
SiO ₂	35.75	35.73	35.67	35.83	35.42	35.29	34.98	35.45
TiO ₂	0.02	0.01	0.02	0.01	0.02	bdl ^c	0.05	bdl
V ₂ O ₃	0.02	0.01	0.01	0.01	0.03	bdl	bdl	bdl
Al ₂ O ₃	0.14	0.18	0.11	0.11	0.08	0.05	0.14	0.04
Cr ₂ O ₃	bdl	bdl	bdl	bdl	0.92	0.21	0.21	0.08
Fe ₂ O ₃ tot	30.79	30.73	30.86	30.91	30.28	31.02	30.44	30.93
MnO	0.02	0.02	0.02	0.02	0.05	0.03	0.03	0.04
MgO	0.21	0.20	0.18	0.18	0.13	0.12	0.12	0.11
CaO	33.40	33.39	33.36	33.37	33.00	33.18	32.93	33.11
Na ₂ O	0.02	0.01	0.01	0.01	bdl	bdl	bdl	bdl
Total	100.36	100.27	100.22	100.45	99.92	99.90	98.90	99.76
Ions calculated on 12 oxygens								
Si	3.007	3.007	3.006	3.011	2.996	2.989	2.990	3.004
Ti	0.001	0.001	0.001	0.001	0.001	bdl	0.001	bdl
V	0.001	0.001	0.001	0.001	0.002	bdl	bdl	bdl
Al	0.014	0.018	0.011	0.011	0.008	0.005	0.014	0.004
Cr	bdl	bdl	bdl	bdl	0.061	0.014	0.015	0.005
Fe ³⁺	1.948	1.946	1.956	1.954	1.927	1.977	1.958	1.972
Mn	0.001	0.001	0.001	0.001	0.003	0.002	0.002	0.003
Mg	0.027	0.026	0.022	0.022	0.016	0.015	0.016	0.014
Ca	3.010	3.011	3.011	3.004	2.990	3.011	3.016	3.005
Na	0.002	0.001	0.002	0.001	bdl	bdl	bdl	bdl
Mol.% end-members								
Andradite	98.14	98.10	98.50	98.53	95.74	98.49	97.83	98.99
Pyrope	0.88	0.84	0.74	0.73	0.54	0.51	0.52	0.46
Grossular	0.71	0.90	0.54	0.55	0.41	0.24	0.70	0.19
Uvarovite	-	-	-	-	3.05	0.69	0.73	0.27
Others	0.26	0.16	0.22	0.18	0.25	0.07	0.23	0.10

^a K and Co were analysed for, but not detected.

^b Analysis points indicated in Figure 6 (left).

^c Abbreviation: bdl = below detection limit.

Chemical Composition

The chemical compositions obtained by EMPA and LA-ICP-MS of demantoid from Balochistan are reported in Tables II and III, respectively.

Electron microprobe analyses showed that the garnets consist of nearly pure andradite (typically ≥98 mol.%), with the exception of Cr-rich zones of the crystals located close to Cr-bearing magnetite inclusions. This composition is typical of gem-quality demantoid (Bocchio et al., 2010; Adamo et al., 2011). Traces of Mg, Al, Ti, V, Cr and Mn also were measured. In particular, Cr ranged from below the detection limit of the microprobe (0.01

wt.%) up to ~1 wt.% Cr₂O₃ measured adjacent to a Cr-bearing magnetite inclusion that itself contained ~16 wt.% Cr₂O₃ (Figure 6). The Cr content of the garnet decreased with increasing distance from such inclusions, as demonstrated by analyses 4-5 through 4-7 in Table II. Magnetite and Cr-rich magnetite are common in demantoid associated with serpentinites, and their presence has been described in detail by Adamo et al. (2009) in demantoid from Val Malenco.

The trace elements measured by LA-ICP-MS are generally comparable with the contents previously reported for demantoid samples with

Table III: Trace-element composition obtained by LA-ICP-MS of demantoid from Balochistan, Pakistan.*

Sample	1	3	4	10	21
Trace elements (ppm)					
Sc	2.50	1.62	2.79	1.25	0.93
Ti	12.7	42.1	33.1	13.7	12.6
V	9.54	8.09	9.72	5.81	3.14
Cr	16.1	18.1	23.6	3.85	3.71
Co	0.93	1.03	0.80	1.02	1.07
Ni	0.79	bdl	1.05	0.38	0.35
Zn	bdl	3.26	bdl	3.08	bdl
Sr	0.04	0.04	0.06	0.07	0.04
Y	0.10	0.09	0.03	0.01	0.04
Zr	0.07	0.04	bdl	bdl	0.10
La	2.04	0.87	0.30	1.05	1.34
Ce	0.66	0.32	0.20	0.19	0.58
Nd	0.11	0.05	0.02	0.06	bdl
Sm	bdl	bdl	bdl	0.12	0.11
Eu	1.99	bdl	bdl	bdl	bdl
Gd	bdl	bdl	0.007	bdl	bdl
Tb	bdl	0.54	bdl	bdl	bdl
Dy	bdl	0.17	0.03	bdl	0.11
Er	0.25	bdl	0.01	0.11	bdl
Yb	0.32	0.04	0.03	bdl	0.14
Lu	bdl	bdl	bdl	0.16	0.35
ΣREE	5.36	1.98	0.60	1.70	2.62

* Average of three analyses each. Abbreviation: bdl = below detection limit.

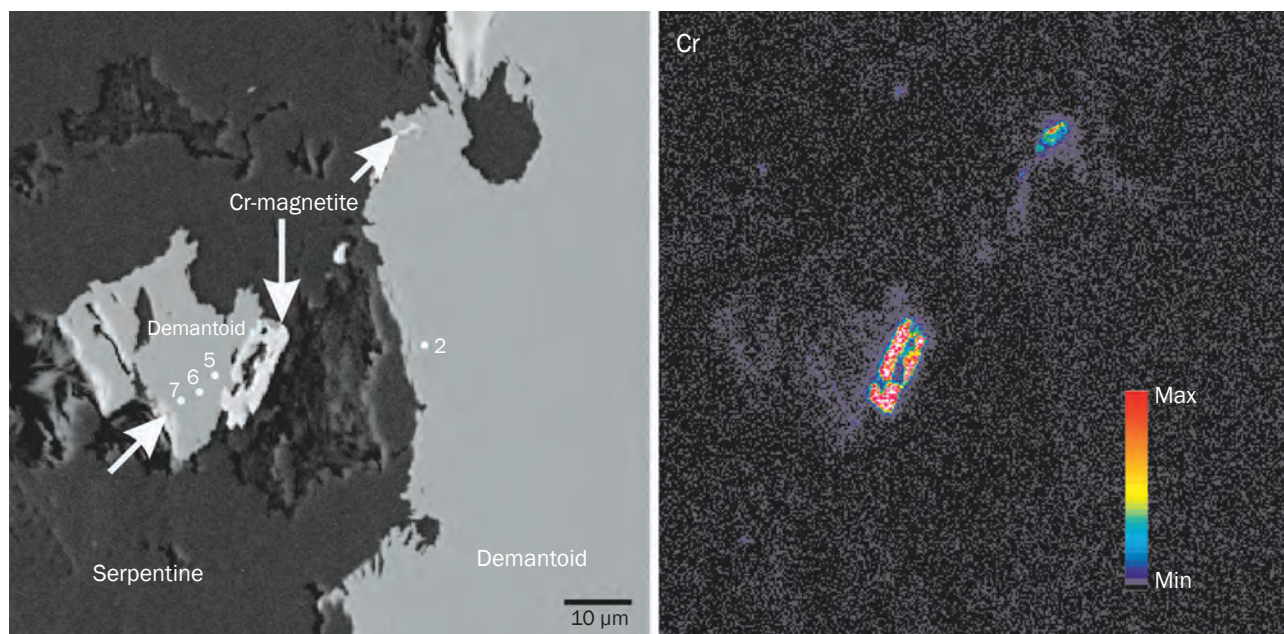
andradite contents of >98 mol.% and related to serpentinitic environments (Bocchio et al., 2010). However, compared to the data of the sample from northern Pakistan (Kaghan Valley) analysed by Bocchio et al. (2010), the Balochistan demantoid appears depleted in all the elements forming the ‘first transition series’ (i.e. Sc, Ti, V, Cr, Co, Ni and Zn) and also contains lower Y and Zr. This is also in agreement with the data of Milisenda et al. (2001), who found higher amounts of chromium (average 0.15 wt.% Cr₂O₃) in demantoid from the Kaghan Valley.

The content of rare-earth elements (REE) compares well with that of other demantoid samples associated with serpentinites, showing a general light rare-earth (LREE) enrichment and heavy rare-earth (HREE) depletion. Conversely, the LREE/HREE ratio (La/Yb = 4.31–14.42) is higher than that calculated for the Kaghan Valley sample (La/Yb = 0.06). Only two of our analyses exhibited a strong Eu anomaly because this element was otherwise not detected.

Concluding Remarks

Demantoid reportedly from Balochistan, Pakistan, appears occasionally in the Peshawar gem market as crystals rarely exceeding 1 ct that are suitable for faceting melee-sized gems (generally smaller than 0.20 ct). The gemmological properties,

Figure 6: This back-scattered electron image (left) and X-ray map showing Cr concentration (right) depict inclusions of serpentine and Cr-bearing magnetite in a demantoid from Balochistan. The high Cr content of the magnetite grain is clearly indicated in the X-ray map. The numbers in the left image correspond to the analyses points given in Table II.



microscopic features and chemical composition of these demantoid gems are consistent with those from other sources associated with serpentinite host rocks. Information about the future potential of the Balochistan deposit is currently unknown.

References

- Adamo I., Bocchio R., Diella V., Pavese A., Vignola P., Prosperi L. and Palanza V., 2009. Demantoid from Val Malenco, Italy: Review and update. *Gems & Gemology*, **45**(4), 280–287, <http://dx.doi.org/10.5741/gems.45.4.280>.
- Adamo I., Gatta G.D., Rotiroti N., Diella V. and Pavese A., 2011. Green andradite stones: Gemmological and mineralogical characterisation. *European Journal of Mineralogy*, **23**(1), 91–100, <http://dx.doi.org/10.1127/0935-1221/2011/0023-2079>.
- Bocchio R., Adamo I. and Diella V., 2010. The profile of trace elements, including the REE, in gem-quality green andradite from classic localities. *Canadian Mineralogist*, **48**(5), 1205–1216, <http://dx.doi.org/10.3749/canmin.48.5.1205>.
- Du Toit G., Mayerson W., van der Bogert C., Douman M., Befi R., Koivula J.I. and Kiefert L., 2006. Demantoid from Iran. *Gems & Gemology*, **42**(3), 131.
- Fritz E.A. and Laurs B.M., 2007. Gem News International: Andradite from Balochistan, Pakistan. *Gems & Gemology*, **43**(4), 373.
- Gübelin E.J. and Koivula J.I., 2005. *Photoatlas of Inclusions in Gemstones*, Vol. 2. Opinio Publishers, Basel, Switzerland, 830 pp.
- Kakar M.I., Mahmood K., Khan M., Kasi A.K. and Manan R.A., 2013. Petrology and geochemistry of gabbros from the Muslim Bagh ophiolite: Implications for their petrogenesis and tectonic setting. *Journal of Himalayan Earth Sciences*, **46**(1), 19–30.
- Krzemnicki M.S., 1999. Diopside needles as inclusions in demantoid garnet from Russia: A Raman microspectrometric study. *Gems & Gemology*, **35**(4), 192–195, <http://dx.doi.org/10.5741/gems.35.4.192>.
- Lind Th., Henn U. and Bank H., 1998. New occurrence of demantoid in Namibia. *Australian Gemmologist*, **20**(2), 75–79.
- Milisenda C.C., Henn U. and Henn J., 2001. Demantoid aus Pakistan. *Gemmologie: Zeitschrift der Deutschen Gemmologischen Gesellschaft*, **50**(1), 51–56.
- Naeem A., Mahmood K. and Kakar M.I., 2014. A study of the gemstones from the Muslim Bagh ophiolite complex, Balochistan, Pakistan. *Earth Sciences Pakistan 2014*, 29–31 August, Peshawar, Pakistan, 99.
- O'Donoghue M., 2006. *Gems*, 6th edn. Butterworth-Heinemann, Oxford, 874 pages.
- Palke A.C. and Pardieu V., 2014. Gem News International: Demantoid from Baluchistan Province in Pakistan. *Gems & Gemology*, **50**(4), 302–303.
- Pezzotta F., Adamo I. and Diella V., 2011. Demantoid and topazolite from Antetazambato, northern Madagascar: Review and new data. *Gems & Gemology*, **47**(1), 2–14, <http://dx.doi.org/10.5741/gems.47.1.2>.
- Phillips W.R. and Talantsev A.S., 1996. Russian demantoid, czar of the garnet family. *Gems & Gemology*, **32**(2), 100–111, <http://dx.doi.org/10.5741/gems.32.2.100>.
- Quinn E.P., 2005. Gem News International: Demantoid from northern Pakistan. *Gems & Gemology*, **41**(2), 176–177.

The Authors

Dr Ilaria Adamo

Italian Gemmological Institute (IGI), Milan, and Dipartimento di Scienze della Terra, Università degli Studi di Milano, Italy
Email: ilaria.adamo@guest.unimi.it

Dr Rosangela Bocchio

Dipartimento di Scienze della Terra
Università degli Studi di Milano, Italy

Dr Valeria Diella

CNR—Istituto per la Dinamica dei Processi Ambientali, Milan, Italy

Dr Franca Caucia

Dipartimento di Scienze della Terra e dell'Ambiente, Università degli Studi di Pavia, Italy

Dr Karl Schmetzer

Petershausen, Germany

Acknowledgements

The authors thank S. Hanken (Waldkraiburg, Germany) for providing the demantoid samples. Microprobe analyses were performed at the Dipartimento di Scienze della Terra, Università degli Studi di Milano, Italy, with the technical assistance of A. Risplendente. LA-ICP-MS analyses were carried out at the CNR—Istituto di Geoscienze e Georisorse, Pavia, Italy, with the technical assistance of Dr A. Zanetti. S. Salvini is also acknowledged for his collaboration during this research.

Nail-head Spicules as Inclusions in Chrysoberyl from Myanmar

Karl Schmetzer and Michael S. Krzemnicki

Multiphase inclusions developed in the form of nail-head spicules in a colourless chrysoberyl crystal from Myanmar were examined by optical means and by Raman microspectroscopy. The growth tubes of the multiphase inclusions contain CO₂, and the grains attached to the ends of these tubes are most likely chrysoberyl crystals (based on Raman spectra and observation of birefringence), some of which are partially covered with an iron-bearing substance, and possibly also negative crystals.

The Journal of Gemmology, 34(5), 2015, pp. 434–438, <http://dx.doi.org/10.15506/JoG.2015.34.5.434>
© 2015 The Gemmological Association of Great Britain

Introduction

Nail-head spicules are sometimes found as inclusions in synthetic gem materials (e.g. synthetic emerald or quartz), but occasionally also in natural gems such as sapphire, spinel, tourmaline and quartz (Schmetzer et al., 1999, 2011; Choudhary and Golecha, 2007). Recently, one of the authors (KS) examined a group of rough and faceted, slightly yellow, greenish yellow or colourless chrysoberyls from Myanmar that afforded an opportunity to augment the foregoing list. The samples had been obtained from a collector, who bought them in the trade. The chrysoberyls were said to originate from the Mogok region of Myanmar. One of them contained nail-head spicules, and this note describes that crystal's morphology and its inclusions.

Results

The colourless chrysoberyl (Figure 1a) consisted of a 6.2 × 5.2 mm tabular crystal with broken ends. The main tabular face was determined

by optical means (i.e. by the position of both optic axes; see Schmetzer, 2011) as the **b** {010} pinacoid. Because the crystal was broken at both ends, we could determine only two additional forms: a smaller **a** {100} pinacoid and a small **m** {110} prism. Several complete slightly yellow or colourless crystals from the same group showed a similar tabular habit with a dominant **b** pinacoid, and one typical example is depicted in Figure 2.

The subject crystal contained several growth tubes running parallel to the c-axis, with colourless or slightly yellowish brown inclusions at one end of the elongated cavities (Figure 1a,b). One of the two larger growth tubes (labelled A in the figures) was completely trapped within the colourless host, but the second (labelled B) was open at its end to the surface of the broken crystal. With permission from the owner of the crystal, one of the **b** faces was polished to allow better examination of the inclusions. Growth tube A was colourless with a homogeneous, transparent appearance, while tube B was partly filled with an inhomogeneous-appearing yellowish brown fine-grained material (Figure 3).

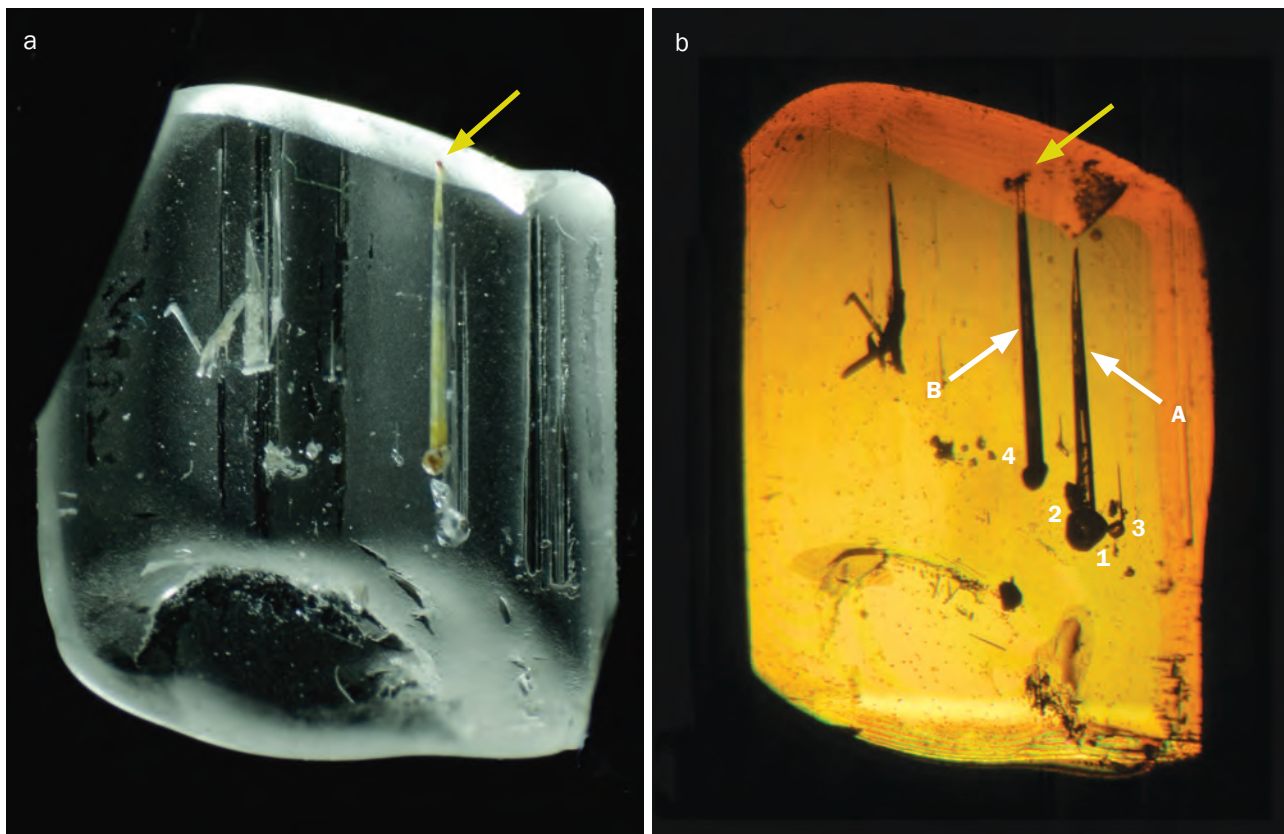


Figure 1: This colourless tabular chrysoberyl crystal (6.2×5.2 mm) reportedly from the Mogok area of Myanmar was studied for this report, and is shown in reflected light (a; photomicrograph by M. S. Krzemnicki) and in immersion between crossed polarizers (b; photomicrograph by K. Schmetzer). It contains multiphase inclusions consisting of growth tubes (labelled A and B) with attached grains (labelled 1–4). Growth tube A is completely trapped within the chrysoberyl host, while tube B is open at its end to the broken surface of the host (yellow arrows).

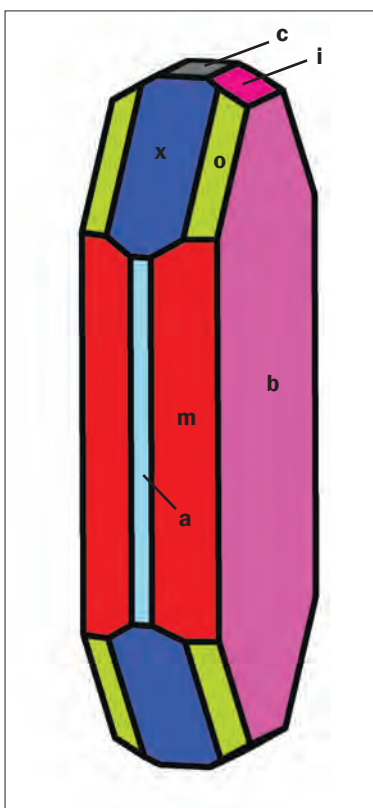
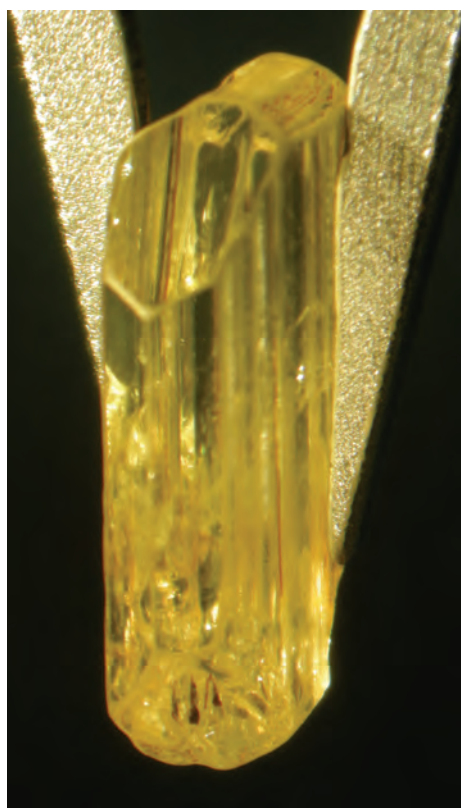


Figure 2: This yellow chrysoberyl crystal (2.8×10.4 mm) reportedly from the Mogok area of Myanmar shows a tabular habit parallel to b $\{010\}$; similar crystals were frequently seen within the group of samples examined. The crystal forms determined are the pinacoids a $\{100\}$, b $\{010\}$ and c $\{001\}$, the prisms i $\{011\}$, x $\{101\}$ and m $\{110\}$, as well as the dipyramid o $\{111\}$. Photomicrograph and crystal drawing by K. Schmetzer.

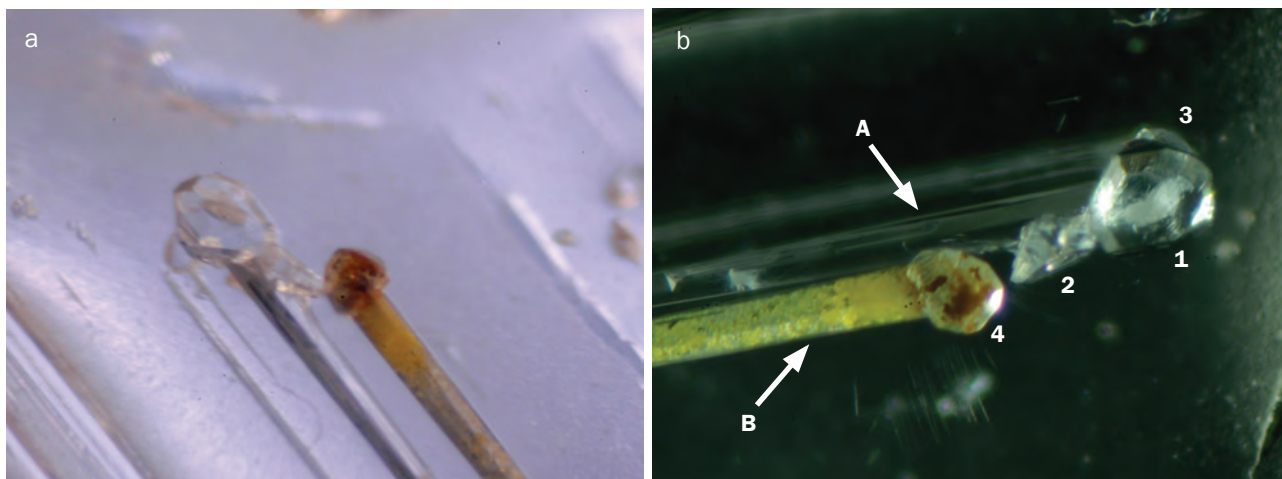


Figure 3: The colourless chrysoberyl crystal contains multiphase inclusions in the form of nail-head spicules. These inclusions consist of growth tubes (A and B) with attached grains showing euhedral crystal forms (1, 3 and 4) or irregular shapes (2). The high-relief appearance of the crystalline inclusions in photo b is due to the use of reflected light with a dark background to obtain the maximum contrast for these tiny colourless inclusions. The field of view of the images is 2.0 × 1.5 mm (a) and 1.8 × 1.3 mm (b); photomicrographs by M. S. Krzemnicki.

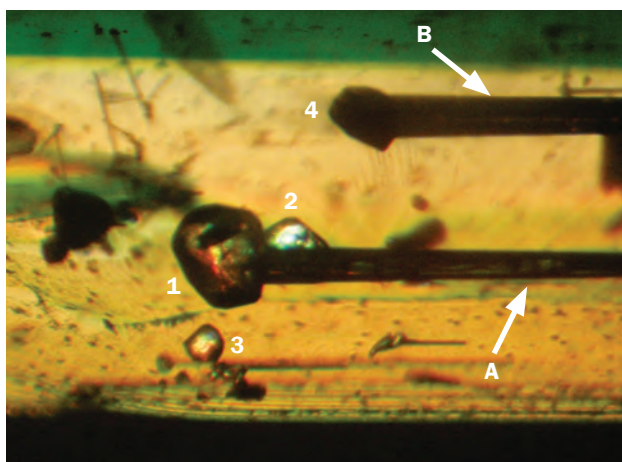
Attached to the end of tube A we observed one irregularly shaped colourless inclusion (labelled 2) and one colourless inclusion (labelled 1) with a tabular habit and clearly visible crystal faces (Figure 3). Within the tabular inclusion 1 was a central area that appeared milky white. Close to this assemblage we observed an additional colourless inclusion (labelled 3) attached to a small growth tube (not labelled in the figures).

At the end of tube B, another inclusion (labelled 4) with plane faces was seen, and part of the surface of this inclusion was covered with a yellowish brown phase (Figure 3). Between

crossed polarizers (Figure 4), the colourless inclusions (1, 2 and 3) attached to closed growth tubes showed birefringence, but grain 4 attached to growth tube B was opaque.

An examination of the inclusions with Raman micro-spectroscopy revealed the presence of CO₂ in growth tube A that was completely trapped within the host chrysoberyl (Figure 5). The various colourless inclusions (1, 2 and 3) at the ends of the enclosed growth tubes showed only the Raman spectra of the chrysoberyl host. Conversely, inclusion 4 at the end of the open tube B, which was at least partly covered with a yellowish brown substance, showed Raman lines for chrysoberyl along with additional peaks corresponding to iron oxides and/or iron hydroxides (Figure 5).

Figure 4: Viewed between crossed polarizers, the grains at the end of the growth tubes (A and B) show birefringence (1, 2 and 3) or appear dark (4). The image was taken in immersion with a field of view of 2.5 × 1.9 mm; photomicrograph by K. Schmetzer.



Discussion

Raman spectroscopy of tiny inclusions trapped in a transparent host frequently reveals a spectrum that consists of the characteristic Raman lines of the host with additional lines of the solid or fluid inclusion. If a solid inclusion is identical to the host, Raman spectroscopy cannot separate the two solid phases. Consequently, a Raman spectrum of an inclusion showing only the lines of the host could indicate either a mineral phase identical with the host or a cavity (i.e. a negative crystal). Grains 1, 2 and

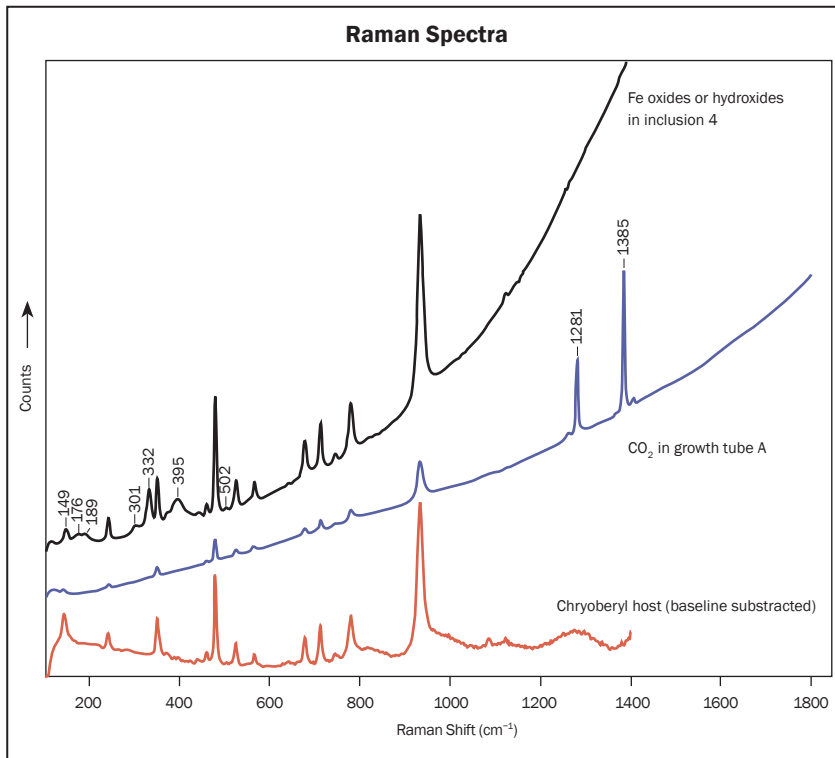


Figure 5: Raman micro-spectroscopy of inclusions in the chrysoberyl showed the presence of iron oxides or hydroxides in the yellowish brown inclusion 4 at the end of the open tube B (top spectrum) as well as the presence of CO₂ in growth tube A (middle spectrum); the bottom spectrum shows only the Raman lines of the host chrysoberyl. Peak labels are provided for the inclusion phases present.

3 showed the Raman spectrum of chrysoberyl and were birefringent. These results indicate that the grains are chrysoberyl. Such inclusions of chrysoberyl in chrysoberyl are rare but have been described occasionally, such as in alexandrite from the Lake Manyara deposit in Tanzania (Schmetzer and Malsy, 2011). In both that alexandrite and the present sample, the orientation of the chrysoberyl inclusions was different from that of the chrysoberyl host.

For grain 4 at the end of tube B that is open to the surface, the Raman spectrum showed lines for chrysoberyl and an additional iron-bearing phase. The microscopic examination did not show birefringence, but this could be due to the low magnification of the gemmological microscope and/or the presence of the iron-bearing material. The yellowish brown substance could cover the surface of a trapped tiny chrysoberyl crystal; could fill, at least partly, the cavity of a negative crystal; or could adhere to the walls of such a negative crystal. However, because a nail-head spicule requires an obstacle during the growth of the host crystal, the first possibility is most likely.

The fine-grained inhomogeneous material in the open tube B may be of secondary origin, a scenario sometimes described as ‘iron staining’. This scenario includes the possibility of iron

staining of at least a part of the surface of a chrysoberyl crystal trapped at the end of such an open tube.

Although we could confirm the presence of chrysoberyl crystals at the ends of other growth tubes—and although the trapping of a tiny chrysoberyl crystal with iron staining is the most likely scenario—the possibility of a negative crystal terminating the open tube B could not be completely excluded. Only a destructive examination (cutting the host crystal to expose the surface of the inclusion) might afford a definitive explanation.

Conclusion

Colourless chrysoberyl, reportedly from Myanmar, may be added to the list of natural gem materials that have been found to contain multiphase nail-head spicules, consisting in this instance primarily of growth tubes with attached euhedral or irregular chrysoberyl crystals.

References

- Choudhary G. and Golecha C., 2007. A study of nail-head spicule inclusions in natural gemstones. *Gems & Gemology*, **43**(3), 228–235, <http://dx.doi.org/10.5741/gems.43.3.228>.

- Schmetzer K., 2011. Measurement and interpretation of growth patterns in chrysoberyl, including alexandrite. *Journal of Gemmology*, **32**(5–8), 129–144, <http://dx.doi.org/10.15506/jog.2011.32.5.129>.
- Schmetzer K. and Malsy A.-K., 2011. Alexandrite and colour-change chrysoberyl from the Lake Manyara alexandrite-emerald deposit in northern Tanzania. *Journal of Gemmology*, **32**(5–8), 179–209, <http://dx.doi.org/10.15506/jog.2011.32.5.179>.
- Schmetzer K., Kiefert L. and Bernhardt H.-J., 1999. Multicomponent inclusions in Nacken synthetic emeralds. *Journal of Gemmology*, **26**(8), 487–500, <http://dx.doi.org/10.15506/jog.1999.26.8.487>.
- Schmetzer K., Bernhardt H.-J. and Hainschwang T., 2011. Chemical and growth zoning in trapiche tourmaline from Zambia – a re-evaluation. *Journal of Gemmology*, **32**(5–8), 151–173, <http://dx.doi.org/10.15506/jog.2011.32.5.151>.

Authors

Dr Karl Schmetzer

Taubenweg 16, 85238 Petershausen, Germany

Email: SchmetzerKarl@hotmail.com

Dr Michael S. Krzemnicki FGA

Swiss Gemmological Institute SSEF, Aeschengraben 26, 4051 Basel, Switzerland

Acknowledgement

The authors are grateful to F. Jurkutat, Einbeck, Germany, for loaning the chrysoberyl samples examined.



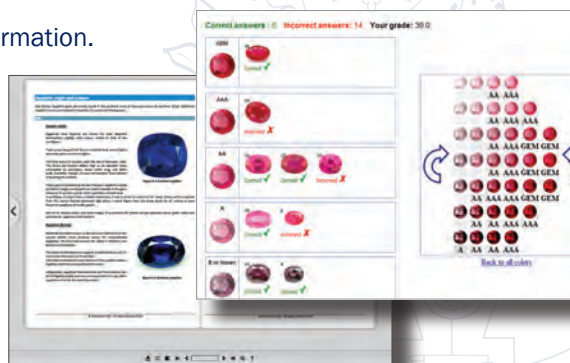
Gem-A

THE GEMMOLOGICAL ASSOCIATION
OF GREAT BRITAIN

Coloured Stones Grading Course

Check out our new **Coloured Stones Grading Course**, in association with GemeWizard® – the leader in gem digital colour communication. At **just £795**, you will learn to grade both common and less common stones, including ruby, sapphire, spinel, chrysoberyl and iolite – an essential skill for anyone considering buying, selling, auctioning or valuing gems or jewellery, then this course is for you.

Contact education@gem-a.com for more information.



Understanding Gems

Join us.



SSEF+

SCHWEIZERISCHES GEMMOLOGISCHES INSTITUT
SWISS GEMMOLOGICAL INSTITUTE
INSTITUT SUISSE DE GEMMOLOGIE



ORIGIN DETERMINATION · TREATMENT DETECTION

DIAMOND GRADING · PEARL TESTING

EDUCATION · RESEARCH



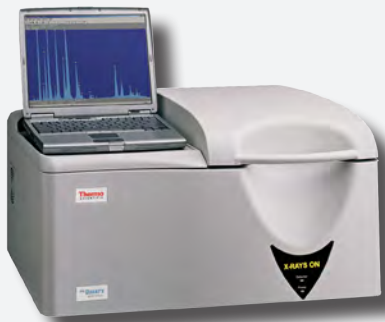
THE SCIENCE OF GEMSTONE TESTING®

tracing gemstone

Whether you're tracking the origin of gems down to their original excavation site or identifying natural from synthetic counterparts, the Thermo Scientific™ ARL™ QUANT'X guarantees reliable EDXRF results. Equipped with the latest silicon drift detector (SDD) technology it offers unsurpassed heavy element sensitivity combined with excellent resolution and short measurement times. Multiple small spot collimators allow for precise analysis of even the smallest of stones while the built-in camera makes positioning really straightforward.

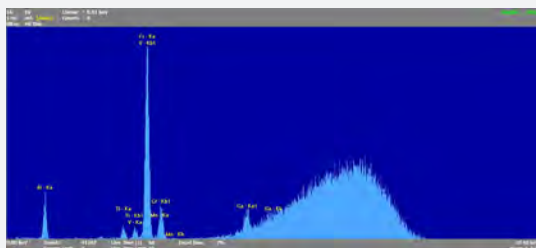
origin and authenticity

• see more details at www.thermoscientific.com/quantx



ARL QUANT'X
Compact, reliable, ultra-performant
EDXRF spectrometer

- Unsurpassed analytical precision
- Excellent resolution
- Better sensitivities
- Rapid, easy installation and on-site customization



Fast analysis of gemstones using ARL QUANT'X

Thermo
SCIENTIFIC
A Thermo Fisher Scientific Brand



Letters

Photoluminescence of Emeralds: Sample Orientation Procedure and Correlation of the R_1 Peak Position with SiO_2 Contents

The *Journal* article by Thompson et al. (2014) presented an interesting new contribution to the matter of emerald origin determination. The authors measured polarized laser-induced photoluminescence spectra of emeralds, focusing on the R_1 and R_2 chromium emission lines, and recorded differences in the peak positions and peak height ratios of these lines. The spectra of 32 natural and synthetic emeralds were measured, including both rough and cut samples.

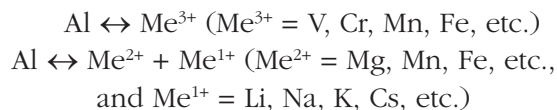
For crystals containing prism faces and, consequently, a known orientation of the c -axis, the authors rotated the samples to obtain spectra with various orientations to the fixed incident laser beam. Because of the known crystallographic orientation, the recorded spectra were easily assigned to $E \parallel c$ and $E \perp c$, since for $E \perp c$, the R_1/R_2 peak-height ratio reached a maximum value. For samples without crystal faces and hence with unknown crystallographic orientation, the emeralds were rotated until the R_1/R_2 peak-height ratio reached such a maximum value, and this direction was considered to represent the $E \perp c$ spectrum. Unfortunately, details of this experimental procedure were not given by the authors, and such information also is not available in previous papers (e.g. Moroz et al., 1998, 2000; Carceller-Pastor et al., 2013) that describe the Cr emissions for crystals with known orientation (i.e. with their c -axis oriented parallel or perpendicular to the incident laser beam).

Upon request, Dr Thompson kindly provided the requisite further details that would enable other scientists to replicate the technique and thereby to obtain comparable results. He explained that two rotation axes were employed, aligned at right angles to each other, and that numerous spectra were recorded in each rotation cycle. A detailed description of the method will be published in a forthcoming paper (D. B. Thompson, pers. comm., 2015).

Regrettably, the chemical properties of the samples analyzed by Thompson et al. (2014) are completely unknown. However, in order to explain the cause of the observed differences in the spectra, especially the shift in the position of the R_1 emission line, the authors correlated this position with chemical properties, in particular with SiO_2 weight percentages of emeralds originating from the same locality as the research samples examined by laser photoluminescence. These chemical data were taken from the PhD dissertation of Huong (2008), who presented numerous graphs showing the compositional variation of major and trace elements in emeralds determined by a combination of LA-ICP-MS and electron microprobe analyses. Although it is widely known that emeralds from a given locality exhibit a range of chemical compositions, the approach by Thompson et al. (2014) might be helpful for providing a very rough indication of the chemical features of the examined samples.

Nonetheless, a shortcoming of the just-described correlation flows from the fact that Huong (2008) provided neither a table with complete chemical properties for the samples with the weight percentages of all elements, nor a calculation of the obtained data for 18 oxygen atoms (according to the normal formula unit of beryl, $\text{Be}_3\text{Al}_2\text{Si}_6\text{O}_{18}$). Yet despite these deficiencies, Thompson et al. (2014) assigned decreasing SiO_2 weight percentages to increasing vacancies or substitutional defects at the Si site of the beryl lattice and speculated about such defects as the cause of the observed shift in the position of the R_1 emission line.

Beryls are subdivided into two groups with different substitutional schemes, specifically octahedral and tetrahedral (Auricchio et al., 1988). In octahedral beryls, two major substitutions are observed for the isomorphic replacement of Al:



In the first case, Al is simply replaced by a trivalent atom; in the second case, Al is replaced by a bivalent atom with charge compensation through the incorporation of an alkali atom in channel sites of the beryl structure.

Tetrahedral beryls are characterized by the replacement of Be^{2+} by Li^{1+} , again with charge compensation by alkalis in channel sites. Nevertheless, in the context of natural and synthetic emeralds, we mainly have to consider the effect of the two octahedral replacement schemes, because tetrahedral substitution of beryllium is limited.

The overview of emerald data presented by Groat et al. (2008) indicates through analyses calculated to 18 oxygen atoms per formula unit (apfu) that a small Si deficiency is occasionally present. However, we have on the one hand to realize that only a part of these data represent full analyses, and for many samples light elements (Be and Li) were not determined. On the other hand, it is equally relevant to keep in mind that many samples are chemically zoned and show a variation of the main elements, including Si. For example, for an emerald crystal from Torrington, New South Wales, Australia, a variation of Si from 5.98 to 6.02 apfu was determined from 353 point analyses (Schmetzer and Bernhardt, 1994).

Consequently, it would make sense to consider the effect of octahedral isomorphous replacement and its influence upon the weight percentage of SiO_2 in emerald. This effect is demonstrated by calculating the SiO_2 contents (in wt.%) for emerald in which Al has been replaced by trivalent metal atoms such as Cr and/or Fe. In such a scenario, although the Si sites show no vacancies or deficiencies ($\text{Si} = 6.0$ apfu for all calculations), we observe a distinct decrease in SiO_2 wt.% values (Figure 1). For this calculation, the small weight difference between Fe_2O_3 and Cr_2O_3 is neglected, because it would only generate very slight alteration in the results. Likewise, a water content of 1.5 wt.% H_2O may be assumed, insofar as a different water content would again lead only to a slight shift of the calculated data points.

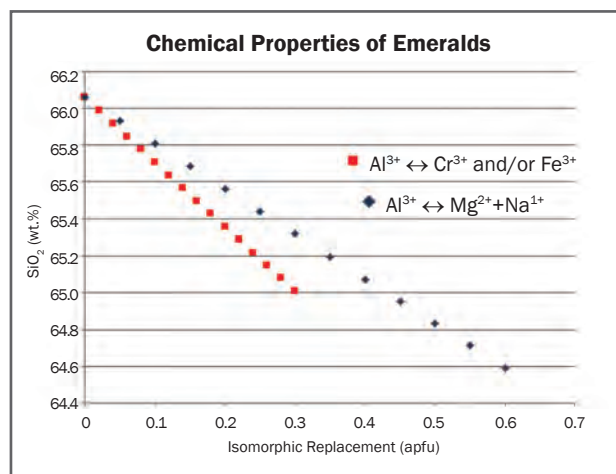


Figure 1: This plot shows the theoretical composition of emeralds with an isomorphous replacement of $\text{Al} \leftrightarrow \text{Fe}^{3+}$ and/or $\text{Al} \leftrightarrow \text{Cr}^{3+}$ or by a coupled substitution of $\text{Al} \leftrightarrow \text{Mg}^{2+} + \text{Na}^{1+}$. The SiO_2 contents were calculated for samples without any silicon vacancies or deficiencies ($\text{Si} = 6.0$ apfu) and for a water content of 1.5 wt.% H_2O . The SiO_2 ranges covered are the variations observed for natural and synthetic emeralds from various sources.

If we calculate the SiO_2 contents, again in wt.%, for the second octahedral replacement scheme involving a coupled substitution of Al by Mg (on Al sites) plus Na (for charge compensation on channel sites), we observe a similar decrease in SiO_2 percentages (Figure 1). These results indicate that for emeralds from different sources, in which both octahedral replacement schemes are always present to a certain degree and with 6 Si atoms per formula unit, the cumulative effects generated by the two isomorphous replacements may cause a reduction in the silicon percentages of up to approximately 2.5 wt.% SiO_2 . Thus, decreasing SiO_2 weight percentages found by chemical analyses do not principally represent Si vacancies or defects, but are mainly a consequence of the different weights of Al_2O_3 compared to Cr_2O_3 , Fe_2O_3 and MgO plus Na_2O .

Accordingly, a correlation in the shift of the R_1 peak position in emerald PL spectra with analytically determined SiO_2 contents (in wt.%) cannot necessarily be attributed to Si vacancies or defects. Rather, the decrease in SiO_2 contents in emerald is mainly due to the different isomorphous replacement schemes. Such a variation of SiO_2 contents is present in all samples, notwithstanding a theoretical value of $\text{Si} = 6$ apfu.

Dr Karl Schmetzer
Petershausen, Germany

References

Aurischio C., Fioravanti G., Grubessi O. and Zanazzi P.F., 1988. Reappraisal of the crystal chemistry of beryl. *American Mineralogist*, **73**(7–8), 826–837.

Carceller-Pastor I., Hutchinson W.D. and Riesen H., 2013. Temperature dependence of the chromium(III) R₁ linewidth in emerald. *Chemical Physics Letters*, **564**, 33–36. <http://dx.doi.org/10.1016/j.cplett.2013.02.009>.

Groat L.A., Giuliani G., Marshall D.D. and Turner D., 2008. Emerald deposits and occurrences: A review. *Ore Geology Reviews*, **34** (1–2), 87–112, <http://dx.doi.org/10.1016/j.oregeorev.2007.09.003>.

Huong L.T.T., 2008. Microscopic, Chemical, and Spectroscopic Investigations on Emeralds of Various Origins. PhD dissertation, University of Mainz, Germany, <http://ubm.opus.hbz-nrw.de/volltexte/2008/1673/pdf/diss.pdf>.

Moroz I., Panczer G. and Roth M., 1998. Laser-induced luminescence of emeralds from different sources. *Journal of Gemmology*, **26**(5), 316–320, <http://dx.doi.org/10.15506/jog.1999.26.5.316>.

Moroz I., Roth M., Boudeulle M. and Panczer G., 2000. Raman microspectroscopy and fluorescence of emeralds from various deposits. *Journal of Raman Spectroscopy*, **31**(6), 485–490, [http://dx.doi.org/10.1002/1097-4555\(200006\)31:6<485::aid-jrs561>3.0.co;2-m](http://dx.doi.org/10.1002/1097-4555(200006)31:6<485::aid-jrs561>3.0.co;2-m).

Schmetzer K. and Bernhardt H.-J., 1994. Isomorphic replacement of Al and Si in tetrahedral Be and Si sites of beryl from Torrington, NSW, Australia. *Neues Jahrbuch für Mineralogie Monatshefte*, **1994**(3), 121–129.

Thompson D.B., Kidd J.D., Åström M., Scarani A. and Smith C.P., 2014. A comparison of R-line photoluminescence of emeralds from different origins. *Journal of Gemmology* **34**(4), 334–343.

Author Reply

We cannot argue with X-ray crystallography measurements showing that defects at Si sites in beryl occur at or below trace-level detection. And so we appreciate Dr Schmetzer’s demonstration that variation of SiO₂ wt.% arises from substitutions of heavier metal ions at Al sites. Following that, we are left with the peculiar result that (region-averaged) SiO₂ wt.% is a better indicator than Al₂O₃ wt.% of Al site defects leading to R-line peak shifts.

D. Brian Thompson
University of North Alabama
Florence, Alabama, USA



The best tools for the job



From 10x loupes to microscopes, Gem-A Instruments stocks a wide range of books and equipment, to aid research and help ensure accurate gem identification.

To download a catalogue visit our website at www.gem-a.com/shop.aspx, or email instruments@gem-a.com.

Understanding Gems

Join us.



Think modular for your personal lab!



GEMMODUL

- MODUL 1 Polariscope and Docking Station for GemLED Refractometer
- MODUL 2 Polariscope and Refractometer Illuminator Base
- MODUL 3 Refractometer and Illuminator Base
- MODUL 4 Polariscope
- MODUL 5 Spectroscope and Coldlight Base
- MODUL 6 UV LW/SW unit

Modules combined into a GemLab at 2 1/2 feet

GEMMASTER

ZEISS 10x – 80x

LEICA 10x – 48x/64x

Cool-touch LED daylight darkfield base

Examination of inclusions in immersion liquids

www.eickhorst.com SYSTEM EICKHORST Made in Germany

Hamburg / Germany · Tel. +49-40-514000-0 · Fax +49-40-514000-30 · info@eickhorst.com

Conferences

AGA Tucson Conference

The 2015 Accredited Gemologists Association Conference in Tucson, Arizona, USA, took place 4 February, with the theme ‘Gems – Facets to Micro-Features’.

Christopher Smith (American Gemological Laboratories [AGL], New York, New York) performed experiments on emerald clarity enhancement using three types of fillers: ‘traditional’ (cedarwood oil, wax, Canada balsam and mineral oil), ‘modern’ (Excel, Opticon, PermaSafe and Palma) and coloured (Joban oil and green Opticon). Overall, he found that the modern fillers were more efficient at hiding fissures than the traditional products, due to three factors: (1) their refractive index, (2) the quality of the contact at the interface between the filler and fissure walls, and (3) the transparency or translucency of the filler. Coloured fillers were found to improve emerald coloration only in lower-quality material (i.e. containing many large fractures and cavities that are filled with the green substance).

Jeffery Bergman (Primagem, Bangkok, Thailand) reviewed collector gems, and noted that the main sources of these stones include Afghanistan, Brazil, Myanmar, Pakistan, Sri Lanka and Tanzania. The growing popularity of these rarities (e.g. taaffeite, painite, jeremejevite and benitoite) is demonstrated by their presence in mainstream sales outlets such as Jewelry Television and eBay.

Lore Kiefert (Gübelin Gem Lab, Lucerne, Switzerland) described several instances in which

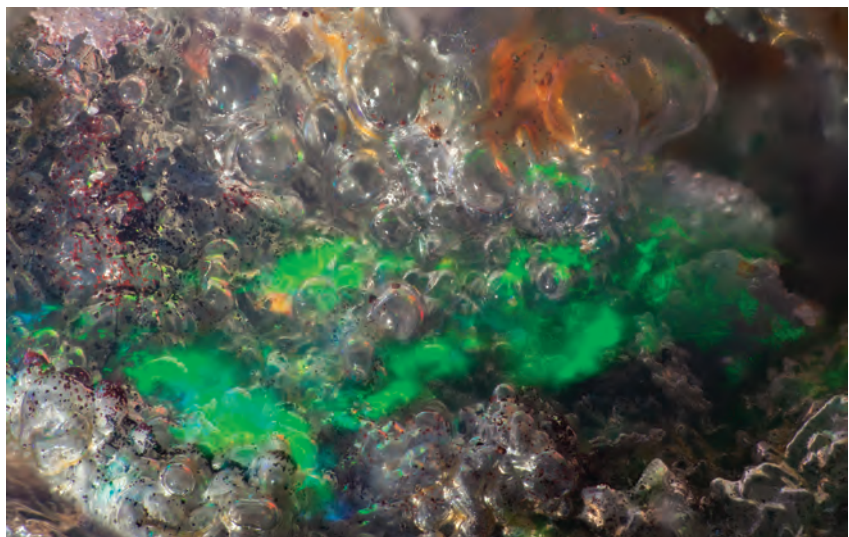
gemmologists should use caution when interpreting their results. For example, the energy-dispersive X-ray fluorescence (EDXRF) chemical analysis of waxed jadeite may show traces of Ca from the wax, which could lead to the misidentification of jadeite as omphacite. Kiefert also described her recent research on black opal from a new deposit in Stayish, Ethiopia. Unlike most of the white opal from Wollo, Ethiopia, this black opal shows negligible hydrophaneity. Its coloration is due to organic carbon, like the black opal from Australia.

Victor Tuzlukov (Russian Faceters Guild, Moscow) examined several factors for evaluating the quality of a gemstone’s faceting. Ideally, the facets should have perfect flatness, sharp interfacial edges and precise symmetry (if appropriate for the facet design). The faceting should also be executed to avoid undesirable optical effects (e.g. unintended reflections), as well as ‘windowing’ of the stone.

Dona Mary Dirlam (Gemological Institute of America [GIA], Carlsbad, California) highlighted the GIA library’s extensive collection of materials dating from 1496 to the present. She also announced an exciting future project of digitizing GIA’s rare book collection using state-of-the-art scanning equipment.

Danny Sanchez (Los Angeles, California, USA) provided several tips for digital photomicrography: lens cleaner works well on polished stones as well as lenses; light diffusers can be made from white film canisters, or even tracing paper (if not in the vicinity

Figure 1: Focus-stacking software was used to capture the globular texture of hyalite in this play-of-colour opal from Magdalena, Jalisco, Mexico. Photomicrograph by Danny Sanchez; image width 4.8 mm.



of hot lights); black foil and mini-reflector cards are useful for manipulating light; and lamps with fans should be placed on a separate surface from the microscope to reduce vibration. He uses Helicon focus-stacking software to blend numerous images (typically around 80) into a single image to show an extreme depth of field (e.g. Figure 1).

In another photomicrography presentation, **Edward Boehm** (RareSource, Chattanooga, Tennessee, USA) described how to take high-quality photos through a microscope with a smart phone. The camera port should be held approximately 1 cm from the microscope's ocular, and darkfield illumination should typically be turned off when using a fibre-optic lamp.

Shane McClure (GIA, Carlsbad) examined three-phase inclusions in emerald and their relationship to country of origin. Jagged three-phase inclusions traditionally have been considered diagnostic of Colombian origin, but very similar inclusions are known in emeralds from Panjshir, Afghanistan, and Musakashi, Zambia. Trace-element analysis can be helpful for separating emeralds from these localities.

The conference was followed by the AGA Gala, where the Antonio C. Bonanno Award for Excellence in Gemology was presented to Thomas Hainschwang and the AGA Lifetime Achievement Award was given to Dona Mary Dirlam.

Brendan M. Laurs

GILC Tucson Conference

The Gemstone Industry & Laboratory Conference took place on 2 February 2015 in Tucson, Arizona.

Shane McClure (GIA, Carlsbad) provided an update on activities by the Laboratory Manual Harmonization Committee (LMHC) during the past year. He indicated that the main function of the LMHC is to come to an agreement on wording on laboratory reports. Two more LMHC information sheets are currently pending, and will be posted at www.lmhc-gemology.org.

In a separate presentation, **McClure** introduced new terminology used on GIA reports for describing the coloration of rubies from Mozambique (and elsewhere) that are attractive but do not have the same appearance as 'pigeon's blood' rubies, which most commonly originate from Mogok, Myanmar. The three new colour categories include 'deep red' (dark red), 'crimson red' (slightly purplish red) and 'scarlet red' (slightly orangy red); the latter two terms cover rubies that would generally be described as 'intense' red.

Christopher Smith (AGL, New York) reviewed the features associated with relatively low-temperature heat treatment of gem corundum. He defined 'relatively low temperature' as below the threshold at which rutile needles begin to dissolve into their corundum host (~1,300°C, depending on various factors). Such temperatures are commonly used to remove a blue colour component (e.g. from ruby and purple sapphire) to produce a purer red/pink coloration, or to decrease or increase yellow colour (to produce colourless sapphire or improve the colour of yellow, orange and padparadscha sapphires). Some microscopic indicators of relatively low-temperature heating include unaltered crystalline inclusions of thermally sensitive minerals such as calcite, diaspore

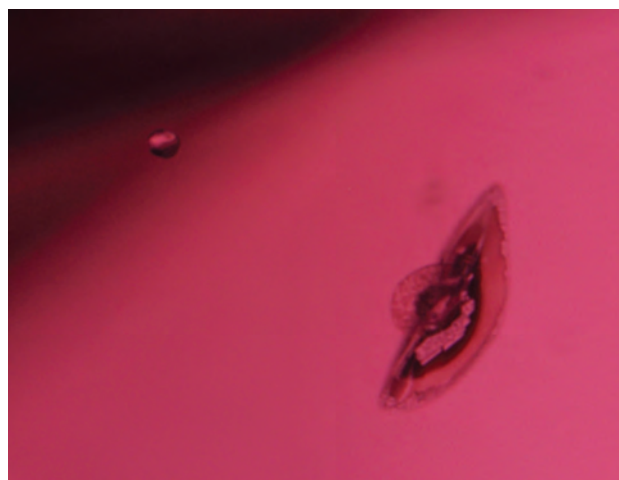


Figure 2: In this pink sapphire from Madagascar, the apatite inclusion on the centre right shows evidence of heat treatment, while the zircon on the upper left does not. Apatite is more thermally sensitive, and therefore such an inclusion scene provides evidence of low-temperature heating. Photomicrograph by Christopher Smith; magnified 40x.

and apatite (but not zircon; Figure 2), and the presence of CO₂-rich fluids in negative crystals.

In a presentation based on research conducted by Colombia's national gemmological laboratory, **Gabriel Angarita** (ACODES, Bogotá, Colombia) proposed that residues in emeralds that are left over from the cutting process, such as emerald dust or diamond powder, should not be mentioned in the clarity enhancement section of reports (e.g. 'insignificant' or 'minor'), since these residues are not a result of enhancement.

The formal presentations were followed by a lively 'Open Forum Session', in which attendees brought up a wide diversity of topics for discussion.

Brendan M. Laurs

GIT2014 Conference

The Gem and Jewelry Institute of Thailand (GIT) hosted the 4th International Gem and Jewelry Conference on 8–9 December 2014 in Chiang Mai, Thailand. The event was attended by more than 250 participants and featured six keynote speakers and two parallel oral sessions, as well as a poster session. The oral presentations attended by this author are briefly described below.

Several presentations covered coloured stones. Keynote speaker **Jean Claude Michelou** (International Colored Gemstone Association, New York) reviewed coloured stone sources and markets. He estimated that more than 100,000 artisanal coloured stone miners are currently active worldwide. However, due to the rising technical challenges of mining the deposits, he predicted a decrease in small-scale operators and an increase in activity by large mining companies in the future. He also suggested that green garnets (demantoid and tsavorite) have good potential for future expansion. **Dr Lore Kiefert** (Gübelin Gem Lab, Lucerne) described new black opal from Stayish, Ethiopia, which is located approximately 30 km from the Wollo white opal mines. The black opal deposit is hosted by the same clay-rich volcanic layer that contains the white opals. The Ba content of the black opals determined by EDXRF shows both volcanic and sedimentary signatures. **Dr Taijin Lu** (National Gems & Jewelry Technology Administrative Center, Beijing, China) indicated that there now are more than 25 different materials that are sold as ‘jade’ in China. Prices are escalating for naturally coloured yellow and red quartzite ‘jade’, which is mined from more than six quarries in China. The coloration of both materials is due to iron compounds (hematite in the red quartzite, and hematite and goethite in the yellow quartzite). **Dr Miro Ng** (The Hong Kong Institute of Gemmology, Central) summarized the cathodoluminescence (CL) colours and the textures in various types of jadeite and its imitations. Quartzite, maw-sit-sit and amphibole-rich rocks can all be easily separated from jadeite with this technique. The grain size of jadeite correlates to its quality, with finer-grained material showing the highest transparency. **Dr Somruedee Satitkune** (Kasetsart University, Bangkok) studied blue sapphires from Phrae Province in northern Thailand. The secondary deposits are derived from a basaltic flow that is 5.6 million years old, and the sapphires are associated with zircon, black spinel and garnet. Internal features consist of colour zoning, crystalline and fluid inclusions, and minute particles. **Dr Le Thi Thu Huong** (VNU University of Science, Hanoi, Vietnam) described the

properties of yellowish brown zircon from Dak Lak in the central highlands of Vietnam. The gems are mined from secondary deposits formed by the weathering of basaltic rocks. EDXRF spectroscopy showed Mg and Al as impurities, and the presence of U³⁺ was revealed by both ultraviolet-visible-near infrared (UV-Vis-NIR) and Fourier-transform infrared spectra. **Jayshree Panjekar** (Panjekar Gem Research & Tech Institute, Pune, India) described aquamarine from Pallapatti village, Karur, Tamil Nadu, India. It shows typical gemmological properties for aquamarine, with internal features consisting of fluid inclusions (two-phase and multiphase) as well as biotite and apatite crystals. **Dr Boontarika Srithai** (Chiang Mai University) used X-ray diffraction (XRD) analysis to determine that the chatoyancy in cat’s-eye opal from Tanzania is caused by needle-like particles of goethite. XRD also showed that it is opal-CT with some cristobalite, tridymite and quartz. **Martin Steinbach** (Gems with a Star, Idar-Oberstein, Germany) gave a well-illustrated lecture that reviewed asterism in gems, including very rare examples of star tanzanite (four rays) and star zircon (eight rays, in a pale yellow stone from Sri Lanka).

On diamond topics, keynote speaker **Dr Lutz Nasdala** (University of Vienna, Austria) reviewed advances in the microspectroscopy of diamond. Hyperspectral Raman mapping can quantitatively show specific areas near diamond inclusions corresponding to compressive and dilative stress, which is of interest for interpreting diamond genesis. This technique can also be used to visualize internal growth textures in diamond that are not visible with an optical microscope. **Dr Wuyi Wang** (GIA, New York) described recent investigations of colourless and near-colourless type IIa CVD synthetic diamond using CL and carbon isotopes. Compared to type IIa natural diamond, the CVD products showed very different growth features under CL, and significantly lighter carbon isotope compositions. **Branko Deljanin** (CGL-GRS Swiss Canadian Gemlab, Vancouver, Canada) described criteria for separating Argyle pink and blue diamonds from CVD-grown synthetic diamonds. Compared to the pink CVD synthetics, the blue CVD-grown products are relatively rare in the market. **Dr Katrien De Corte** (HRD Antwerp, Belgium) indicated that the low-pressure, high-temperature treatment of type IIa diamond can be done in 3–15 minutes with desktop equipment at pressure of <1 atmosphere and temperatures of 2,000–2,200°C; hydrogen gas is used to prevent graphitization. The properties of diamonds treated by this technique are similar to those of HPHT-treated stones, since similar temperatures are used.



Figure 3: These sapphires from Nigeria are shown before heating (left, 0.07–0.40 g) and after traditional heat treatment (right, 0.03–0.76 g). Photo by T. Sripoonjan.

Gem treatments were covered in several presentations. **Thanong Leelawatanasuk** (GIT, Bangkok) examined heated and untreated sapphires from the Mambilla area of Nigeria (Figure 3), near the border with Cameroon. The rough material was typical of magmatic-type sapphire derived from secondary deposits. Heated samples showed melted crystalline inclusions with partially healed tension halos, frosted 'fingerprints' and a brownish appearance for dense clouds of microscopic particles. **Boontawee Sriprasert** (GIT, Bangkok) performed further studies of treated 'black' (very dark blue) sapphires that were previously described on GIT's website. He found additional evidence for the Fe-Ti diffusion treatment of these stones, which were submitted to the GIT laboratory in January and August 2014. **Shane McClure** (GIA, Carlsbad) discussed problems associated with describing the degree of emerald clarity enhancement on identification reports: a stone may be treated or re-treated after being submitted for a report, and there are inconsistencies between how various laboratories evaluate the degree of enhancement. **Roman Serov** (MSU Gemmological Center, Lomonosov Moscow State University, Russia) performed heating experiments on Russian demantoid. After heating to 650°C under reducing conditions (stones embedded in charcoal powder) for one hour, the brown colour component decreased and the samples became greener; subsequent heating of those same samples to 650°C under oxidizing conditions (in air) caused them to become browner.

On the topic of pearls, **Shigeru Akamatsu** (Central Gem Laboratory, Tokyo, Japan) highlighted some of the problematic materials being used for bead nuclei in pearl culturing: (1) Giant clam (*Tridacna spp.*) shell easily breaks when it is drilled, and it is also an illegal product included in Appendix II of CITES; (2) beads made from Chinese freshwater mussel shell are commonly treated with toxic chemicals to bleach

them white; and (3) glued bead nuclei consisting of three pieces of shell that are cemented together are susceptible to falling apart, even from exposure to hot water.

Dr Seriwat Saminpanya (Srinakharinwirot University, Bangkok, Thailand) studied ancient glass beads from Mae Hong Son, northern Thailand. The beads were recovered from a log coffin burial site dated 12,000 years ago. UV-Vis-NIR spectroscopy showed that copper and iron cause the colours of the blue and green beads, whereas iron is responsible for the colour of the yellow and black beads; some lead was also present.

Business topics presented at the conference varied considerably. Keynote speaker **Prida Tiasuwan** (Pranda Jewelry Group, Bangkok) discussed the business implications for the gem and jewellery industry of the Association of Southeast Asian Nations Economic Community (AEC). The goal of the AEC is regional economic integration of ASEAN nations by the end of 2015 through a single market and a production base that is fully integrated into the global economy. The free flow of goods will be encouraged, and although value-added tax will be paid in the country of sale, there will be no import duty. Keynote speaker **Burak Cakmak** (Swarovski, London) reviewed his company's efforts to embrace corporate social responsibility (CSR). Swarovski has a 120-year history of involvement with CSR, and seeks to balance and maximize three critical aspects of their business: 'Planet, People and Profit'. Keynote speaker **Franco Pianegonda** (Franco Pianegonda, Vicenza, Italy) explained the philosophy behind his jewellery designs. He focuses on the customer who will wear his jewellery, rather than being concerned with innovating fast enough to meet new desires. By contrast, in a presentation titled 'Developing at 10,000 pieces of jewelry per hour', keynote speaker **Thomas Nyborg** (Pandora Production Co., Bangkok) described the policies and procedures that are used by Pandora in their large jewellery manufacturing business. The company is based entirely in Thailand, and employs 7,934 people with an average age of 27. **Kennedy Ho** (AIGS Laboratory, Bangkok) discussed the challenges of doing business in Myanmar. The government offers little protection for investors, so there is a lot of risk, but also an abundance of business opportunities with good potential.

The e-proceedings volume for this conference, and also for prior GIT conferences (2012, 2008 and 2006), can be purchased at www.git.or.th/shopping_cart/e-book.aspx?lang=en.

Brendan M. Laurs

Gem-A Notices

GIFTS TO THE ASSOCIATION

The Association is most grateful to the following for their gifts for research and teaching purposes:

- Angelett Gallery**, London, for eight pieces of 'highly mineralized ground' from the Salsigne mine, France, and a piece of rock from the goldfields of Western Australia (see *Gems & Jewellery*, Vol. 24, No. 2, 2015, 30–31).
- Anura Wijemanne Associates**, Colombo, Sri Lanka, for mixed-colour sapphires weighing a total of 29.26 carats.
- Than Aung**, Mogok, Myanmar, for miscellaneous gem rough and a collection of calcites and ruby in calcite from Mogok.
- Jason Baskin Minerals**, Flemington, New Jersey, USA, for garnets in graphite schist and faceted garnets from the Red Embers mine, Erving, Massachusetts, USA (see *The Journal*, Vol. 34, No. 4, 2014, 286–287).
- John Bradshaw** of Coast-to-Coast Rare Stones, Nashua, New Hampshire, USA, for a large selection of rare gemstones.
- Eric Braunwart** of Columbia Gem House Inc., Vancouver, Washington, USA, for iolite, corundum and kyanite rough from Palmer Canyon, Wyoming, USA.
- Pat Daly FGA**, London, for two books and 28 magazines.
- Richard Eddy**, Cheshire, Oregon, USA, for three pieces of opalised wood and three specimens showing the stages of opal treatment.
- Sterling Foutz and Mary Hecht** of Sterling Opal, Tempe, Arizona, USA, for samples of synthetic opal.
- Farooq Hashmi and Michael Puerta** of Intimate Gems, Glen Cove, New York, USA, for samples of tourmaline and natrolite from Mwajanga, Tanzania.
- Prof. U Tin Hlaing**, Shan State, Myanmar, for a bracelet composed of beads of jade-like materials (see *The Journal*, Vol. 34, No. 3, 2014, 197–198).
- Syed Iftikhar Hussain** of Syed Trading Co., Islamabad, Pakistan, for two peridot crystals, rough pieces of nephrite and spessartine, and an actinolite cabochon (all from Pakistan), and a slab of trapiche quartz from Russia.
- Brett and Allyce Kosnar** of Kosnar Gem Co., Black Hawk, Colorado, USA, for a piece of rough and three cabochon samples of stabilized shattuckite from DRC.
- Milenyum Mining Ltd.**, Milas, Turkey, for rough and cut Csarite (colour-change diaspore).
- U San Myo**, Yangon, Myanmar, for samples of spinel, ruby and green apatite, and a selection of marble host rock from Mogok.
- Saeko Nagao FGA**, Fukushima, Japan, for beryl and rainbow garnet.
- Mauro Pantò** of The Beauty In The Rocks, Laigueglia, Italy, for the following faceted stones: 'black' axinite (source unknown); quartz from Madagascar (one with lazulite and another with piemontite inclusions); tantalite and columbite from Colorado, USA; fuchsite from the Kola Peninsula, Russia; shungite from New Mexico, USA; and 'liparsite' (manmade glass from Italy).
- Denis Pho**, for interference figure specimens, jadeite, 11 trapiche cabochons and more than 220 g of spinel crystals.
- Hemant Phophaliya** of AG Color Inc., New York, New York, USA, for a 19.09 ct tanzanite.
- Werner Radl** of Mawingu Gems, Liesenfeld, Germany, for two pieces of rough chrysoprase from Kondoa District, Tanzania, and beryl with inclusions from Haneti, Tanzania.
- Sein Sein**, Mogok, for tourmaline and aquamarine from Pein-pyit and quartz with tourmaline from Leplanha, Myanmar.
- U Tin Kyaw Than FGA** of the Gemmological Science Centre, Yangon, Myanmar, for a box of miscellaneous faceted gems from Myanmar.
- Ian Thompson FGA**, Wood Green, London, for a selection of books.
- Dominic Turk** of G. Turk Ltd., London, for a treated opal.
- Wards**, Birmingham, West Midlands, for tektites.

MEMBERSHIP

At a meeting of the Council held on 25 February 2015, Alan D. Hart FGA DGA was appointed to serve on the Council. The following were elected to membership:

Fellowship and Diamond Membership (FGA DGA)

Higgo, Emma, *Hindhead, Surrey*
Kwok Men Yee, *Kam Tin, Hong Kong*

Fellowship (FGA)

Clark, Christopher, *Knoxville, Tennessee, USA*
Deng Heng, *Guilin, Guangxi, P.R. China*
Durocher, Beatrice, *Marseille, France*
Huang Jiajun, *Guangzhou, Guangdong, P.R. China*
Hui Wan Man, *North Point, Hong Kong*
Jiamanusorn, Siriwat, *Bangkok, Thailand*
Jin, Apple, *London*
Johansson, Sandra, *Västra Götaland, Sweden*
Kang Zhiyuan, *Shanghai, P.R. China*
Kitching, Laura, *Northampton, Northamptonshire*
Lee Tak Fai, Eric, *Kowloon, Hong Kong*
Lescuyer, Loic, *Francheville, France*
Lloyd, Samantha, *Leicester, Leicestershire*
Marleau, Diane, *Mont-Royal, Quebec, Canada*
Martin-Gutierrez, Francesca, *Bounds Green, London*
Minelli, Adriana, *Toronto, Ontario, Canada*
Ootani, Wakana, *Tokyo, Japan*
Rafalimanana, Laza Andriamizaka, *Antsirabe, Madagascar*
Raheeriririna, Haingo, *Antananarivo, Madagascar*
Recchi, Jean-Noel, *Marseille, France*
Rochambeau, David, *Montreal, Quebec, Canada*
Rong Zhen, *Shanghai, P.R. China*
Rykova, Elena, *Paris, France*
Sampson, Suzanne, *Leicester, Leicestershire*
Shi Yang, *Guilin, Guangxi, P.R. China*
So Sau Man, *Tsing Yi, Hong Kong*
Sugawara, Naoyuki, *Saitama, Japan*
Takebayashi, Maya, *Yokohama City, Kanagawa, Japan*
Thompson, Noah, *Chiddingfold, Surrey*
Van Colen, Louise, *Montreal, Quebec, Canada*
Wong Man Ho, *Kowloon, Hong Kong*
Yamazaki, Junichi, *Kambei-gun, Iwate, Japan*
Zhang Shengnan, *Beijing, P.R. China*
Zhu Ying, *Shanghai, P.R. China*

Diamond Membership (DGA)

Arioli, Elena, *London*
Burton, Amy Louise, *London*
Burton, Guy Christopher, *London*
Leung Hang-Fai, Henry, *Kowloon, Hong Kong*
Thung Chi Ming, Herbert, *Kowloon, Hong Kong*
Wong Nga Sze, Jennifer, *Foton, Hong Kong*

Associate Membership

Akgun, Murat, *Mugla, Turkey*
Akgun, Guzide, *Mugla, Turkey*
Alexander, Sheila, *Potters Bar, Hertfordshire*
Auerbach, Roy, *Dallas, Texas, USA*
Campbell, Alan, *Edinburgh*
Colucci, Thomas, *Alexandria, Virginia, USA*
Coquel, Isabelle, *Singapore*
Donn, Nigel, *Manchester, Greater Manchester*
Downes, Claire, *London*
Drammeh, Hamed, *Surutue, Nigeria*
Fujiki, Otoo, *Tokyo, Japan*
Grimwood, Brett, *Nelson, New Zealand*
Hennelly, Jacinta, *Galway, RO Ireland*
Hopkins, Gary, *East Grinstead, West Sussex*
Hughes, Gill, *Chelford, Cheshire*
Ito, Akira, *Tokyo, Japan*
Johnston, Christopher, *Erongo, Namibia*
Kanevskij, Aleksandr, *Antwerp, Belgium*
Lai Yuen Wan, Eva, *Wan Chai, Hong Kong*
Li Jing, *London*
Molliere, Pascal, *Farnborough, Hampshire*
Quinn, Charles, *Varna, Bulgaria*
Tom, Graham, *London*
Watt, Martin, *Belfast, County Antrim*
Weller, Thomas, *Oberwil, Switzerland*
Yamashita, Mei, *Miura City, Kanagawa, Japan*
Zhang Xiaole, *Solibull, West Midlands*

Corporate Membership

Milenyum Mining Ltd., *Milas, Turkey*

At a meeting of the Council held on 25 March 2015, the following were elected to membership:

Fellowship

De Vismes, Raphaelae, *Larchmont, New York, USA*
Genet, Julie, *Cagnes-sur-Mer, France*
Swaving, Christine, *The Hague, The Netherlands*

Associate Membership

Bradshaw, John, *Nashua, New Hampshire, USA*
Breitsprecher, Charles, *Sacramento, California, USA*
Finleon, Deborah, *Alexandria, Virginia, USA*

Fitzpatrick, John, *White County, Illinois, USA*
Fogelberg, Kenneth, *Santa Maria, California, USA*
Goldman, Ira, *N. Miami, Florida, USA*
Haindel, Mary Virginia, *Metairie, Louisiana, USA*
Henderson, Corinna, *Shipley, West Yorkshire*
Lindenbergh, Idzarda, *Rotterdam, The Netherlands*
Morrier, Yves, *Montreal, Quebec, Canada*
Morrison, Jeffrey, *Yarmouth, Maine, USA*
Prince, Nick, *Atlanta, Georgia, USA*

Sammon, Christopher, *London*
Smith, Rosalind, *Chelmsford, Essex*

Annual General Meeting

The 2015 Annual General Meeting of The Gemmological Association of Great Britain will be held on Wednesday 24 June (not 17 June as previously notified) at 11:00 a.m. The venue is to be confirmed.

OBITUARY

Dr James Bowman Nelson

1913–2015

Dr Jamie Nelson PhD FGS FInstP FGA (D.1980), of Hampstead, London, died on 17 March 2015 at the age of 101.

Dr Nelson was an ebullient Scottish physicist, X-ray crystallographer, mineralogist, gemmologist and inventor of scientific instruments. His more recent scientific interests centred on gemmology (which he started at an age when most people retire), but his contributions to the scientific world were more wide ranging. As managing director of McCrone Scientific Ltd. (London) his inventions were numerous including the McCrone micronising mill which has received much acclaim from users of X-ray diffraction.

A life-long mineral collector, he has been well-known for only about a quarter of a century in gemmological circles. Jamie was fascinated by the wonders of the behaviour of light. He invented and commissioned various devices to investigate and demonstrate the ways light interacts with gemstones. His laboratory was an Aladdin's cave packed to the ceiling with instruments (most of which he had designed), papers (many of which he had written) and a collection of specimens. He used the latter to demonstrate the principles he always expounded with great enthusiasm. In his late 90s, his ardour, acumen and critical faculties were undiminished and his physical stamina and ability would have done credit to someone several decades younger.

Jamie was born on 7 June 1913 in Stenhousemuir, Scotland. His formal education in Scotland and Canada ended at the age of 14 when he left school to support his mother and sister. However, just before leaving, he was awarded a gold medal for obtaining the highest high school entrance exam marks in the Niagara Falls district. He returned to the UK in the 1930s where he met Doris Holden. They were married in 1942 and for 67 years they were totally devoted to each other.

After working for Cussons Soap Factory, Jamie was employed as chief analytical chemist by Magnesium Elektron in Manchester during most of World War II. In early 1944 he transferred to the coal research establishment BCURA, to take charge of a new X-ray service section. He was based at the Cavendish Laboratory, Cambridge, where he measured the thermal expansion of graphite, obtaining accurate measurements up to 800°C using his own high-temperature X-ray diffraction camera. Graphite was used to slow down the neutrons in nuclear fission electricity generators then under construction in the UK. During all these early years he published many accounts of his own physical analytical methods including UV emission spectroscopy and X-ray diffraction analysis.

Doris discovered a clause in the Cambridge University Admissions Regulations whereby, without formal qualifications, if 'an applicant possessed sufficient background knowledge to profit from a path of instruction leading to a PhD, the enrolment could proceed'. Jamie was made aware of Doris's application on his behalf on the morning of a Viva Voce with three university Fellows. He then received an official letter advising him to seek enrolment at a college and provide himself with cap and gown of Master status. Without Doris's help and her support during his student days at Cambridge, he claims he would have starved. As a couple, they were renowned for their Cambridge parties, a tradition they continued all their lives.

Jamie successfully completed his thesis with Professor Sir Lawrence Bragg as his supervisor. He then regarded himself as a card-carrying crystallographer. Sir Lawrence generously gave Jamie many of the crystal specimens on which Sir Lawrence himself had



Dr Jamie Nelson during his 100th birthday celebration with his good friends Sara Mark (left) and Jean Prentice.

determined the atomic structure over the previous 30 years. Jamie became a Fellow of the Geological Society in 1956 and was by then already a Fellow of the Institute of Physics.

In the 1950s, Jamie transferred to Morgan Crucibles until 1964 when he left to establish McCrone Scientific Ltd. In the early years he was involved in various problem-solving projects and he collaborated with Dr Walter McCrone of McCrone Associates, Chicago, Illinois, USA, providing his X-ray analytical expertise. But Jamie's main love was invention, including the McCrone micronising mill, low-load hardness tester, and wavelength and reflectance standards.

Jamie made a poor start in gemmology. In 1980, after three examination attempts, he achieved only a pass mark. Since then he has more than made up for this inauspicious beginning. Starting in 1984, Jamie published 17 original articles on gemmology, almost all of which were in *The Journal of Gemmology*. In 1988 Jamie and Alan Jobbins were invited by the University of Geosciences in Wuhan, China, to advise on the setting up of gemmological courses and a gem testing laboratory. Subsequently the correspondence courses of the Gemmological Association of Great Britain were translated into Chinese which enabled students in China to access and enrol for the Association's Diploma in Gemmology.

For his seminal work on the explanation of the optical 'flash effect', used to detect glass fracture-filling in diamonds, he was awarded the Gemmological

Association's Research Diploma in 1993. Since its inception in 1945 there have been only six recipients of this award.

In 2001, Jamie received the prestigious August Köhler Medal, an award of the State Microscopical Society of Illinois (Chicago), 'for outstanding contributions to optical microscopy'.

Starting in 1994, Jamie was engaged in helping to produce the first comprehensive database of the Raman spectra of minerals, gems and their inclusions. The Renishaw compilation now amounts to over 1,500 mineral species and chemical compounds, all of which have come from his considerable collection. He also developed several gemmological instruments, such as: (1) an accessory for the Renishaw Raman microspectrometer that recorded the low-temperature photoluminescence spectroscopy of diamond, which enabled the distinction of HPHT-treated diamonds from other colourless diamonds, and (2) a compact and inexpensive device for detecting short-wave UV transparency, a helpful pre-screening method for HPHT-treated colourless diamonds. All of Jamie's custom-built products were made and marketed by his one-man company, Nelson Gemmological Instruments.

Jamie will be greatly missed, not just for his scientific abilities but also for his wonderful humour and generous hospitality.

*Gwyn Green
Barnt Green, West Midlands*

An innovator in gemstone reporting

- Identification of colored gemstones • Country of origin determination • Full quality and color grading analysis



AMERICAN GEMOLOGICAL LABORATORIES

AGL

580 5th Ave • Suite 706 • New York, NY 10036, USA
www.aglglab.com • +1 (212) 704 - 0727

Learning Opportunities

CONFERENCES AND SEMINARS

CIBJO Congress 2015

4–6 May 2015
Salvador, Brazil
<http://congress2015.cibjo.org>

3rd Annual New England Mineral Conference

8–10 May 2015
Newry, Maine, USA
www.nemineralconference.org

ICA Congress

16–19 May 2015
Colombo, Sri Lanka
<http://congress.gemstone.org>

The Santa Fe Symposium

17–20 May 2015
Albuquerque, New Mexico, USA
www.santafesymposium.org

Society of North American Goldsmiths' 44th Annual Conference

20–23 May 2015
Boston, Massachusetts, USA
www.snagmetalsmith.org/conferences/impact-looking-back-forging-forward

9th International Conference on New Diamond and Nano Carbons

24–28 May 2015
Shizuoka, Japan
www.ndnc2015.org

AGA Las Vegas Conference

28 May 2015
Las Vegas, Nevada, USA
<http://accreditedgemologists.org/currevent.php>

JCK Las Vegas Show

29 May–1 June 2015
Las Vegas, Nevada, USA
<http://lasvegas.jckonline.com/Education--Events/Education-Schedule>
Notes: Educational lectures and events will take place 28–30 May.

Maine Pegmatite Workshop 2015

29 May–6 June 2015
Poland, Maine, USA
<http://pegworkshop.com>

XIVèmes Rendez-Vous Gemmologiques de Paris

8 June 2015
Paris, France
<http://tinyurl.com/njx6yu7>

PEG 2015: 7th International Symposium on Granitic Pegmatites

17–21 June 2015
Lower Silesia, Poland
www.peg2015polandczech.us.edu.pl

Sainte-Marie-aux-Mines Mineral and Gem Show

25–28 June 2015
Sainte-Marie-aux-Mines, Haut-Rhin, France
www.sainte-marie-mineral.com
Note: Lectures, workshops and gem/mineral-related films will be offered during the show.

1st Mediterranean Gemmological & Jewellery Conference

27–28 June 2015
Athens, Greece
<http://gemconference.com>

JTV Gem Lovers' Conference

22–24 July 2015
Knoxville, Tennessee, USA
www.jschoolinstitute.com/gem-lovers-conference-2015

Jewelry Camp 2015: Antique Jewelry & Art Conference

30–31 July 2015
West Harrison, New York, USA
www.jewelrycamp.org

NAJA 44th ACE IT Annual Mid-Year Educational Conference

8–11 August 2015
Washington D.C., USA
www.najaappraisers.com/index.html

12th International Congress for Applied Mineralogy

10–12 August 2015
Istanbul, Turkey
<http://icam2015.org>
Note: One of the congress themes is 'Industrial Minerals, Gems, Ores, and Mineral Exploration'

Northwest Jewelry Conference 2015

14–16 August 2015

Compiled by Georgina Brown and Brendan Laurs

Bellevue, Washington, USA
www.nwgem.com

Goldschmidt 2015

16–21 August 2015
Prague, Czech Republic
<http://goldschmidt.info/2015>

Session of interest: Mantle-Derived Intraplate Magmas, their Xenolith and Diamond Cargo: Processes, Timescales, and Geodynamic Implications

Dallas Mineral Collecting Symposium

21–22 August 2015
Dallas, Texas, USA
www.dallassymposium.org/2015-symposium

International Gemmological Conference (IGC)

23 August–3 September 2015
Vilnius, Lithuania
www.igc-gemmology.net

13th Biennial Meeting of the Society of Geology Applied to Mineral Deposits (SGA 2015)

24–27 August 2015
Nancy, France
<http://sga2015.blog.univ-lorraine.fr>
Session of interest: Gems and Industrial Minerals

8th International Congress on the Application of Raman Spectroscopy in Art and Archaeology

1–5 September 2015
Wrocław, Poland
<http://raa.chem.uni.wroc.pl>

26th International Conference on Diamond and Carbon Materials

6–10 September 2015
Bad Homburg, Germany
www.diamond-conference.elsevier.com

8th European Conference on Mineralogy and Spectroscopy (ECMS 2015)

9–11 September 2015
Rome, Italy
www.ecms2015.eu

Institute of Registered Valuers Loughborough Conference

12–14 September 2015
Loughborough
www.jewelleryvaluers.org/Loughborough-Conference

48th Annual Denver Gem & Mineral Show

18–20 September 2015
Denver, Colorado, USA
www.denvermineralshow.com
Note: Lectures and seminars will follow the show theme 'Minerals of the American Southwest'.

Canadian Gemmological Association Gemmology Conference 2015

16–18 October 2015
Vancouver, British Columbia, Canada
www.gemconference2015.com

The Munich Show

30 October–1 November 2015
Munich, Germany
<http://munichshow.com/en>
Note: The Forum Minerale will offer lectures and films on gems and minerals.

36th Annual New Mexico Mineral Symposium

14–15 November 2015
Socorro, New Mexico, USA
<https://geoinfo.nmt.edu/museum/minsymp/home.cfml>

Gem-A Conference, incorporating the 18th FEEG Symposium

21–22 November 2015
London
www.gem-a.com

EXHIBITS

Europe

Bellissima—Italy and High Fashion 1945–1968

Until 3 May 2015
MAXXI National Museum of XXI Century Arts, Rome, Italy
www.fondazionemaxxi.it/2014/07/01/bellissima/?lang=en

Anton Cepka—Kinetic jewellery

Until 7 June 2015
Pinakothek der Moderne, Munich, Germany
<http://www.pinakothek.de/en/kalender/2015-03-14/49069/anton-cepka-kinetic-jewellery>

Déboutonner la mode

Until 19 July 2015
Les Arts Décoratifs, Paris, France
www.lesartsdecoratifs.fr/francais/musees/musee-des-arts-decoratifs/actualites/expositions-en-cours/mode-et-textile/deboutonner-la-mode

Emaux de Bresse...et aujourd'hui?

Until 15 November 2015
Museum of Bresse—Domain Planon, Saint-Cyr-sur-Menthon, France
www.ain.fr/jcms/cd_7944/exposition-temporaire-et-animations-2014-au-musee-departemental-de-la-bresse

130 ans de création joaillière à Bastia: l'atelier Filippi

Until 19 July 2016

Musée Municipal d'Art et d'Histoire, Bastia, Corsica
<http://www.musee-bastia.com/musee-bastia/musee.php?nav=16&lang=en>

Inspired: Festival of Silver 2015

18–23 May 2015

Goldsmiths' Centre, London
www.thegoldsmiths.co.uk/events/festival-of-silver-2015-

An Adaptable Trade: The Jewellery Quarter at War

14–27 June 2015

Museum of the Jewellery Quarter, Birmingham
www.jewelleryquarter.net/event/first-world-war-centenary-exhibition

Bejewelled Treasures: The Al Thani Collection

21 November 2015–28 March 2016

Victoria and Albert Museum, London
www.vam.ac.uk/content/exhibitions/exhibition-bejewelled-treasures-the-al-thani-collection

Smycken: Jewellery

On display (closing date to be determined)

Nordiska Museet, Stockholm, Sweden
www.nordiskamuseet.se/en/utstallningar/jewellery

Middle East

Urartian Jewellery Collection

Until 31 July 2015

Rezan Has Museum, Istanbul, Turkey
www.rhm.org.tr/en/event/rezan-has-museum-urartian-jewellery-collection

North America

Ancient Luxury and the Roman Silver Treasure from Berthouville

Until 17 August 2015

The Getty Villa, Pacific Palisades, California, USA
www.getty.edu/art/exhibitions/ancient_luxury

Generations of Mastery: Gemstone Carvings by Dreher

Until October 2015

Gemological Institute of America, Carlsbad, California, USA
www.gia.edu/gia-museum-generations-mastery-gemstone-carvings-dreher

Beneath the Surface: Life, Death, and Gold in Ancient Panama

Until 1 November 2015

Penn Museum, Philadelphia, Pennsylvania, USA
www.penn.museum/press-releases/1163-beneath-the-surface.html

Bent, Cast, and Forged: The Jewelry of Harry Bertoia

Until 29 November 2015

Cranbrook Art Museum, Bloomfield Hills, Michigan, USA
www.cranbrookart.edu/museum/CAMec3.html

Fabergé: From a Snowflake to an Iceberg

Until 31 December 2015

Houston Museum of Natural Science, Texas, USA
www.hmns.org/index.php?option=com_content&view=article&id=594&Itemid=621

Maker and Muse: Women and Early Twentieth Century Art Jewelry

Until 3 January 2016

Driehaus Museum, Chicago, Illinois, USA
www.driehausmuseum.org

Glittering World: Navajo Jewelry of the Yazzie Family

Until 10 January 2016

The National Museum of the American Indian, New York, New York, USA
<http://nmai.si.edu/explore/exhibitions/item/838>

Arts of Islamic Lands: Selections from the al-Sabah Collection, Kuwait

Until 30 January 2016

Museum of Fine Arts, Houston, Texas, USA
www.mfah.org/exhibitions/arts-islamic-lands-selections-al-sabah-collection-

Turquoise, Water, Sky: The Stone and Its Meaning

Until 2 May 2016

Museum of Indian Arts and Culture, Santa Fe, New Mexico, USA
www.indianartsandculture.org/current?&eventID=1989

Fabergé from the Matilda Geddings Gray Foundation Collection

Until 27 November 2016

Metropolitan Museum of Art, New York, New York, USA
www.metmuseum.org/exhibitions/listings/2011/faberge

Glitterati—Portraits & Jewelry from Colonial Latin America

Until 27 November 2016

Denver Art Museum, Denver, Colorado, USA
<http://denverartmuseum.org/exhibitions/glitterati>

Gold and the Gods: Jewels of Ancient Nubia

Until 14 May 2017

Museum of Fine Arts, Boston, Massachusetts, USA
www.mfa.org/exhibitions/gold-and-gods

Fabergé: Jeweler to the Tsars

20 June–27 September 2015
Oklahoma City Museum of Art, Oklahoma, USA
www.okcmoa.com/see/exhibitions/faberge/

Gemstone Carvings: Crystals Transformed Through Vision & Skill

On display (closing date to be determined)
Houston Museum of Natural Science, Houston, Texas, USA
www.hmns.org/index.php?option=com_content&view=article&id=481&Itemid=502

City of Silver and Gold: From Tiffany to Cartier

On display (closing date to be determined)
Newark Museum, New Jersey, USA
www.newarkmuseum.org/SilverAndGold.html

Australia and New Zealand

A Fine Possession: Jewellery and Identity

Until 20 September 2015
Powerhouse Museum, Sydney, Australia
www.powerhousemuseum.com/exhibitions/jewellery

OTHER EDUCATIONAL OPPORTUNITIES

Gem-A Workshops and Courses

Gem-A, London
www.gem-a.com/education/course-prices-and-dates.aspx

Antoinette Matlins 'Hands-on' Gem Course

14–17 May 2015
Woodstock, Vermont, USA
www.antoINETTEMATLINS.com/seminars_woodstock.html

ASA Course on Recognizing Treated Gems and Origin Issues

16–17 May 2015
Chicago, Illinois, USA
www.appraisers.org/Education/ViewClass?ClassID=3333

The Goldsmiths' Company Assay Office: Hallmarking Information Day

22 May 2015
Goldsmiths' Hall, London
<http://tinyurl.com/o2m8tgh>

Gem-A Trip to Idar-Oberstein

13–20 June 2015
Idar-Oberstein, Germany
www.gem-a.com/news--events/events/idar-oberstein-2015.aspx

Fakes and Forgeries

14 June 2015
Art Antiques Fair, London
www.societyofjewelleryhistorians.ac.uk/news

Jewels of 'Blacknesse' at the Jacobean Court with Daniel Packer

23 June 2015
Society of Antiquaries of London, Piccadilly, London
www.societyofjewelleryhistorians.ac.uk/current_lectures

Montreal School of Gemmology: Gem and Jewellery Appraisal Course

6–29 July 2015 (in English and French)
Montreal, Quebec, Canada
www.ecoledegemmologie.com/en/c/10

Golden Threads: Filigree in Islamic Jewellery with Michael Spink

22 September 2015
Society of Antiquaries of London, Piccadilly, London
www.societyofjewelleryhistorians.ac.uk/current_lectures

Beauty and Belief: Techniques and Traditions of Omani Jewellery with Aude Mongiatti and Fahmida Suleman

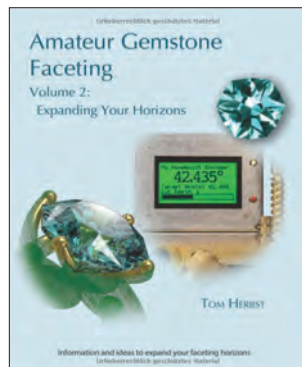
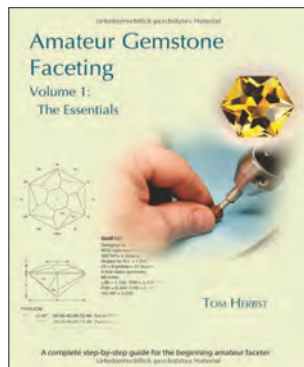
27 October 2015
Society of Antiquaries of London, Piccadilly, London
www.societyofjewelleryhistorians.ac.uk/current_lectures

Digital Tools and New Technologies in Contemporary Jewellery with Dauvit Alexander

24 November 2015
Society of Antiquaries of London, Piccadilly, London
www.societyofjewelleryhistorians.ac.uk/current_lectures

New Media

Amateur Gemstone Faceting



Tom Herbst, 2014.

Vol. 1: *The Essentials*, 428 pages, illus., softcover, ISBN 978-3000474743.

Vol. 2: *Expanding Your Horizons*, 456 pages, illus., softcover, ISBN 978-3000474750.

Self-published by Facetable Books, www.facetingbook.com. US\$19.95/volume.

This two-volume book on faceting by Tom Herbst covers a wide range of topics about gem cutting that are of interest to the beginner through master faceter. The word *amateur* in the title might be misleading since a large part of the content is very interesting for professional faceters, as well as for hobbyists with many years of experience. This monumental work, totalling almost 900 pages, is the state-of-the-art publication for this field of knowledge, offering comprehensive information on modern advances and techniques introduced to precision gem faceting during the past few decades.

Volume 1, called *The Essentials*, gives basic information on materials, equipment and techniques involved with gem faceting. A complete review of faceting machines, grinding and polishing laps, and additional equipment is given, together with detailed

explanations and tips for gem rough selection, dopping, and cutting and polishing procedures. Elaborate step-by-step instructions for the beginning faceter will guide the reader through the exciting experience of faceting their first stone, with comments on the possible problems encountered at each step and troubleshooting advice.

Volume 2, called *Expanding Your Horizons*, includes valuable information for faceters who want to better understand the science behind cutting gemstones and introduces modern computer-aided techniques related to faceting. The reader will find detailed explanations of gemstone mathematics, geometry and optics, properties of common gem materials, and an explanation of treatments. Computer programs for creating new faceting designs and optical optimization of existing cuts are also explained, together with a case study of creating a new design and a collection of original faceting designs developed by the author. The last chapter invites faceters to improve their equipment with several interesting do-it-yourself projects.

The author provides an explanation of faceting processes from a solid scientific perspective, with information not only regarding how but also why, from the point of view of materials science, optics, mechanics, gemmology and other related fields. Nevertheless, all of the scientific information is presented in easy-to-understand and informal language, with side-bar stories on the history of science and the author's faceting experience that make this book even more enjoyable.

The book is very well illustrated, and has a glossary of faceting terms and a subject index for both volumes. More details and selected pages (as free downloads) are available on the book's website, together with other reader resources and several downloadable items relating to various chapters of the book.

Dr Egor Gavrilenko

Eleventh Annual Sinkankas Symposium—Ruby, rev. edn.



Lisbet Thoresen, Ed., 2014. Pala International, Fallbrook, California, USA, 126 pages, illus., softcover, ISBN 978-0991532001, www.sinkankassymposium.net/ order-pubs. US\$45.00.

This lavishly illustrated proceedings volume, published in February 2014, commemorates a symposium held in April 2013 at the Gemological Institute of America in Carlsbad, California, that was co-sponsored by the San Diego Mineral & Gem Society. The book contains contributions by 10 authors, some of whom were speakers at the symposium. Not all of the presentations at the conference are represented by articles in this volume.

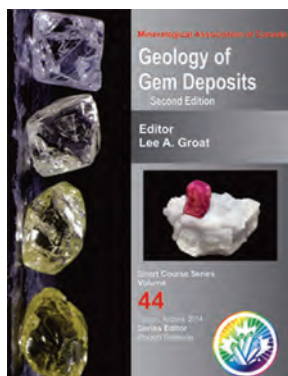
The book starts with biographies of the speakers and authors, followed by abstracts of the symposium presentations. The bulk of the volume consists of a

series of contributions that cover a broad diversity of topics on ruby: geology and localities (Dr James Shigley); treatments (Shane McClure); a historical account of mining in Mogok, Burma (reprint of a 1907 article by W. G. Fitz-Gerald); a description of a 1996 visit to Mogok (Richard Hughes); Nepalese rubies and sapphires (Elise Skalwold); an update on ruby mining in Afghanistan and Tajikistan (Gary Bowersox); a selected bibliography (Dr James Shigley); a collector's guide to literature on rubies and sapphires (Richard Hughes); mineral illustrations by Gamini Ratnavira and Eberhard Equit (Lisbet Thoresen); and a poem titled 'The Conundrum' (Robert Weldon). The book closes with a series of beautiful photographs of rubies from the collection of William F. Larson.

This eclectic compendium provides useful reference information as well as entertaining reading, and will appeal to a wide audience including hobbyists, collectors, gemmologists, bibliophiles, historians, earth scientists and armchair travellers. It is printed on sturdy paper and the colour reproduction of the photos is excellent. It would have been nice to have dimensions or weights for all specimens pictured (as well as the field-of-view for photomicrographs). Also, it seemed unusual to have the bibliography and literature listing appear in the middle of the volume, rather than at the end. But these are minor issues that do not detract from an otherwise very interesting and informative work on ruby.

Brendan M. Laurs

Geology of Gem Deposits, 2nd edn.



Lee A. Groat, Ed., 2014.
Short Course Series
Vol. 44, Mineralogical
Association of Canada,
Ottawa, Ontario, 405 pages,
illus., softcover, ISBN
978-0921294542, www.
mineralogicalassociation.ca.
US\$60.00.

of faceted gem materials. Nevertheless, a thorough synthesis of this subject would require another volume in itself. The final chapter in the book, on coloured gemstones from Canada (which also appeared in the first edition), may at first seem out of place in a volume on the geology of gem deposits. However, the geological setting of the various localities is provided, and considering the Canadian origin of this publication, this chapter must certainly be appreciated by many readers.

The volume contains a wealth of up-to-date information on the localities, geochemistry, geological origin and in some cases exploration criteria for the gem varieties that it covers. Two chapters (on chrysoberyl and topaz) are noticeably shorter than the others. The end of each chapter contains a useful reference list, which is particularly extensive for jade and corundum. This reviewer appreciated that not all of the deposits described in this volume are of economic significance, since much can be learned from studying the geology of minor showings in addition to important localities.

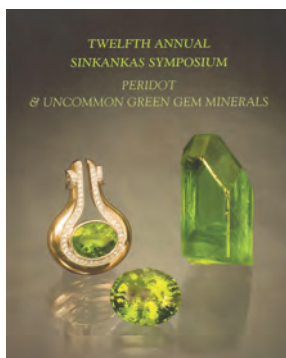
The book is printed on high-quality paper stock and is appropriately illustrated with many colour figures (diagrams as well as specimen photos). Some minor quibbles are that author names are not listed for all of the chapters in the table of contents, and two pages (216 and 256) were left entirely blank, evidently due to the decision to start each chapter on a right-hand page. Dimensions or weights were not included for some of the specimens pictured.

This volume serves as a valuable compendium on the geology of gem deposits, and belongs on the bookshelf of anyone who is involved with gem exploration, mining or origin determination. In addition, the book provides a useful reference for enthusiastic collectors with a desire to know more about the unusual and dynamic forces that have created a wide variety of gem treasures.

Brendan M. Laurs

This impressive volume accompanied a Mineralogical Association of Canada short course that took place in February 2014 during the Tucson gem shows. This second edition follows the same format as an earlier *Geology of Gem Deposits* volume published in 2007 (now out of print). It has been extensively updated, with the same principal authors for most of the chapters in both editions (i.e. Dr Thomas Stachel, Dr Gaston Giuliani, Dr Lee Groat, David Turner, Dr Daniel Marshall, Dr William 'Skip' Simmons, Dr George Harlow and Bradley Wilson). Chapters are included on the following gem materials: diamond, corundum (ruby and sapphire), emerald, other beryls, chrysoberyl, tanzanite and tsavorite, topaz, gem-bearing pegmatites and jade (jadeite and nephrite). New to the second edition is a chapter on the geology of gems and their geographic origin. This section is quite welcome, although it appears at an odd location between the chapters on gem corundum and emerald, rather than at the end of the volume where it might be expected. In addition, although it provides good summaries of the deposit types for various gems, this chapter is written solely from a geological perspective, so gemmologists will be disappointed by the lack of criteria presented for the origin determination

Twelfth Annual Sinkankas Symposium—Peridot and Uncommon Green Gem Minerals



Lisbet Thoresen, Ed., 2014. Pala International, Fallbrook, California, USA, 146 pages, illus., softcover, ISBN 978-0991532018, www.sinkankassymposium.net/order-pubs. US\$45.00.

The 12th Annual Sinkankas Symposium, on peridot and uncommon green gem minerals, was held in April 2014 at the Gemological Institute of America in Carlsbad and was co-sponsored by the San Diego Mineral & Gem Society. (See *The Journal*, Vol. 34, No. 2, 2014, pp. 156–157 for a report on this conference.) The format of this proceedings volume is similar to that of the previous symposium's volume on ruby (see review on pp. 457–458), with several contributions by a variety of authors, not all of whom were speakers at the symposium. Some of the presentations given at the conference are not represented by articles in this volume.

The book begins with a listing of the symposium programme, followed by abstracts of the presentations and then biographies of the speakers and authors. There are 12 contributions on peridot (the uncommon green gems covered in the symposium are not included): mineralogy and crystallography (Dr William 'Skip' Simmons); ancient gem peridot from Zabargad Island in Egypt (Dr James A. Harrell);

archaeogemmology (Lisbet Thoresen and Dr James A. Harrell); an historical overview of peridot at the Muséum National d'Histoire Naturelle, Paris, France (Dr François Farges); geology (Dr James E. Shigley); worldwide sources (Si and Ann Frazier); peridot from Supat, Pakistan (Pir Dost); peridot from Pyaung-gaung, Mogok Stone Tract, Myanmar (Dr George Harlow and Kyaw Thu); the manufacture of a suite of peridot jewellery (Robert E. Kane); extraterrestrial peridot (Si and Ann Frazier); and a selected bibliography (Dr James E. Shigley). The volume closes with several pages of attractive photos of peridot and other green minerals from the collection of William F. Larson.

To this reviewer's knowledge, this is the only modern volume devoted entirely to peridot. The quality of the printing is very high and the illustrations are outstanding, even capturing the subtle nuances of green coloration in various rough and cut specimens. Unfortunately, dimensions or weights were not included for all specimens pictured, and the ordering of the contributions could have been more logical (i.e. with geology and worldwide localities appearing closer to mineralogy and crystallography). There are also a few typos in the book (e.g. 'pocalities' in the table of contents and an inconsistent spelling of 'Supat' and 'Sapat Gali' in the volume). Nevertheless, these small items are overshadowed by the exceptional amount of interesting and useful information on peridot that has been assembled for this volume, which will appeal to gemmologists, mineralogists, geologists, archaeologists, historians and bibliophiles.

Brendan M. Laurs

OTHER BOOK TITLES*

Diamonds

Research on the Origin of Diamonds under the Kimberley Process Certification Scheme of the United Nations

By Beili Zhang, Hua Chen, Zhili Qiu and others, 2013. Geological Publishing House, Beijing, China, 410 pages, ISBN 978-7116086531 (in Chinese). ¥198.00 hardcover.

Gem Localities

Gem Trails of Washington, 2nd edn.

By Garret Romaine, 2014. Gem Guides Book Co., Upland, California, USA, 248 pages, ISBN 978-1889786537. US\$18.95 softcover.

Minéraux de Bretagne

By Louis Chauris, 2014. Les Editions du Piat, Saint-Julien-du-Pinet, France, 336 pages, ISBN 978-2917198223 (in French). €85.00 hardcover.

Namibia—Mineralien und Fundstellen

By various authors, 2014. extraLapis No. 47, Christian Weise Verlag, Munich, Germany, 124 pages (in German). €19.80 softcover.

The Nature of California Guidebook: Gemstones from the Pala Pegmatites

By Ron Schmidling II, 2015. Self-published, 33 pages, ASIN B00S5OP47M. £6.33 Kindle edition.

General Reference

Beginners Guide to Gem Carving

By Jason Hollis, 2014. Self-published, 24 pages, ASIN B00QOR8032. £6.89 Kindle edition.

* Compiled by Georgina Brown and Brendan Laurs

Gem & Jewelry Pocket Guide: A Traveler's Guide to Buying Diamonds, Colored Gems, Pearls, Gold and Platinum Jewelry

By Renée Newman, 2015. International Jewelry Publications, Columbus, Ohio, USA, 160 pages, ISBN 978-0929975306. US\$11.95 softcover or US\$4.99 Kindle edition.

Gemstone Tumbling, Cutting & Drilling: A Simple Guide to Finishing & Polishing Rough Stones

By James Magnuson and Val Carver, 2015. Adventure Publications, Cambridge, Minnesota, USA, 128 pages, ISBN 978-1591934608. US\$14.95 softcover.

Miller's Field Guide: Silver

By Judith Miller, 2015. Mitchell Beazley, London, 240 pages, ISBN 978-1784720360. £7.99 softcover.

Jewellery and Objets d'Art

Answers to Questions about Old Jewelry, 1840–1950, 8th edn.

By C. Jeanenne Bell, 2015. Krause Publications, Iola, Wisconsin, USA, 400 pages, ISBN 978-1440240188. £23.99 softcover.

Anton Cepka: Jewelry and Objects

By The International Design Museum, 2015. Arnoldsche Art Publishers, Stuttgart, Germany, 224 pages, ISBN 978-3897904385. £45.00 hardcover.

Antonio and Piero del Pollaiuolo: "Silver and Gold, Painting and Bronze..."

By Andrea Di Lorenzo and Aldo Galli, 2015. Skira Editore, Milan, Italy, 288 pages, ISBN 978-8857224749. £29.00 hardcover.

Art of the Land of Maharajas: Indian Jewellery and Arms of the XVII–XIX Centuries from Alexander Feldman's Collection

By Eugene Sivachenko and Victoria Bulgakowa, 2015. Hirmer Verlag Publishers, Munich, Germany, 280 pages, ISBN 978-3777422299. £52.33 hardcover.

Cartier Royal: High Jewelry and Precious Objects

By Francois Chaille, 2015. Flammarion, Paris, France, 260 pages, ISBN 978-2080201942. £80.00 hardcover.

Cycles of Life: Rings from the Benjamin Zucker Family Collection

By Sandra Hindman, 2014. Paul Holbertson Publishing, London, 260 pages, ISBN 978-0991517237. £35.00 softcover.

Damiani: Alchemy of Desire. A Story, a Family, and an Italian Passion

By Cristina Morozzi, 2014. Rizzoli International Publications, New York, New York, USA, 240 pages, ISBN 978-0847842834. US\$100.00 hardcover.

Eesti Rahvapärased Hõbeehetud. Estonian National Silver Jewellery

By Eevi Astel, 2014. Estonian National Museum, Tartu, Estonia, 96 pages, ISBN 978-9949417957. €19.00 hardcover.

Fabergé Eggs by Victor Mayer

By Anne-Barbara Kern, 2015. Arnoldsche Art Publishers, Stuttgart, Germany, 128 pages, ISBN 978-3897904354. £30.00 hardcover.

Inspired by Light and Land: Designers and Makers in Western Australia 1829–1969

By Dorothy Erickson, 2014. Western Australian Museum, Welshpool, Australia, 492 pages, ISBN 978-1920843199. AUS\$90.00 hardcover.

Jewellery 1970–2015: Bollmann Collection.

Fritz Maierhofer—Retrospective

Karl Bollmann, Graziella Folchini Grassetto, Christoph Thun-Hohenstein and Elisabeth Schmuttermeyer, 2015. Arnoldsche Art Publishers, Stuttgart, Germany, 144 pages, ISBN 978-3897904286. US\$50.00 hardcover.

Jewels of the Renaissance

By Yvonne Hackenbroch, 2015. Assouline Publishing, London, 200 pages, ISBN 978-1614282037. £120.00 hardcover.

Jewels on Queen

By Anne Schofield, 2014. NewSouth Publishing, Sydney, Australia, 128 pages, ISBN 978-1742231433. £19.99 softcover.

Maker and Muse: Women and Early Twentieth Century Art Jewelry

By Elyse Zorn Karlin, 2015. The Monacelli Press, New York, New York, USA, 256 pages, ISBN 978-1580934046. US\$50.00 hardcover.

Non-Figural Designs in Zuni Jewelry

By Toshio Sei, 2015. Schiffer Publishing, Atglen, Pennsylvania, USA, 160 pages, ISBN 978-0764347276. US\$24.99 hardcover.

Piaget: Watchmakers and Jewellers Since 1874

By Florence Müller, 2015. Abrams Books, New York, New York, USA, 344 pages, ISBN 978-1419716881. US\$85.00 hardcover.

The Rings from the Hashimoto Collection of the National Museum of Western Art

National Museum of Western Art, 2014. National Museum of Western Art, Tokyo, Japan, 318 pages, ISBN 978-4907442040. ¥2,400 hardcover.

Surviving Desires: Making and Selling Native Jewellery in the American Southwest

By Henrietta Lidchi, 2015. University of Oklahoma Press, Norman, Oklahoma, USA, 272 pages, ISBN 978-0806148502. US\$34.95 softcover.

Understanding Jewellery, 4th edn.

By David Bennett and Daniela Mascetti, 2015. Antique Collectors' Club, Woodbridge, Suffolk, 526 pages, ISBN 978-1851496976. £45.00 hardcover.

Untamed Encounters: Contemporary Jewelry from Extraordinary Gemstones

By Mimi Lipton, 2014. Thames and Hudson, London, 248 pages, ISBN 978-0500970638. £60.00 hardcover.

Wartski: The First 150 Years

By Geoffrey C. Munn, 2015. Antique Collectors' Club, Woodbridge, Suffolk, 288 pages, ISBN 978-1851497843. £65.00 hardcover.

Mineralogy

Crystals and Crystal Growth

By Wilfred Carter, 2015. Nova Science Publishers, Hauppauge, New York, USA, 108 pages, ISBN 978-1634637916. US\$82.00 softcover.

Gold for Collectors

By Scott Werschky, Carles Curto and Joaquim Callén, 2014. Mineral Up Editions, Barcelona, Spain, 288 pages, ISBN 978-8469713464. US\$99.99 hardcover.

Lapis Mineralienverzeichnis – Alle Mineralien von A bis Z und ihre Eigenschaften

By Stefan Weiß, 2014. Christian Weise Verlag, Munich,

Germany, ISBN 978-3921656808 (in German). €19.80 softcover.

Introducing Mineralogy

By John Mason, 2014. Dunedin Academic Press, Edinburgh, 160 pages, ISBN 978-1780460284. £14.99 softcover.

Social Studies

Most Captivating Diamond Heists of Our Time: A Look at the Worlds Biggest Heists

By Jason Bozzuto, 2014. Self-published, Kobo, Toronto, Canada. US\$9.99 eBook.

Erratum

The book *Jadeite: Identification & Price Guide*, 4th edn. should not have been listed in Vol. 34, No. 4, 2014, p. 374, as it deals with glassware and not jadeite gem material.



Stone Group Laboratories

Where technology and experience meet.


- Gem Identification
- Treatment Analysis
- Consultation
- Research

www.StoneGroupLabs.com



Crown Color

Fine Rubies, Sapphires and Emeralds
Bangkok - Geneva - Hong Kong - New York



Crown Color is a proud supporter of the *Journal of Gemmology*

Head Office: Crown Color Ltd., 14/F, Central Building, suite 1408
1-3 Pedder Street, Central Hong Kong SAR, Tel: +852-2537-8986
New York Office: + 212-223-2363 | Geneva Office: + 41-22-8100540



YOUR GLOBAL PARTNER

Gem Identification Report and Gemstone Memo

GIT, The utmost advanced Gem and Precious Metal Testing Laboratory in Thailand, is recognized by CIBJO (The World Jewellery Confederation) and also a member of LMHC and ICA, we are well equipped with the world's most advanced instruments operated by highly experienced gemologists.

LABORATORY SERVICES

ensuring the authenticity of your valuable gems & jewelry



The Gem and Jewelry Institute of Thailand (Public Organization)
140 ITF Tower, Silom Rd., Bangkok 10500, Thailand
TEL : +66 2634 4999 FAX : +66 2634 4970
<http://www.git.or.th> E-mail: jewelry@git.or.th



Literature of Interest

Coloured Stones

Agate investigation with particular emphasis on iris agate. G. Pearson and R. Green, *Australian Gemmologist*, **25**(8), 2014, 279–287.

Classification of raw jadeite (gambling jadeite). J. Pan, *Journal of Gems & Gemmology*, **16**(3), 2014, 12–23 (in Chinese with English abstract).

The color mechanism analysis of Dushan jade. X. He, Y. Xue, W. Jiang and H. Zhao, *Acta Petrologica et Mineralogica*, **33**(Supp.), 2014, 69–75 (in Chinese with English abstract).

Colored gemstones: Impacts on availability and pricing from 2000–2014. E. Braunwart, *GemGuide*, **34**(1), 2015, 2–8.

Coloring mechanism of tiger's eyes with different colors. S. Luo, K. Li and Y. Liu, *Acta Petrologica et Mineralogica*, **33**(Supp.), 2014, 76–82 (in Chinese with English abstract).

Colouring agent of blue spinel and cobalt spinel from Vietnam. M. Furuya, *Gem Information*, **42**, 2014, 1–3 (in Japanese).

Gemological study on trapiche style amethyst. S. Zhou, *China Gems & Jades*, **z1**, 2014, 154–157 (in Chinese).

Ion substitutions and structural adjustment in Cr-bearing tourmalines. O.S. Vereshchagin, I.V. Rozhdestvenskaya, O.V. Frank-Kamenetskaya and A.A. Zolotarev, *European Journal of Mineralogy*, **26**(2), 2014, 309–321, <http://dx.doi.org/10.1127/0935-1221/2014/0026-2372>.

Mondstein—eine aktuelle Betrachtung [Moonstone—A current observation]. U. Henn, T. Häger and F. Schmitz, *Gemmologie: Zeitschrift der Deutschen Gemmologischen Gesellschaft*, **63**(3/4), 2014, 81–100 (in German with English abstract).

Optical and cathodoluminescence investigations of the green microcrystalline (chrysoprase) quartz. M. Hatipoğlu and Y. Yardımcı, *Journal of Luminescence and Applications*, **1**(2), 2014, 87–104, <http://dx.doi.org/10.7726/jla.2014.1008>.*

Une pezzottaïte exceptionnelle au LFG [Exceptional pezzottaite in LFG]. A. Droux, E. Fritsch and O. Segura, *Revue de Gemmologie A.F.G.*, **190**, 2014, 14–15.

Reading pegmatites: Part 1—What beryl says. D. London, *Rocks & Minerals*, **90**(2), 2015, 138–153, <http://dx.doi.org/10.1080/00357529.2014.949173>.

The story of one spodumene. V.A. Tuzlokov, *Mineralogical Almanac*, **20**(1), 2015, 69–71.

Unusual colour changes in gemstones. M. Furuya, *Gem Information*, **42**, 2014, 4–6 (in Japanese).

Cultural Heritage

Characterization of the lapis lazuli from the Egyptian treasure of Tôd and its alteration using external μ -PIXE and μ -IBIL. T. Calligaro, Y. Coquinot, L. Pichon, G. Pierrat-Bonnefois, P. de Campos, A. Re and D. Angelici, *Nuclear Instruments and Methods in Physics Research Section B: Beam Interactions with Materials and Atoms*, **318**, Part A, 2014, 139–144, <http://dx.doi.org/10.1016/j.nimb.2013.06.063>.

Gem quality and archeological green 'jadeite jade' versus 'omphacite jade'. A. Coccato, S. Karampelas, M. Wörle, S. van Willigend and P. Pétrequine, *Journal of Raman Spectroscopy*, **45**, 2014, 1260–1265, <http://dx.doi.org/10.1002/jrs.4512>.

The history of emerald mining in Colombia: An examination of Spanish-language sources. B. Brazeal, *The Extractive Industries and Society*, **1**(2), 2014, 273–283, <http://dx.doi.org/10.1016/j.exis.2014.08.006>.*

In situ identification of gemstone beads excavated from tombs of the Han Dynasties in Hepu County, Guangxi Province, China using a portable Raman spectrometer. J. Dong, Y. Han, J. Ye, Q. Li, S. Liu and D. Gu, *Journal of Raman Spectroscopy*, **45**(7), 2014, 596–602, <http://dx.doi.org/10.1002/jrs.4501>.

Les premières pierres précieuses de l'antiquité [The first gems of antiquity]. H.-J. Schubnel, *Revue de Gemmologie A.F.G.*, **190**, 2014, 10–13.

Nadir Shah and the myth of the Kuh-e Nur's name. A. Malecka, *Australian Gemmologist*, **25**(8), 2014, 288–289.

Diamonds

Chromism in pink diamonds. J. Chapman, *Australian Gemmologist*, **25**(8), 2014, 268–271.

Diamonds: A sketch portrait (History of discovery of the Russian deposits and their genesis). V.K. Garanin and M.B. Leybov, *Mineralogical Almanac*, **19**(1), 2014, 30–47.

Exceptional pink to red diamonds: A celebration of the 30th Argyle diamond tender. J. King, J.E. Shigley and C. Jannucci, *Gems & Gemmology*, **50**(4), 2014, 268–279, <http://dx.doi.org/10.5741/GEMS.50.4.268>.*

Compiled by Brendan Laurs

* Article freely available for download, as of press time

Hydrous mantle transition zone indicated by ringwoodite included within diamond.

D.G. Pearson, F.E. Brenker, F. Nestola, J. McNeill, L. Nasdala, M.T. Hutchison, S. Matveev, K. Mather, G. Silversmit, S. Schmitz, B. Vekemans and L. Vincze, *Nature*, **507**, 2014, 221–224, <http://dx.doi.org/10.1038/nature13080>.

Introduction of the theory of optical performance of diamond. M. Furuya, *Gem Information*, **42**, 2014, 7–9 (in Japanese).

Lomonosov diamond mine in Arkhangelsk, Russia. M. Furuya, *Gem Information*, **42**, 2014, 10–14 (in Japanese).

O momento é dos diamantes coloridos [The moment is of colored diamonds]. J.L. Brusa, *Diamond News*, **41**, 2014, 53–58 (in Portuguese).

Rough diamond auctions: Sweeping changes in pricing and distribution. R. Shor, *Gems & Gemology*, **50**(4), 2014, 252–267, <http://dx.doi.org/10.5741/GEMS.50.4.252>.*

Study of the Blue Moon diamond. E. Gaillou, J.E. Post, K.S. Byrne and J.E. Butler, *Gems & Gemology*, **50**(4), 2014, 280–286, <http://dx.doi.org/10.5741/GEMS.50.4.280>.*

A trajetória do Brasileiro diamante [The source of Brazilian diamond]. J.L. Brusa, *Diamond News*, **41**, 2014, 7–13 (in Portuguese).

Gem Localities

Adun Chilon [Russian beryl locality]. W.E. Wilson, *Mineralogical Record*, **46**(2), 2015, 228–232.

Advances in trace element “fingerprinting” of gem corundum, ruby and sapphire, Mogok area, Myanmar. F. Lin Sutherland, K. Zaw, S. Meffre, T. Yui and K. Thu, *Minerals* **5**(1), 2015, 61–79, <http://dx.doi.org/10.3390/min5010061>.*

The Afghan pocket, Pederneira mine (Brazil). D. Trinchillo and F. Pezzotta, *Minerals—The Collector’s Newspaper*, **9**, 2015, 1–4, http://spiriferminerals.com/foto_artyk/minerals/Minerals9-net.pdf.*

Australian opalised fossils – Earth treasures from dried mud and deep time. E.T. Smith, *Australian Gemmologist*, **25**(8), 2014, 272–278.

Chrysoberyl-sillimanite association from the Roncadeira pegmatite, Borborema Province, Brazil: Implications for gemstone exploration.

H. Beurlen, R. Thomas, J.C. Melgarejo, J.M.R. Da Silva, D. Rhede, D.R. Soares and M.R.R. Da Silva, *Journal of Geosciences*, **58**(2), 2013, 79–90, <http://dx.doi.org/10.3190/jgeosci.142>.*

Composition and genesis of green nephrites from the Karakax River in Hetian, Xinjiang. Z. Wen, M. Abuduwayiti and F. Lu, *Acta Petrologica et Mineralogica*, **33**(Supp.), 2014, 19–27 (in Chinese with English abstract).

The Diamond Hill mine, Abbeville County, South Carolina. C. Karwoski, *Mineralogical Record*, **46**(2), 2015, 249–263.

First ruby and pink sapphire mine coming to Greenland. M. Feliciano, *JNA*, **367**, 2015, 64–66.

Gemological and mineralogical characteristics of green nephrite from Cassiar, Canada. Q. Wu, R. Wu, Y. Zhao and W. Shi, *Acta Petrologica et Mineralogica*, **33**(Supp.), 2014, 43–47 (in Chinese with English abstract).

Granite pegmatites of the Borisovskiy Pluton, South Urals. S.V. Kolisnechenko, V.I. Popova and V.A. Popov, *Mineralogical Almanac*, **19**(1), 2014, 14–29.

Great topaz find: Tribute pocket, CO, USA. J. Cowman and P. Persson, *Minerals—The Collector’s Newspaper*, **9**, 2015, 1, 6–10, http://spiriferminerals.com/foto_artyk/minerals/Minerals9-net.pdf.*

Mineral inclusions in sapphire from the basalt-related deposit in Bo Phloi, Kanchanaburi, western Thailand: Indication of their genesis.

P. Khamloet, V. Pisutha-Arnond and C. Sutthirat, *Russian Geology and Geophysics*, **55**(9), 2014, 1087–1102, <http://dx.doi.org/10.1016/j.rgg.2014.08.004>.

Mineralogy and geochemistry of gem vanadanium-chromian grossulars (tsavorite) from East Africa. L. Lyu, B. Mao and X. He, *Journal of Gems & Gemmology*, **16**(4), 2014, 1–13 (in Chinese with English abstract).

The Pederneira mine, São José da Safira, Minas Gerais, Brazil. D. Trinchillo, F. Pezzotta and A. Dini, *Mineralogical Record*, **46**(1), 2015, 1–138.

The Piteiras emerald mine, Minas Gerais, Brazil: Fluid-inclusion and gemmological perspectives.

E.P. Lynch, A. Costanzo, M. Feely, N.J.F. Blamey, J. Pironon and P. Lavin, *Mineralogical Magazine*, **78**(7), 2014, 1571–1587, <http://dx.doi.org/10.1180/minmag.2014.078.7.04>.

Prase opal from Tanzania. H. Zhao, X. Zhang and X. He, *Journal of Gems & Gemmology*, **16**(4), 2014, 14–21 (in Chinese with English abstract).

Smaragde aus der Provinz Laghman, Afghanistan: ein Vergleich mit Smaragden aus dem Panjshir-Tal [Emeralds from Laghman Province, Afghanistan: Comparison with emeralds from Panjshir Valley]. U. Henn and F. Schmitz, *Gemmologie: Zeitschrift der Deutschen Gemmologischen Gesellschaft*, **63**(3/4), 2014, 101–106 (in German with English abstract).

Study on gemmological characteristics and ore genesis of nephrite from Tanghe, Hebei Province. C. Chen, X. Yu and S. Wang, *Journal of Gems & Gemmology*, **16**(3), 2014, 1–11 (in Chinese with English abstract).

A study of gemological characteristics of green nephrite in Ospa 11* mining area of Russia. Y. Zhao, R. Wu, Q. Qu and W. Shi, *Acta Petrologica et Mineralogica*, **33**(Supp.), 2014, 37–42 (in Chinese with English abstract).

A study of gemological and color influencing ions of green nephrite from Ospinsk No.7 mining area, Russia. M. Yuan, R. Wu and J. Zhang, *Acta Petrologica et Mineralogica*, **33**(Supp.), 2014, 48–54 (in Chinese with English abstract).

Instruments and Techniques

Gamma-rays attenuation of zircons from Cambodia and South Africa at different energies: A new technique for identifying the origin of gemstone. P. Limkitjaroenporn and J. Kaewkhao, *Radiation Physics and Chemistry*, **103**, 2014, 67–71, <http://dx.doi.org/10.1016/j.radphyschem.2014.05.035>.

La spectrométrie d'émission accessible à tous—3ème partie [Portable emission spectrometry—Part 3]. D. Peyresaubes, M. Schoor and J.-C. Boulliard, *Revue de Gemmologie A.F.G.*, **190**, 2014, 17–18.

3 in 1 photo lens for iPhone. T. Linton, A. Smallwood and A.C. Paul, *Australian Gemmologist*, **25**(8), 2014, 290–291.

Jewellery Manufacturing

Additive manufacture of fashion and jewellery products: A mini review. Y. Yap, *Virtual and Physical Prototyping*, **9**(3), 2014, 195–201, <http://dx.doi.org/10.1080/17452759.2014.938993>.*

News Press

Colored diamonds: Asia's new fancy best friend. M. Yuan, *Forbes*, 2 May 2015, www.forbes.com/sites/myuan/2015/02/05/colored-diamonds-asias-new-fancy-best-friend.*

Mogok miners hold out hope for remaining rubies. K.H. Mon, *The Irrawaddy*, 4 March 2015, www.irrawaddy.org/feature/mogok-miners-hold-out-hope-for-remaining-rubies.html.*

Precious rebound—Coloured gemstones coming into their own after being outshone by diamonds for decades. I. Solomons, *Mining Weekly*, 13 February 2015, www.miningweekly.com/article/coloured-gemstones-coming-into-their-own-after-being-outshone-by-diamonds-for-decades-2015-02-13-1.*

Organic Gems

Characteristics of trace elements in freshwater and seawater cultured pearls. E. Zhang, F. Huang, Z. Wang and Q. Li, *Spectroscopy and Spectral Analysis*, **34**(9), 2014, 2544–2547 (in Chinese with English abstract).

Comparative Fourier transform infrared investigation of oltu-stone (natural carbon black) and jet. M. Hatipoğlu, S.N. Cesaro and D. Ajò, *Spectroscopy Letters*, **47**(3), 2014, 161–167, <http://dx.doi.org/10.1080/00387010.2013.785435>.

Contribution of donor and host oysters to the cultured pearl colour in *Pinctada martensii*. G. Zhifeng, H. Fengshao, W. Hai, G. Kai, Z. Xin, S. Yaohua and W. Aiming, *Aquaculture Research*, **45**(7), 2014, 1126–1132, <http://dx.doi.org/10.1111/are.12052>.

Crystallography of calcite in pearls. A. Pérez-Huerta, J.-P. Cuif, Y. Dauphin and M. Cusack, *European Journal of Mineralogy*, **26**(4), 2014, 507–516, <http://dx.doi.org/10.1127/0935-1221/2014/0026-2390>.

Einblicke in eine außergewöhnlich große Südseezuchtperle mittels Röntgen-Mikrocomputertomographie [A look inside a remarkably large beaded South Sea cultured pearl]. L. M. Otter, U. Wehrmeister, F. Enzmann, M. Wolf and D. E. Jacob, *Gemmologie: Zeitschrift der Deutschen Gemmologischen Gesellschaft*, **63**(3/4), 2014, 69–80 (in German with English abstract).

The ivory pandemonium. C. Lule, *GemGuide*, **33**(6), 2014, 4–6.

Pérolas em Santa Catarina [Pearls in Santa Catarina]. C.M. de Lima e Silva, G. Caetano Manzoni and M.I. Bonotto Brusa, *Diamond News*, **41**, 2014, 42–51 (in Portuguese).

A preliminary study of inclusions in the burmite (Myanmar amber) and their significance. B. Lu, D. Yang, H. Fang and G. Shi, *Acta Petrologica et Mineralogica*, **33**(Supp. 2), 2014, 117–122 (in Chinese with English abstract).

Synthetics and Simulants

The development of sintered polycrystalline diamond compact (PCD&PDC). Y. Zhao, S. Zhao and S. Yan, *Superhard Material Engineering*, **26**(2), 2014, 45–49 (in Chinese with English abstract).

Fake it till you make it—The uncanny art of forging amber. M.E. Eriksson and G.O. Poinar, *Geology Today*, **31**(1), 21–27, <http://dx.doi.org/10.1111/gto.12083>.*

Gemmological characteristics of dark green jadeite imitations. R. Li, Z. Xu, Y. Xiong, P. Zhang and Y. Zhang, *Journal of Gems & Gemmology*, **16**(5), 2014, 49–54 (in Chinese with English abstract).

Identification characteristics of composite coral. H. Li, Z. Yue, J. Liang, T. Lu, J. Zhang and J. Zhou, *Journal of Gems & Gemmology*, **16**(5), 2014, 44–48 (in Chinese with English abstract).

Identification characteristics of HPHT synthetic diamonds in jewelry with cluster setting. H. Zhu, T. Li and G. Li, *Journal of Gems & Gemmology*, **16**(5), 2014, 28–33 (in Chinese with English abstract).

Identification and spectroscopy characteristics of three natural minerals similar to turquoise.

X. Zhang, M. Yang, J. Di and P. Wang, *Journal of Gems & Gemmology*, **16**(3), 2014, 38–45 (in Chinese with English abstract).

A preliminary study on the separation of natural and synthetic emeralds using vibrational spectroscopy.

L.T.-T. Huong, W. Hofmeister, T. Häger, S. Karampelas and N.D.-T. Kien, *Gems & Gemology*, **50**(4), 2014, 287–292, <http://dx.doi.org/10.5741/GEMS.50.4.287>.*

Premiers diamants synthétiques déposés pour analyse au Laboratoire Français de Gemmologie [First synthetic diamonds submitted for analysis to the French Gemological Laboratory].

A. Delaunay and E. Fritsch, *Revue de Gemmologie A.F.G.*, **190**, 2014, 4–8.

Treatments

Gambling-jadeite and characteristics of an inner-filled gambling-jadeite.

A. Ling and Z. Chen, *Acta Petrologica et Mineralogica*, **33**(Supp.), 2014, 97–100 (in Chinese with English abstract).

Identification characteristics of emeralds filled by ExCel.

J. Su, T. Lu, R. Wei and J. Zhang, *Journal of Gems & Gemmology*, **16**(6), 2014, 34–38 (in Chinese with English abstract).

Research on heat treatment of ruby from Burma and Vietnam.

W. Wang and J. Di, *Journal of Gems & Gemmology*, **16**(4), 2014, 29–38 (in Chinese with English abstract).

A study of dyed opals from Ethiopia.

F. Yu, G. Fan, S. Weng, Y. Liu, M. Sun and Y. Xu, *Acta Petrologica et Mineralogica*, **33**(Supp. 2), 2014, 123–139 (in Chinese with English abstract).

Miscellaneous

Appraising worn jewelry and damaged gemstones for insurance.

R.B. Drucker, *GemGuide*, **34**(1), 2015, 13–14.

Can traditional methods be still useful in exploration and mining of gem deposits?—A review.

S. W. Nawaratne, *Journal of Geological Society of Sri Lanka*, **16**, 2014, 151–158, www.gsslweb.org/wp-content/uploads/2015/03/Article-15.pdf.*

Healing images. Gems and medicine. V. Dasen, *Oxford Journal of Archaeology*, **33**(2), 2014, 177–191, <http://dx.doi.org/10.1111/ojoa.12033>.

Il museo mineralogico e gemmologico “Luigi Cellèri”, San Piero in Campo, Isola d’Elba

["Luigi Celleri" mineralogical and gemological museum, San Piero in Campo, Elba Island].

F. Pezzotta, *Rivista Mineralogica Italiana*, **2**, 2014, 114–122, (in Italian).

The influence of pearl oyster farming on reef fish abundance and diversity in Ahe, French Polynesia.

L. Cartier and K. Carpenter, *Marine Pollution Bulletin*, **78**(1–2), 2014, 43–50, <http://dx.doi.org/10.1016/j.marpolbul.2013.11.027>.

A study on the symbolic features and wearing types of pearl necklaces.

J. Cho, *Journal of the Korean Society of Clothing and Textiles*, **37**(8), 2013, 1029–1043, <http://dx.doi.org/10.5850/jksct.2013.37.8.1029> (in Korean with English abstract).*

Compilations

Gem News International. Demantoid from Balochistan, Pakistan • Ethiopian black opal • Non-nacreous beaded cultured pearl • Beryl and topaz doublet • Coated lawsonite • Composite ruby rough • Dyed marble imitations of jadeite and sugilite • Synthetic spinel with unusual short-wave UV reaction • Online U.S. diamond sales • Gem auctions • *Margaritologia* newsletter • Gemology session at GSA meeting. *Gems & Gemology*, **50**(4), 2014, 302–315, www.gia.edu/gems-gemmology.*

Gemmologie Aktuell [Gemmology News].

Mosandrite • Sugilite imitation • Glass imitation of colour-zoned quartz. *Gemmologie: Zeitschrift der Deutschen Gemmologischen Gesellschaft*, **63**(3/4), 2014, 63–68 (in German and English).

Lab Notes. Colourless type IaB diamond with Si-V defect • Screening of yellow diamond melee • Large irradiated yellow diamond • Natural pearl aggregates from *Pteria* mollusks • Lead-glass-filled Burmese rubies • Spinel inclusion in spinel • Fancy Vivid pinkish orange CVD synthetic diamond • Mixed-type HPHT synthetic diamond with unusual growth features • Black nano-polycrystalline synthetic diamond. *Gems & Gemology*, **50**(4), 2014, 293–301, www.gia.edu/gems-gemmology.*

Conference Proceedings

4th International Gem and Jewelry Conference.

8–9 December 2014, Chiang Mai, Thailand, www.git.or.th/shopping_cart/e-book.aspx?lang=en.

World of Gems Conference IV.

20–21 September 2014, Rosemont, Illinois, USA, <http://gemguide.com/events/world-of-gems-conference>.



Gain a European Certificate in Gemmology

Founded in 1995, The Federation for European Education in Gemmology (FEEG) supports a European gemmology qualification that is recognized by all gem and jewellery bodies and institutions across Europe.

FEEG comprises 11 gemmological organizations from eight European countries. Graduates of these organizations can take the exam (available in five languages) to gain the European Certificate in Gemmology. **Graduates of Gem-A's Gemmology Diploma are eligible to take the exam.**

If you are a Gemmology Diploma graduate and want to find out more, contact information@gem-a.com.

Participating organizations:

- **WIFI Oberösterreich**
Linz, Austria
- **Academie voor Mineralogie**
Antwerp, Belgium
- **Société Belge de Gemmologie**
Etterbeek, Belgium
- **Institut National de Gemmologie**
Paris, France
- **Deutsche Gemmologische Gesellschaft**
Idar-Oberstein, Germany
- **Istituto Gemmologico Italiano**
Milan, Italy
- **Netherlands Gemmological Laboratory**
Leiden, The Netherlands
- **Dutch Gemmological Institute**
Schoonhoven, The Netherlands
- **Escola de Gemmologia de la Universitat de Barcelona**
Barcelona, Spain
- **Instituto Gemológico Español**
Madrid, Spain
- **Gem-A**
London, United Kingdom



The 18th FEEG Symposium will be held in conjunction with Gem-A's 2015 Conference — email events@gem-a.com to be added to the mailing list

*For they who have the time
even the jungle is a paradise.*

— Sri Lankan saying



Palala International
Palagems.com / Palaminerals.com
800-854-1598 / 760-728-9121

Natural Sapphire, Sri Lanka • 9.71 ct • 12.5 x 10.85 x 8.23 mm
Photo: Mia Dixon